

GENETIC CHARACTERIZATION AND STRAIN DIFFERENTIATION OF FELINE CALICIVIRUS  
AMONG CAT POPULATION IN THAILAND BY HIGH RESOLUTION MELTING ANALYSIS



A Dissertation Submitted in Partial Fulfillment of the Requirements  
for the Degree of Doctor of Philosophy in Veterinary Pathobiology

Department of Veterinary Pathology

FACULTY OF VETERINARY SCIENCE

Chulalongkorn University

Academic Year 2021

Copyright of Chulalongkorn University

ลักษณะทางพันธุกรรมและการวิเคราะห์แยกสายพันธุ์ของไวรัสคาลิซึ ในประชากรแมวของประเทศไทย  
ไทยโดยวิธีวิเคราะห์ด้วยวิธี High Resolution Melting Analysis



วิทยานิพนธ์นี้เป็นส่วนหนึ่งของการศึกษาตามหลักสูตรปริญญาวิทยาศาสตรดุษฎีบัณฑิต  
สาขาวิชาพยาธิชีววิทยาทางสัตวแพทย์ ภาควิชาพยาธิวิทยา  
คณะสัตวแพทยศาสตร์ จุฬาลงกรณ์มหาวิทยาลัย  
ปีการศึกษา 2564  
ลิขสิทธิ์ของจุฬาลงกรณ์มหาวิทยาลัย

Thesis Title	GENETIC CHARACTERIZATION AND STRAIN DIFFERENTIATION OF FELINE CALICVIRUS AMONG CAT POPULATION IN THAILAND BY HIGH RESOLUTION MELTING ANALYSIS
By	Miss Kannika Phongroop
Field of Study	Veterinary Pathobiology
Thesis Advisor	Associate Professor SOMPORN TECHANGAMSUWAN, DVM, MSc, Ph.D
Thesis Co Advisor	Professor ANUDEP RUNGSIPIPAT, Ph.D.

---

Accepted by the FACULTY OF VETERINARY SCIENCE, Chulalongkorn University in Partial Fulfillment of the Requirement for the Doctor of Philosophy

..... Dean of the FACULTY OF VETERINARY SCIENCE  
(Professor SANIPA SURADHAT, Ph.D.)

#### DISSERTATION COMMITTEE

..... Chairman  
(Associate Professor WIJIT BANLUNARA, Ph.D.)

..... Thesis Advisor  
(Associate Professor SOMPORN TECHANGAMSUWAN, DVM, MSc, Ph.D)

..... Thesis Co-Advisor  
(Professor ANUDEP RUNGSIPIPAT, Ph.D.)

..... Examiner  
(Associate Professor Dr. AUNYARATANA THONTIRAVONG)

..... Examiner  
(Instructor Dr. Kasem Rattanapinyopituk, D.V.M., M.Sc., Ph.D)

..... Examiner  
(Associate Professor Dr. Sirilak Surachetpong)

..... External Examiner  
(Associate Professor Dr. Jatuporn Rattanasrisomporn)

กรรมกร พงษ์รูป : ลักษณะทางพันธุกรรมและการวิเคราะห์แยกสายพันธุ์ของไวรัสคาลิซิ ในประชากรแมวของประเทศไทยโดยวิธีวิเคราะห์ด้วยวิธี High Resolution Melting Analysis. ( GENETIC CHARACTERIZATION AND STRAIN DIFFERENTIATION OF FELINE CALICIVIRUS AMONG CAT POPULATION IN THAILAND BY HIGH RESOLUTION MELTING ANALYSIS) อ.ที่ปรึกษาหลัก : รศ. สพ.ญ. ดร.สมพร เตชะงามสุวรรณ, อ.ที่ปรึกษาร่วม : ศ. น.สพ. ดร.อนุเทพ รังสีทิพัฒน์

ไวรัสคาลิซิในแมวเป็นที่รู้จักอย่างแพร่หลายว่าเป็นหนึ่งในไวรัสก่อโรคที่สำคัญซึ่งทำให้เกิดโรคของระบบทางเดินหายใจส่วนบนและโรคในช่องปากในแมว ในรอบสิบปีที่ผ่านมา ไวรัสคาลิซิสายพันธุ์รุนแรงซึ่งส่งผลให้อัตราการตายของแมวที่ติดเชื้อเพิ่มขึ้นนั้นได้มีรายงานการเกิดขึ้นทั่วโลกสูงขึ้นอย่างเห็นได้ชัด ในขณะที่การใช้วัคซีนสำหรับป้องกันและลดความรุนแรงของโรคมียังไม่แพร่หลายทั่วโลกและในแมวไทย อย่างไรก็ตามข้อมูลของความชุกและการศึกษาถึงลักษณะทางพันธุกรรมของไวรัสคาลิซิที่มีอยู่ในแมวไทยนั้นยังไม่เคยมีการรายงานอย่างเป็นทางการ ดังนั้น การศึกษาครั้งนี้จึงมุ่งที่จะให้เห็นภาพรวมของอุบัติการณ์และลักษณะทางพันธุกรรมของไวรัสคาลิซิในแมวที่หมุนเวียนอยู่ในแมวไทยในช่วงปี ค.ศ. 2016-2021 นอกจากนี้ผู้วิจัยได้มีการใช้เทคนิคการวิเคราะห์แบบไฮริโซลูชันเมลตติ้งเพื่อวินิจฉัยและคัดแยกสายพันธุ์ในปฏิกิริยาเดียวกัน และได้ทำการย้อมสีอิมมูโนฮิสโตเคมีร่วมกับใช้เทคนิคอินไซโตไฮบริดเคชัน เพื่อระบุการมีอยู่ของไวรัสในเนื้อเยื่อของแมวที่มีการติดเชื้อ ผลการศึกษาแสดงให้เห็นถึงอุบัติการณ์ของไวรัสคาลิซิในแมวไทยที่หมุนเวียนช่วงปีดังกล่าวเท่ากับร้อยละ 46.7 และความสัมพันธ์กับรอยโรคเหงือกอักเสบถูกแสดงให้เห็นด้วยค่าอัตราส่วนออกเท่ากับ 9.02 (95% CI: 2.61-30.46;  $p < 0.001$ ) สายพันธุ์ของไวรัสคาลิซิที่ตรวจพบจากการศึกษานี้ถูกจัดกลุ่มอยู่ในจีโนกรุ๊ป 1 และไม่พบการเกิดไวรัสลูกผสมของไวรัสคาลิซิในแมวไทย ทั้งนี้ทางผู้วิจัยสามารถได้มาซึ่งลำดับสารพันธุกรรมที่สามารถถอดรหัสได้อย่างสมบูรณ์ของไวรัสคาลิซิในแมวจากหนึ่งตัวอย่างศึกษา ที่มีการแสดงออกของอาการทางคลินิกสอดคล้องกับอาการที่ปรากฏในสายพันธุ์รุนแรง และเป็นสาเหตุให้เกิดการเสียชีวิตอย่างเฉียบพลัน นอกจากนี้ การศึกษานี้ยังสามารถพัฒนาเทคนิคการวิเคราะห์แบบไฮริโซลูชันเมลตติ้งที่สามารถแยกแยะระหว่างสายพันธุ์ของวัคซีน 2 ยี่ห้อที่ทางผู้วิจัยนำมาใช้เป็นตัวควบคุมบวก และ 5 สายพันธุ์ของไวรัสคาลิซิที่ไหลเวียนอยู่ตามธรรมชาติในแมวไทย ในการศึกษาครั้งนี้ทางผู้วิจัยได้ทำการเก็บตัวอย่างจากแมวที่เสียชีวิตแบบเฉียบพลันโดยแสดงอาการทางคลินิกก่อนเสียชีวิตสอดคล้องกับอาการที่แสดงออกของไวรัสคาลิซิสายพันธุ์รุนแรงโดยการตรวจสอบเบื้องต้นด้วยปฏิกิริยาลูกโซ่โพลีเมอเรสแบบย้อนกลับได้แสดงผลบวกต่อไวรัสคาลิซิในทุกเนื้อเยื่ออวัยวะ จากนั้นผู้วิจัยได้ทำการยืนยันตำแหน่งการมีอยู่และการกระจายตัวของไวรัสในเนื้อเยื่อต่าง ๆ โดยใช้เทคนิคอิมมูโนฮิสโตเคมี อินไซโตไฮบริดเคชัน และ การส่องดูด้วยกล้องจุลทรรศน์อิเล็กตรอนแบบส่องผ่าน เป็นที่น่าสนใจอย่างยิ่งว่านอกจากเซลล์เป้าหมายชนิดอีพิทีเลียมและเอ็นโดทีเลียมซึ่งมักพบการมีอยู่ของไวรัสเป็นปกตินั้น ในการศึกษาครั้งนี้ได้ตรวจพบแอนติเจนทั้งในรูปแบบโปรตีน จีโนม และการพบอนุภาคไวรัสในเซลล์ประสาทหลายชนิดในระบบประสาท แม้ว่าไวรัสคาลิซิจะมีได้ถูกบ่งชี้ว่าเป็นไวรัสที่ก่อโรคของระบบประสาทก็ตาม โดยสรุปจากการศึกษาในครั้งนี้ชี้ให้เห็นว่าการหมุนเวียนของไวรัสคาลิซิในแมวไทยยังคงมีอยู่ในระดับสูงแม้ว่าจะมีการใช้วัคซีนเพื่อควบคุมและลดความรุนแรงของโรคกันอย่างแพร่หลาย ดังนั้นการเฝ้าติดตามสายพันธุ์ที่สามารถต่อต้านวัคซีน และอาจมีความรุนแรงยิ่งขึ้นซึ่งอาจพัฒนาเกิดขึ้นใหม่ได้ยังคงมีความจำเป็น สุดท้ายนี้การศึกษาเชิงลึกเกี่ยวกับการติดเชื้อของไวรัสคาลิซิเข้าสู่เซลล์ของระบบประสาทยังคงต้องการการศึกษาวิจัยเพิ่มเติมเพื่อเข้าใจถึงกลไกทางพยาธิวิทยาได้ดียิ่งขึ้น

สาขาวิชา พยาธิชีววิทยาทางสัตวแพทย์

ปีการศึกษา 2564

ลายมือชื่อนิสิต .....

ลายมือชื่อ อ.ที่ปรึกษาหลัก .....

ลายมือชื่อ อ.ที่ปรึกษาร่วม .....

# # 5975501731 : MAJOR VETERINARY PATHOBIOLOGY

KEYWORD: melting analysis, cat, Feline calicivirus, Thai cats

Kannika Phongroop : GENETIC CHARACTERIZATION AND STRAIN DIFFERENTIATION OF FELINE CALICIVIRUS AMONG CAT POPULATION IN THAILAND BY HIGH RESOLUTION MELTING ANALYSIS.  
 Advisor: Assoc. Prof. SOMPORN TECHANGAMSUWAN, DVM, MSc, Ph.D Co-advisor: Prof. ANUDEP RUNGSIPIPAT, Ph.D.

Feline calicivirus (FCV) is widely known as one of the significant causative viral pathogens causing self-limited upper respiratory tract and oral disease in cats. In the last decade, severe FCV form, as named a virulent systemic feline calicivirus (VS-FCV), has distinctly emerged worldwide even though commercially available vaccines for FCV are typically used in Thai cats. However, the data of either prevalence or molecular characterization has never been officially noticed in Thailand. Thus, this study aimed to provide molecular epidemiology and characterization of the FCV circulating in Thai cats during 2016-2021. Moreover, the high-resolution melting analysis (HRM) is utilized for simultaneous detection and strain typing. Immunohistochemical staining (IHC) and in situ hybridization (ISH) were also performed for viral localization in tissues. Our results demonstrated FCV incidence circulating in Thai cats as 46.7% and associated with gingivostomatitis lesion with an odds ratio of 9.02 (95% CI: 2.61-30.46;  $p < 0.001$ ). The FCV Thai strains (FCV-THs) were clustered in genogroup I without any viral recombination evidence. One of our cases had shown clinical signs, likely VS-FCV, and became sudden death, and we could complete the whole genome coding sequence of these samples. Moreover, our study successfully validated the HRM technique that could segregate between two commercially available FCV vaccine strains and five wild-type FCV Thai strains within a single PCR reaction. Furthermore, the reverse-transcription polymerase chain reactions (RT-PCRs) disclosed positive results in various organ tissues in one VS-FCV dead cat, which represented related clinical signs of virulent strain. Afterward, IHC, ISH, and transmission electron microscopy (TEM) were performed to confirm the localization, distribution, and existence of viral pathogens. As known that target cells of FCV are epithelial and endothelial cells, interestingly, our findings represented FCV antigen either protein or genomic signal in the neuronal cells. This was confirmed the existing intranuclear virion by TEM. In conclusion, we suggested that FCV circulation in Thai cats is still on a big scale, even though the vaccination is widely used. So, monitoring emerging vaccine breakdown strains and possibly influencing the evolution undergone positive selection is still needed. Lastly, the insight study about FCV-associated neuropathy should be more investigated in further research

Field of Study: Veterinary Pathobiology

Academic Year: 2021

Student's Signature .....

Advisor's Signature .....

Co-advisor's Signature .....

## ACKNOWLEDGEMENTS

I am overwhelmed in all humbleness and gratefulness to acknowledge my depth to my principal advisor Assoc. Prof. Dr. Somporn Techangamsuwan, who gave me the golden opportunity to do this wonderful project and my co-advisor Prof. Dr. Anudep Rungsipipat for valuable guidance, support and encouragement to help me achieve my educational goal. I would like to express my appreciation to committee members, Assoc. Prof. Dr. Wijit Banlunara, Assoc. Prof. Dr. Siriluck Surachetpong, Assoc. Prof. Dr. Aunyaratana Thontiravong, Instructor Dr. Kasem Rattanapinyopitukand, and Assoc. Prof. Dr. Jatuporn Rattanasrisomporn, who provided valuable advices in this research project. In the deepest of my heart, I also appreciate to thank Dr. Chutchai Piewbang, Senior Postdoctoral fellowship, Department of Pathology, Faculty of Veterinary science, Chulalongkorn University, who have been accompany contributed in this studies especially the topic of pathological identification. I also deeply extend my thanks to the Small Animal Teaching Hospital, Faculty of Veterinary Science, Chulalongkorn University, Kasetsart University, and many private clinics in Thailand for providing samples. Moreover, I also would like to thank all CU-Vet Path's staff and my beloved lab mates who walk together even in the bad or good time and helped me a lot in finalizing this project within the limited time frame. Last but not least, I would like to thank Chiang Mai University for supporting the Doctoral Scholarship and The 90th Anniversary of Chulalongkorn University Fund (Ratchadaphiseksomphot Endowment Fund) for funding of my PhD project. Besides, I would like to dedicate this thesis to my parents, my husband and my son who always stand beside me and being the wind beneath my wing. Finally, I would like to thank myself for being patient and able to overcome many limitations until can do the impossible thing being a possible.

CHULALONGKORN UNIVERSITY

Kannika Phongroop

## TABLE OF CONTENTS

	Page
ABSTRACT (THAI).....	iii
ABSTRACT (ENGLISH).....	iv
ACKNOWLEDGEMENTS.....	v
TABLE OF CONTENTS.....	vi
LIST OF TABLES.....	xi
LIST OF FIGURES.....	xii
ABBREVIATIONS.....	14
CHAPTER I.....	16
Introduction.....	16
Importance and rationale.....	16
Literature reviews.....	18
Characterization and genome organization of Family Caliciviridae.....	18
Feline calicivirus (FCV).....	22
Genome characterization of FCV.....	22
Clinical finding of FCV infection.....	25
Host receptors of FCV.....	27
Pathogenesis and pathology of FCV.....	28
Diagnostic assays of feline upper respiratory virus.....	29
Melting curve analysis (MCA).....	30
High resolution melting analysis (HRM).....	31
Objectives of the study.....	33

Hypothesis.....	33
Conceptual Framework .....	34
Advantages of the study .....	35
CHAPTER II.....	36
Molecular Epidemiology and Strain Diversity of Circulating Feline Calicivirus in Thai Cats.....	36
Authors.....	36
Abstract.....	37
Introduction.....	38
Materials and Methods.....	41
Sample collection .....	41
Nucleic acid extraction and complementary DNA (cDNA) construction .....	41
FCV and FHV-1 detection using real-time polymerase chain reaction (qPCR)...	42
FCV genetic sequencing .....	44
Genetic characterization and phylogenetic analysis .....	44
Recombination and selective pressure analyses .....	45
Statistical analysis.....	45
Results.....	46
Incidence of FCV and FHV-1 detection circulating in Thai cats .....	46
Associations between FCV, FHV-1, and co-detection with clinical variables .....	47
Sequencing and phylogenetic analysis .....	48
Discussion .....	59
Conclusion.....	62
Acknowledgment .....	63



Ethics Statement.....	63
Data accessibility.....	63
Declaration of competing interest.....	64
CHAPTER III.....	65
Simultaneous Detection and Differentiation between Feline Calicivirus Vaccine and Wild-type Thai Strain in Clinical Samples Using .....	65
High-Resolution Melting Analysis.....	65
Abstract.....	67
Introduction.....	68
Materials and Methods.....	70
Sample collection, RNA extraction, and complementary DNA (cDNA) synthesis .....	70
Primer design.....	70
FCV screening detection.....	71
FCV vaccine strain preparation.....	74
Standard reference synthesis of FCV strains.....	74
RT-qPCR and HRM assay.....	76
Sensitivity and specificity evaluation of HRM assay .....	76
Efficacy to detect a mixed infection.....	77
Data analysis and interpretation.....	77
Result.....	77
FCV screening by RT-PCR .....	77
RT-qPCR and HRM assay.....	78
Sensitivity and Specificity evaluation .....	80

Efficiency in detecting the FCV mixed infection.....	81
Determination of the clinical sample.....	81
Discussion .....	87
Acknowledgment .....	89
Ethics Statement.....	90
Data accessibility.....	90
Declaration of competing interest.....	90
CHAPTER IV .....	91
Pathological Identification of Virulent Systemic Feline Calicivirus in Naturally Infected Cat revealed Neurotropism Aspect.....	91
Authors.....	91
Abstract.....	92
Introduction.....	93
Materials and Methods.....	95
Necropsied cats and sample collection .....	95
Samples preparation and feline viral detection by molecular technique .....	95
Sequencing and phylogenetic analysis .....	97
Histopathology .....	98
Immunohistochemistry (IHC) .....	98
Riboprobe preparation and <i>in situ</i> hybridization (ISH).....	99
Transmission electron microscopy (TEM) .....	100
Results.....	100
Sample collection and FCV molecular screening.....	100
Sequencing and phylogenetic analysis .....	103

Gross lesion and histopathology .....	104
Immunohistochemistry.....	107
<i>In situ</i> hybridization .....	109
Transmission electron microscopy.....	109
Discussion .....	111
Acknowledgment .....	113
Ethics Statement.....	113
Data accessibility.....	114
Declaration of competing interest.....	114
CHAPTER V .....	115
DISCUSSION AND CONCLUSION.....	115
General discussion.....	115
Limitation of the study and suggestion for the further study.....	117
Conclusion .....	118
APPENDIX.....	118
Supplementary data of Chapter II.....	118
REFERENCES .....	130
VITA.....	146

## LIST OF TABLES

	Page
Table 1 Primer sequences for feline calicivirus (FCV) and feline herpesvirus type-1 (FHV-1) detection and full-length FCV genome amplification .....	44
Table 2 Incidence of feline calicivirus (FCV), feline herpesvirus type-1 (FHV-1), and co-detection from 184 cats from different regions in Thailand during 2016-2021 .....	48
Table 3 The multinomial logistic regression analysis of variables associated with feline calicivirus (FCV) and feline herpesvirus-1 (FHV-1) detection from 184 cats in Thailand during 2016-2021 .....	50
Table 4 Deduced amino acid identity between 14 feline calicivirus Thai (FCV-TH) strains and other 43 FCV strains deposited in GenBank database .....	53
Table 5 Physicochemical property of remarkable amino acid residue position on hypervariable region E (HVR-E) of VP1 major capsid protein gene hypothesized to differentiate between classical FCV and VS-FCV pathotype .....	59
Table 6 Evidence of positive and negative selection using various detection methods .....	60
Table 7 Nucleotide sequence, position, and amplicon size of primers used in this study.....	74
Table 8 List of synthetic reference strains and wild-type Thai strain of feline calicivirus (FCV).....	76
Table 9 Linear regression model showing the relationship between % C:G of PCR product sequence and melting temperature deriving from HRM assay.....	79
Table 10 Mean melting temperature ( $T_m$ ) and standard deviation (SD) within the group of each feline calicivirus (FCV) strain detected from clinical samples .....	83
Table 11 Molecular screening result of feline viral pathogen and organs of detection .....	103

## LIST OF FIGURES

	Page
Figure 1 Cryo-electron microscope structure of Feline calicivirus (FCV). .....	20
Figure 2 Illustration demonstrates open reading frame (ORFs) and gene order in family Caliciviridae.....	21
Figure 3 Illustration of <i>Caliciviridae</i> members genome organization.....	22
Figure 4 Illustration of Feline calicivirus genomic organization.....	24
Figure 5 The genome mapping of feline calicivirus (FCV). modified from (Henzel et al., 2012).....	25
Figure 6 Structural of FCV major capsid protein, VP1.....	26
Figure 7 Fluorescent melting analysis.....	32
Figure 8 Intercalating dyes.....	33
Figure 9 Phylogenetic tree is constructed based on 33 complete nucleotide sequences of feline calicivirus (FCV).....	51
Figure 10 Phylogenetic trees of full-length VP1.....	54
Figure 11 Phylogenetic trees of P2 subdomain.....	55
Figure 12 Phylogenetic trees of Hypervariable E region (HVR-E).....	56
Figure 13 The multiple deduced amino acid sequence alignment of partial RNA dependent RNA polymerase (RdRp) protein (aa1615-1763).....	58
Figure 14 The multiple nucleotide alignment of partial RNA dependent RNA polymerase (RdRp) sequence (nucleotide position 5214-5343).....	73
Figure 15 Feline calicivirus (FCV) strain differentiation by melt curve analysis.....	80
Figure 16 Linear regression analysis of the relationship between % C:G content of PCR product and $T_m$ value.....	81
Figure 17 Analytical sensitivity of HRM assay.....	85

Figure 18 Analytical specificity of HRM assay.....	86
Figure 19 Analytical HRM assay of the mimetically mixed-infection model of FCV-TH strain (Wild type) and vaccine strain (FCV-Vac).....	87
Figure 20 RT-PCR results of Feline calicivirus (FCV) were determined using capillary electrophoresis (Qiaxcel®).....	104
Figure 21 Phylogenetic correlation of FCV from cat. no.1 (red circle) with distinct strains from the GenBank database.....	105
Figure 22 Gross lesion of cat no.1.....	106
Figure 23 Histological features of FCV were associated with numerous affected tissues by Hematoxylin & eosin staining (H&E).....	107
Figure 24 Feline calicivirus protein antigen was revealed by immunohistochemical (IHC) strain in various organs of cat no.1. ....	109
Figure 25 In situ hybridization (ISH) identified FCV genomic antigen in respiratory epithelial cells.....	111
Figure 26 In situ hybridization (ISH) signals indicated the FCV genome in various cells. ....	111
Figure 27 The ultrastructure of the mixed infected brain of cat no 1.....	112

## ABBREVIATIONS

3'HVR-E: 3' hypervariable region E  
 5'HVR-E: 5' hypervariable region E  
 Cons-E: conserve central region  
 FCGS: feline chronic gingivostomatitis  
 fJAM-A: feline junctional adhesion molecule A  
 FHV-1: feline herpesvirus-1  
 FNoV: feline norovirus  
 FCV: feline calicivirus  
 FCV-THs: feline calicivirus Thai strains  
 FCV-Vac: feline calicivirus vaccine strain  
 FURTD: Feline upper respiratory tract disease  
 gRNA: genomic RNA  
 HRM: High resolution melting analysis  
 IHC: Immunohistochemistry  
 ISH: In situ hybridization  
 LC: leader capsid  
 MCA: melting curve analysis  
 NTA: N-terminal arm  
 NTPase: 2C-like helicase  
 ORFs: Open reading frames  
 P: protrusion domain  
 PCR: polymerase chain reaction  
 PolyA: polyadenylated  
 Pro: 3C-like protease  
 RT-qPCR: reverse transcription-quantitative polymerase chain reaction  
 RdRp: RNA dependent RNA polymerase  
 S: shall domain  
 sgRNA: subgenomic RNA

TEM: Transmission electron microscope

T<sub>m</sub>: melting temperature

UTR: un-translation region

VPg: viral genome-linked protein

VP1: a major structural protein

VP2: a minor structural protein

VS-FCV: virulent systemic feline calicivirus





## CHAPTER I

### Introduction

#### Outline of the thesis

The dissertation is composed of five chapters. The first chapter starts with an overview of the thesis, including the general introduction, importance and rationale, objectives of the studies, review literature, and advantages of the studies. Chapter two to chapter four in the dissertation represent all the studies. Firstly, we provide the overview of molecular epidemiology and characterization of the feline calicivirus (FCV) circulating in Thai cats during 2016-2021. Then, the fashionable simultaneous diagnostic and strain differentiation technique is developed and validated in this study based on the principal knowledge of molecular characterization of FCV Thai strains (FCV-THs). Furthermore, viral pathogen localization, distribution, and existence are achieved by using various techniques, including immunohistochemistry (IHC), in situ hybridization (ISH), and transmission electron microscope (TEM). Finally, the last chapter will offer a general discussion and conclusion.

#### Importance and rationale

Feline upper respiratory tract disease (FURTD) is a complex disease typified by rhinotracheitis, conjunctivitis, gingivitis, stomatitis, and faucitis. Although there are several pathogens involved with FURTD, including bacteria and viruses, clinical signs are similarly revealed. Feline calicivirus (FCV) is recognized as one of the common viral pathogens of FURTD that cause acute feline respiratory problems and oral disease (Fernandez et al., 2017) The clinical features present in FCV infected cats are various, including rhinitis, conjunctivitis, stomatitis, glossitis, oral ulceration, and

pneumonia (Hurley and Sykes, 2003; Monne Rodriguez et al., 2018). Usually, the mortality rate of FCV infection is low, and recovery cats can become an asymptomatic carrier stage after recovering and shedding the virus for more than 30 days (Wardley, 1976; Hou et al., 2016). On the other hand, we occasionally recognize developing fatal pneumonia in the kitten (Monne Rodriguez et al., 2014; Caringella et al., 2019).

The common replication site of FCV is the oropharynx (Wardley, 1976), and most feline chronic gingivostomatitis (FCGS) cases show an association with the presence of FCV (Thomas et al., 2017). Interestingly, although the typical clinical sign and detection of FCV is respiratory tract and oral diseases, some publications have also identified the virus in fecal of healthy and diarrhea cats (Zhang et al., 2014). Moreover, the replication ability in the enteric tract of some FCV strains has been reported (Mochizuki, 1992; Radford et al., 2007), but the etiological role and pathogenesis are still unclear. Due to other viruses in different genera, but the same family of FCV, such as Norovirus, can cause gastrointestinal disease in humans. Recently, it has been demonstrated that FCV and feline norovirus (FNoV) infection are associated with acute diarrhea in kittens (Castro et al., 2015).

Genetic diversity leads to quasispecies virus evolution, especially RNA virus. Besides, the mortality rate of FCV infection is previously recognized as low (1-2%) (Wong et al., 2013). However, a severe clinical sign and a higher mortality rate raising to 60% have been published several times in the last ten years (Hurley et al., 2004; Prikhodko et al., 2014). Although the FCV vaccine seems likely to deduct the severity of classical signs of FCV infection, it does not show potency to protect the animal from either infection or reduce the clinical sign of virulence systemic FCV (VS-FCV) symptoms (Radford et al., 2007; Caringella et al., 2019). In addition, genetic characterization of this atypical FCV is studied and identified as an emerging FCV virulent strain (Meyer et al., 2011; Battilani et al., 2013). Moreover, recombination of

FCV has been reported both *in vitro* (Symes et al., 2015) and naturally-occurring recombinants (Coyne et al., 2006c).

The traditional and gold standard viral identification method is still a cell culture technique, but it is a time-consuming, laborious, and high-cost procedure. High resolution melting (HRM) analysis, in which the broadening application of real-time PCR, is a rapid, cost-efficient, and close-tube system that post-PCR processing is unnecessary (Marin et al., 2016). Moreover, HRM is widely used for simultaneous detection and typing pathogens in humans (Toi and Dwyer, 2008a; Tajiri-Utagawa et al., 2009) and animal field (Marin et al., 2016; Vaz et al., 2019). On the other hand, using the HRM technique for differentiation of FCV variant had never been documented.

Even though there are preliminary reports of FCV prevalence in Thailand (Phongroop et al., 2018a; Phongroop et al., 2018b), the genetic background of these have never been identified. Therefore, the genomic approach of FCV circulating in Thailand may be essential for understanding and surveillance strain diversity of FCV in Thai cats. Thus, developing a diagnostic technique that is less time-consuming, affordable advantage, and can perform both detection and typing pathogen simultaneously, such as the HRM technique, might be helpful.

## Literature reviews

### Characterization and genome organization of Family Caliciviridae

The *Caliciviridae* member can widely infect various animal species, such as humans, swine, marine mammals, lagomorphs, cattle, sheep, dogs, and cats. Pathogenic caliciviruses commonly cause signs in their specific host, including enteric, oral, respiratory, and systemic diseases (Maclachlan et al., 2016). The family *Caliciviridae* currently consists of eleven genera, including most members (7 genera) infect the mammals (*Lagovirus*, *Norovirus*, *Nebovirus*, *Recovirus*, *Sapovirus*, *Valovirus*,

and *Vesivirus*), two of genera infect birds (*Bavovirus*, *Nacovirus*). In addition, two genera infect fish (*Minovirus* and *Salovirus*) (Vinje et al., 2019). The members of the *Caliciviridae* family consist of a virus with a single-stranded, positive-sense RNA genome ranging from 6.4 to 8.5 kb (Vinje et al., 2019). The calicivirus virions are non-enveloped icosahedral capsid, 27-40 nm in diameter range (Figure 1) (Conley et al., 2019). The viral capsid consists of 180 copies of a single major structural protein (VP1) with 55-70 kDa, which is arranged in a T-3 icosahedral lattice (90 dimers) (Figure 1b).

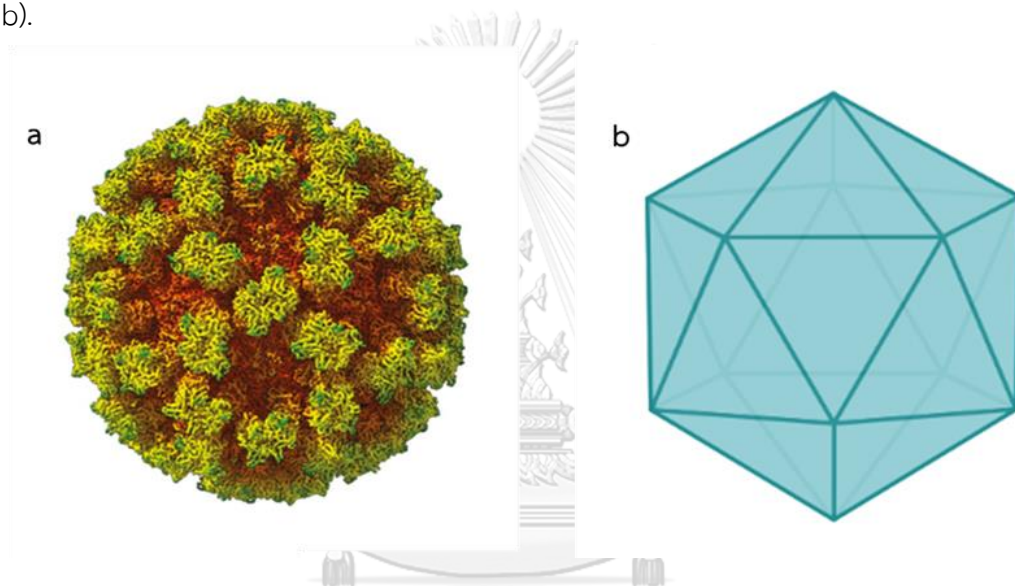


**Figure 1** Cryo-electron microscope structure of Feline calicivirus (FCV).

**a**, an icosahedral 3D reconstruction of FCV virion by the shells of capsid are shown in color orange and the outer faces of the protruding capsomeres are demonstrated in yellow and green (Conley et al., 2019). **b**, an illustration of T=3 icosahedral capsid gathers from 90 dimers of major capsid protein (VP1)

The calicivirus genome includes the nonstructural and structural proteins encoded by a different open reading frame (ORFs). The number of ORFs in the full-length genome of *Caliciviridae* members is established into 2-4 ORFs (Figure 2) (Vinje et al., 2019).

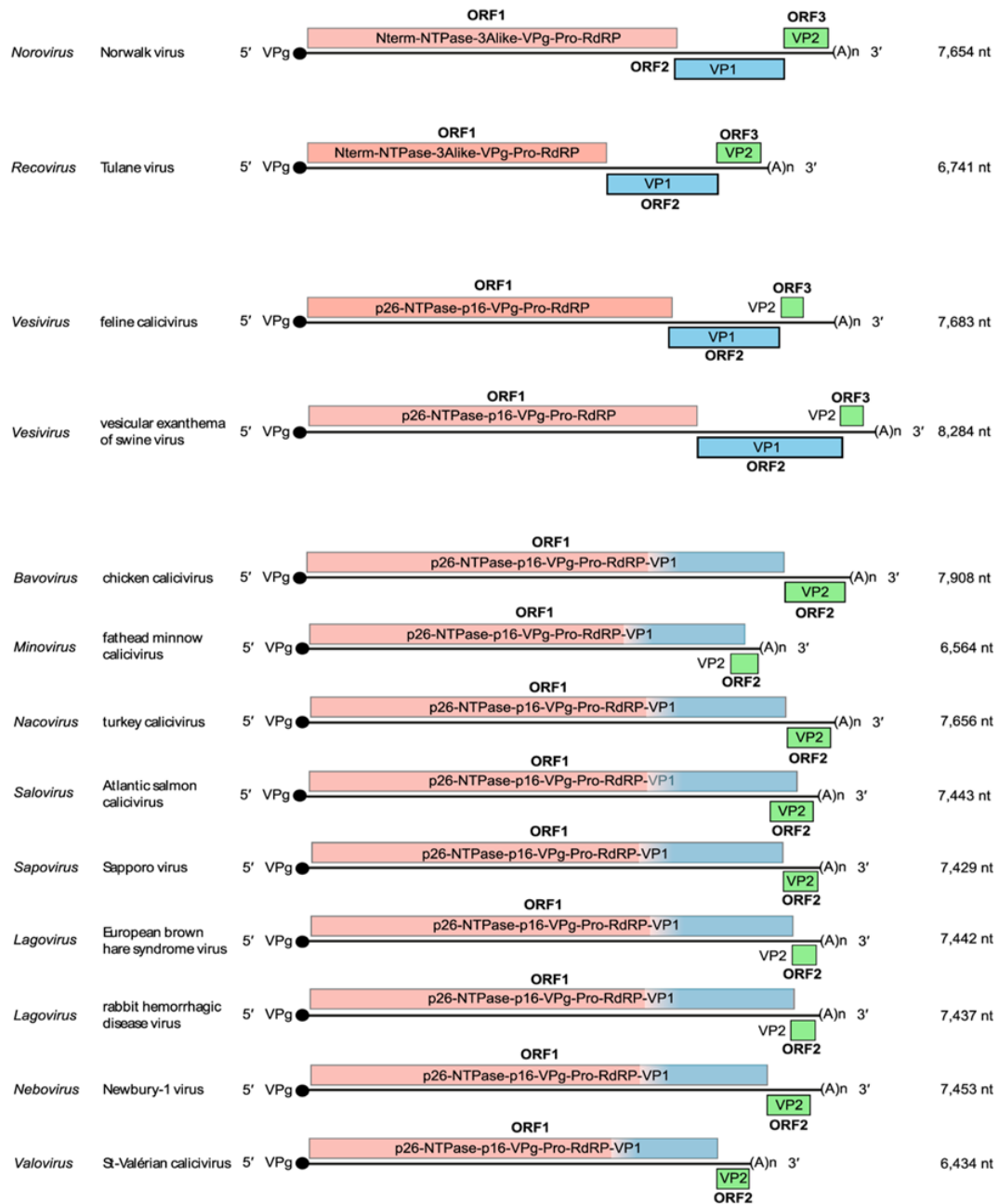


Figure 2 Illustration demonstrates open reading frame (ORFs) and gene order in family *Caliciviridae*.

The full-length genome of indicated genera is characterized as 2-4 ORFs with 6.5 – 8.3 kb (Vinje et al., 2019).

In all *Caliciviridae* members, a viral genome-linked protein (VPg), ranging 13-16 kDa, is covalently bound at 5' end, then followed with an un-translation region (UTR); meanwhile, the polyadenylated (PolyA) is following UTR and attached at the 3' end in both genomic RNA (gRNA) and subgenomic RNA (sgRNA) (Figure 3) (Vinje et al., 2019). Moreover, the transcription of 3' co-terminal sgRNA also occurs during infection, so the initial translations are driven by both calicivirus gRNA and sgRNA (Royall and Locker, 2016; Urban and Luttermann, 2020).

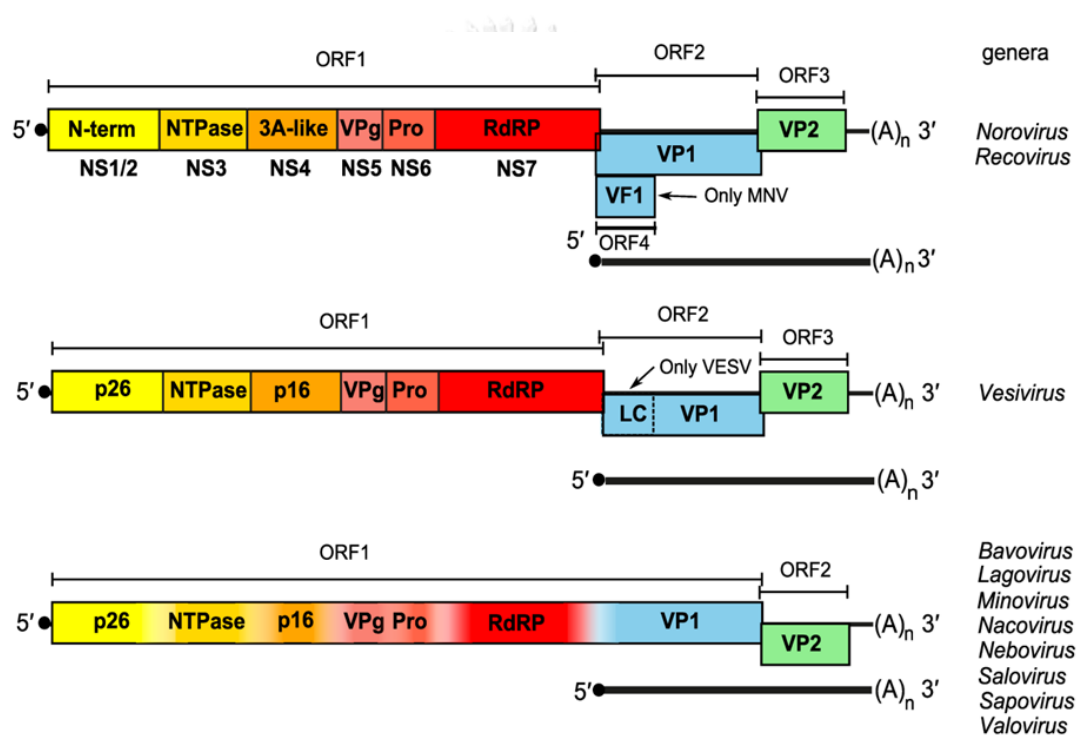


Figure 3 Illustration of *Caliciviridae* members genome organization.

VPg is covalently linked to the 5'-ends of both genomic and subgenomic RNAs and is displayed as a black circle (Vinje et al., 2019).

## **Feline calicivirus (FCV)**

### **Genome characterization of FCV**

FCV belongs to the genus *Vesivirus*, the family *Caliciviridae* (Weiblen et al., 2016). FCV is a small RNA virus with approximately 7.7 kb that can be separated into 3 ORFs, including ORF1, ORF2, and ORF3 (Figure 4) (Symes et al., 2015; Pereira et al., 2018; Smertina et al., 2019). ORF1, which is located at the 5' end of the genome, encodes the nonstructural proteins, whereas ORF2 encodes the leader capsid (LC) and the major capsid protein (VP1), and ORF3 encodes the minor structural protein (VP2) (Radford et al., 2007). Likely other viruses, ORF1 is the largest coding sequence of FCV and encode the polyproteins that can be post-translational cleaved as six nonstructural proteins containing p5.6, p32, 2C-like helicase (NTPase), p30, 3C-like protease (Pro), and RNA dependent RNA polymerase (RdRp), and VPg. In addition, RdRp plays an important key in being responsible for viral replication; moreover, it also can speed up the viral evolution cause of its error-prone nature (Smertina et al., 2019). Additionally, the evidence refers that the sequence identity between ORF1 and ORF2 is susceptible to be a majority recombination hot spot site of some *Caliciviridae* member; Noroviruses and Feline calicivirus, has been reported (Katayama et al., 2002b; Kojima et al., 2002; Symes et al., 2015).

A unique characteristic of *Vesivirus* members is that it has a translation initiation mechanism by using a LC as a precursor for the initial generator of the VP1 (Urban and Luttermann, 2020). Following the amino acid sequence alignment and antigenic analyses, the VP1 can be divided into six distinct regions (A to F), in which region A corresponds to the LC protein (Cubillos-Zapata et al., 2020)

The LC protein functionally acts as an essential element in viral spread by associated with cytopathic effect; meanwhile, the VP1 is responsible for capsid formation and reveals to correlate with the replication complex (Urban and Luttermann, 2020). Regions B, D, and F are relatively conserved, whereas regions C

and E are highly divergent among FCV isolates. Region E is the immunodominant region where further differentiated into 5' (5' HVR-E) and 3' hypervariable regions (3' HVR-E), split by a conserve central region (Cons-E) (Figure 5) (Radford et al., 1999; Neill et al., 2000). Importantly, it has been identified that the 5' HVR-E region played a role as an immunodominant region in which encoded major B-cell epitope being targeting for virus-neutralizing antibodies (Radford et al., 1999; Geissler et al., 2002; Pereira et al., 2018). Moreover, the high variation E region is commonly used for molecular study and differentiated FCV strain (Radford et al., 1998; Sato et al., 2002).

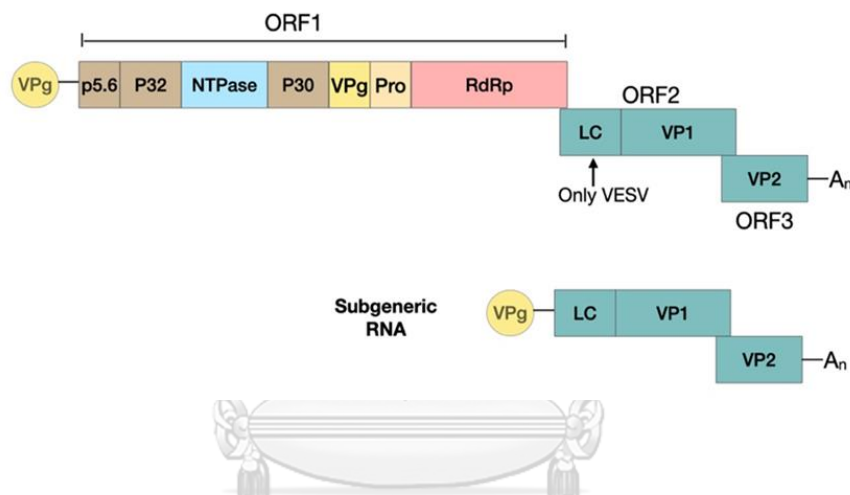
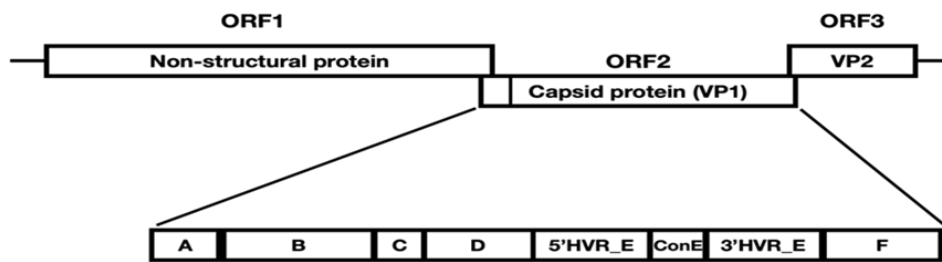


Figure 4 Illustration of Feline calicivirus genomic organization.

**a**, Genomic full-length RNA of about 7.5 kb contains three ORFs; ORF1 encodes a polyprotein that undergoes posttranslational cleavage into non-structural proteins; ORF2 and ORF3 encode the major and minor structural proteins (VP1 and VP2) respectively. **b**, Sub-genomic RNA of vesiviruses also encodes VP1, VP2, and a small leader of the capsid protein (LC). The coding sequences are demonstrated by color boxes that are flanked by untranslated sequences (lines). Circle shapes refer to the viral protein genome-linked (VPg) that is covalently bound to the 5' end of genomic and sub-genomic RNA.  $A_n$  substitute the polyA tail at the 3' end of genomic and sub-genomic RNA. (Modified from (Smertina et al., 2019))





**Figure 5** The genome mapping of feline calicivirus (FCV). modified from (Henzel et al., 2012)

The VP1 monomer contains three structural domains, including an N-terminal arm (NTA), a shell domain (S), and a protrusion domain (P) (Figure 6). The P domain is a flexible protruding part and further divided into P1 and P2 subdomains, by the latter subdomain located as a surface-exposed region of the viral capsid. Likewise, two distinct linear epitopes that have been recognized by neutralizing and non-neutralizing monoclonal antibodies were discovered at the outermost capsid surface (P2 subdomain) of VP1 within the 5' HVR-E region (Cubillos-Zapata et al., 2020). In addition, some amino acid residues, including 438, 440, 448, 452, and 492 of the HVR-E regions, had been significantly disclosed associated with VS-FCV pathotype variance (Brunet et al., 2019). However, a few studies have shown results that do not support the hypothesis that this amino acid property can differentiate between respiratory and VS-FCV pathotypes (Di Martino et al., 2020; Bordicchia et al., 2021).

The last FCV genome component, VP2 minor capsid protein, has a function to form a channel in the capsid via a portal-like assembly for transporting the viral genome to the cytoplasm of the host cell (Conley et al., 2019).

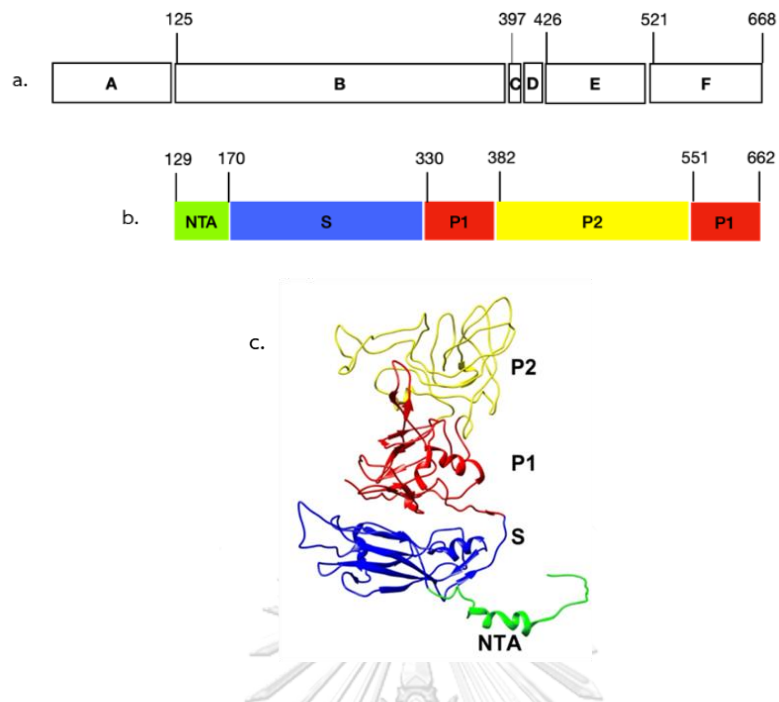


**Figure 6 Structural of FCV major capsid protein, VP1.**

a, Presentation of deduce amino acid region by A refer to leader capsid protein (LC) position. b, Display the infer amino acid position (Reference GenBank accession number AAA79324) of VP1 structural protein (NTA, N-terminal arm; S, a shell domain; P1 and P2, Protruding domain). c, Ribbon model refer to the VP1 protein structure (Protein Data Bank [PDB] accession number 3M8L) and the VP1 structural domains also demonstrate (Cubillos-Zapata et al., 2020).

### Clinical finding of FCV infection

FCV is recognized as one of the primary viral pathogens for FURTD. Most FCV-infected cats present either non-clinical symptoms (Uri, 2014) or acute respiratory disease and oral ulceration as the typical sign (Pesavento et al., 2008). Furthermore, many cats suffering from feline chronic gingivostomatitis (FCGS) are also associated with FCV infection (Thomas et al., 2017). Prevalence of FCV infection detecting in both household and shelter cats have been reported worldwide between 8% (Bannasch and Foley, 2005) to 50% (Schulz et al., 2015; Phongroop et al., 2018a), and

indistinct predisposing risk factor such as age, sex, and sterilization are demonstrated (Bannasch and Foley, 2005; Gourkow et al., 2013).

Classically, FCV-infected cats are characterized being self-limited infections and more rarely relative to sudden death (Gaskell et al., 2012). After recovery, infected cats mostly became the carriers by shedding the virus for more than 30 days (Wardley, 1976; Hou et al., 2016). In the last decade, the emerging highly virulent FCV strain, known as a virulent systemic disease (VS-FCV), was published continuously (Pesavento et al., 2004; Willi et al., 2016; Caringella et al., 2019). VS-FCV was firstly described when its outbreak in 1998 (Pedersen et al., 2000a). Clinical signs of VS-FCV were involved multiple organs, including subcutaneous edema, oral and cutaneous ulceration, mainly auricle and plantar pad (Pedersen et al., 2000a; Hurley et al., 2004). The mortality rate of VS-FCV highly reaches 50% (Hurley and Sykes, 2003). Radford et al. (Radford et al., 2009) represented that VS-FCV outbreak is usually initiated in the multi-cat community, resulting in rapid onset, spread, and high mortality (Radford et al., 2009). Although several data indicated that VS-FCV emerging had liberated from genetically distinct FCV strain (Coyne et al., 2006b; Reynolds et al., 2009; Schulz et al., 2011), assays to characterize genetic pattern to clarify the highly virulent FCV biotype had been unclear (Abd-Eldaim et al., 2005; Foley et al., 2006; Rong et al., 2006; Willi et al., 2016).

RNA viruses are acceptable to be the subject with rapid evolution, influenced by the poor proofreading of the RNA polymerase (Domingo et al., 1996). Caliciviruses are counted as viral families that show rapid evolution, resulting from intergenomic recombination (Posada et al., 2002). Many FCV publications have recognized the recombination both *in vitro* systems (Symes et al., 2015) and in endemically infected cat colonies (Coyne et al., 2006a; Symes et al., 2015). Interestingly, Symes et al. (Symes et al., 2015) have been noticed as a “hot spot” of recombination events

between ORF1 and ORF2 with a recombination rate of at least  $6.8 \times 10^{-6}$  single direction recombinant genomes per parental viral genome. In addition, the viral recombination may be potentially a consequence of viral evolution producing novel emerging strain, so understanding and monitoring the viral involvement is essential (Symes et al., 2015).

### Host receptors of FCV

Virus-receptor interaction is crucial in the disease's host range, tissue and cell tropism, and pathogenesis. The binding of the virus to the receptor at the cell surface is essential for triggering the downstream mechanism of viral infection. At the beginning of infection, FCV binds to the feline junctional adhesion molecule A (fJAM-A). Then, the conformation change in VP1 is initiated after receptor engagement for genome release after internalization (Conley et al., 2019). FCV passes into cells via clathrin-mediated endocytosis (Stuart and Brown, 2006). Endosomal acidification is an essential step for the viral entering process, even though the virus's mechanism evades the endosomal degradation and transports their genome into host cell cytosol is uncertain (Penaflor-Tellez et al., 2019).

fJAM-A has been identified as a functional receptor of FCV (Makino et al., 2006). Junctional adhesion molecules-A (JAMs-A) is a type I transmembrane glycoprotein containing two extracellular immunoglobulin (Ig) like domains, D1 and D2, a transmembrane domain, and a short cytoplasmic tail (Lu et al., 2018). It is usually found at the tight junctions of endothelial and epithelial cells and on platelets and leucocytes (Liu et al., 2000; Ebnet et al., 2004). The previous reports have suggested that the conserved surface residues on P2 subdomain on the capsid surface are a key for regulating fJAM-A interaction and downregulating the conformation changes.

These mechanisms seem likely to influence the kinetics of infection and virulence of different FCV isolates (Ossiboff et al., 2010; Lu et al., 2018).

### **Pathogenesis and pathology of FCV**

The incubation period of FCV infection is 2-6 days. In cats infected with less virulent virus strains, the lesions are usually limited within the upper respiratory tract, oral cavity, and conjunctiva. Additionally, oral ulceration begins as vesicles that quickly rupture; then, the recovery consumes the subsequent 2-3 weeks. Besides, oral ulceration is also characteristic of VS-FCV infections. They usually affect the tongue, gingiva, and hard palate; moreover, they work on the nasal cavity and skin epithelium. Lesions in the footpads range from mild hyperemia to sloughing of the entire pad (Maclachlan et al., 2016).

Moreover, subcutaneous edema, mainly on the head and limbs also involves (Monne Rodriguez et al., 2014). Interstitial pneumonia has developed in cats or kittens either infected with a virulent strain or co-infected with another feline respiratory virus, such as feline herpesvirus-1 (FHV-1) (Pesavento et al., 2004; Monne Rodriguez et al., 2014; Monne Rodriguez et al., 2018). Multiorgan necrosis, especially in the lung, liver, spleen, and pancreas, is occasionally noticed in VS-FCV infected cats (Pedersen et al., 2000b) by the antigen of the virions detected on both intranuclear and intracytoplasmic (Pesavento et al., 2004). Infection of endothelial cells with subsequent vascular injury potentially describes the striking facial and limb edema in cats with the systemic form of the disease.

In the last decade, detection of FCV in normal and clinical gastroenteritis has been frequently presented (Zhang et al., 2014; Castro et al., 2015; Di Martino et al., 2020). Moreover, the replication ability in the enteric tract of some FCV strains has been reported (Mochizuki, 1992; Radford et al., 2007), and there are some

suggestions that some FCVs strains may promote enteric tropism and ultimately serve as enteric pathogens (Di Martino et al., 2020). Thus, FCV should be considered a causative viral pathogen in the diagnostic algorithm of feline viral enteric diseases. Lastly, Although FCV is not a neurotropic virus, reports of FCV in the neuronal cell are also discovered (Battilani et al., 2013; Wardhani et al., 2021). However, the way to deliver the virus to neuronal cells is still poorly understood.

### **Diagnostic assays of feline upper respiratory virus**

Previously, FURTD was diagnosed by relying on clinical signs, epidemiological data, and medical data, which provided the least accuracy. However, using laboratory techniques for viral detection directly is precisely enhancing the accuracy of diagnosis (Weiblen et al., 2016). Nowadays, molecular diagnostic methods, either conventional polymerase chain reaction (PCR) or quantitative polymerase chain reaction (qPCR), are more frequently used to diagnose FCV due to its less expensive, less cumbersome, and rapid turn-around-time than traditional viral identification, such as viral isolation (Ruch-Gallie et al., 2011). However, conventional PCR assay cannot differentiate between the vaccine strain and natural strains of FCV (Maggs and Clarke, 2005). Therefore, the application of genome sequencing is usually additionally operated to verify between vaccine and field strain (Weiblen et al., 2016), especially has been utilized to identify vaccine outbreak strain (VBS) of FCV (Ohe et al., 2007).

In the last decade, qPCR application using melting curve analysis (MCA) has been utilized to differentiate genotype of viral sequence, by without probe, in the principle of different C:G ration given divergent melting temperature ( $T_m$ ). Helps et al. have ever differentiated 17 FCV strains from MCA of 60 PCR products (Helps et al., 2002). Moreover, Wilhem and Truyen had also presented the advantage of RT-qPCR

with MCA to detect genomic variation of different FCV isolates (Wilhelm and Truyen, 2006)

### **Melting curve analysis (MCA)**

MCA principally determines the dissociation of double-stranded DNA (dsDNA) during heating. Double-stranded DNA incorporated with saturated fluorescence will strongly present in the low-temperature situation of ending PCR reaction. When the temperature is raised in the melting analytical phase, dsDNA starts to separate by the temperature that 50% of DNA is denatured, known as the melting temperature ( $T_m$ ). In the denaturation phase, the fluorescence signal will decrease slowly at first. Then, the fluorescence signal will dramatically reduce at a particular temperature, indicating the melting of double-strand DNA inverts to single-strand DNA (Figure 7) (Reed et al., 2007). The melting temperature and characteristic pattern in the melting curve of amplified products are highly influenced by G:C content, length, and the nucleotide sequence (Marin et al., 2016). Therefore, the fluorescence reporter molecule is the key to detection in MCA by determining the total amount of accumulated DNA during DNA amplification (Mao et al., 2007).

Many DNA-binding dyes have been used for the application, including SYBR Green I, SYTO9, and others (Mao et al., 2007). SYBR Green is the most famous qPCR dye; however, it still has several disadvantages. One of the problems is that the limitation concentration,  $<0.5 \mu\text{M}$ , can use in the reaction due to their tendency to inhibit PCR reaction (Figure 8) (Giglio et al., 2003). Consequently, the new generation of saturated dyes has been developed for a better result to determine the single-base variant and others applicable of MCA.

### High resolution melting analysis (HRM)

High resolution melting analysis (HRM) is a DNA analysis technique which has been firstly introduced in 2002 (Reed et al., 2007). HRM is an extended analysis tool after the qPCR application, by it is a modern high-resolution MCA that uses novel saturated dye and high-resolution instrument (Reed et al., 2007). It principally determines the alteration of fluorescence saturating dye that does not inhibit PCR reaction after the PCR amplification. The melting profile of PCR products that are influenced by their G:C content, length, and genotyping variation have been utilized to study DNA structure and arrangement for many years (Vossen et al., 2009).

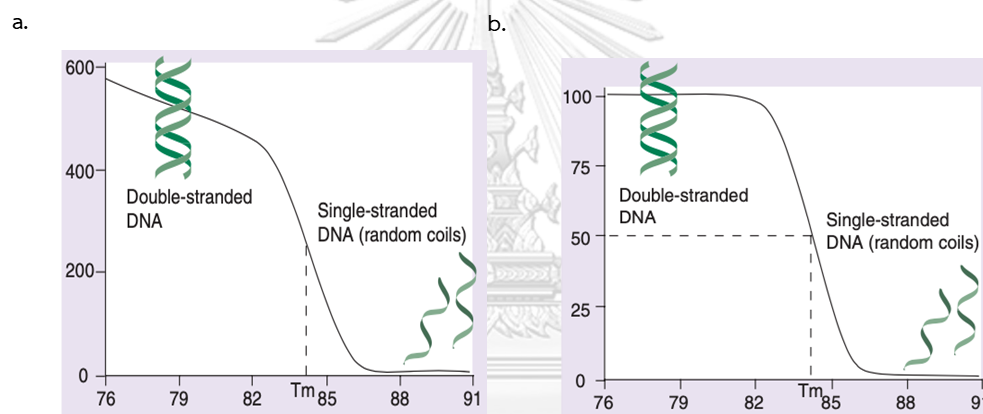


Figure 7 Fluorescent melting analysis.

**a**, the original fluorescence data presenting a linear decrease of signal at low temperature, then go along with a rapid reduction around the melting temperature ( $T_m$ ). The lowest fluorescence signal is revealed when the DNA is single stranded. **b**, the original fluorescence is normalized as 0 to 100 after background withdrawal (Reed et al., 2007)

Cause of the limitation of SYBER Green I that can inhibit PCR reaction and dye re-localization possible to occur during melting. Many saturated dyes, such as LCGreen®



and EvaGreen<sup>®</sup>, have been established for solving the problem. HRM can detect genotyping, even single base substitution modified sequence by dispensable fluorescence probe. HRM has been widely utilized in several manners, including mutation scanning, repeat typing, and genetic variants screening (Reed et al., 2007). In human medicine, HRM is an advantageous technique for simultaneous detection and pathogen genotyping differentiation. For example, in 2008, Toi and Dwyer had used an HRM application to detect single nucleotide polymorphism (SNP) and to differentiate between vaccine and wild-type varicella-zoster virus (VZV) strain (Toi and Dwyer, 2008a). Moreover, Tajiri-Utagawa et al. had developed HRM for routine detection and genotyping of Norovirus from clinical samples (Tajiri-Utagawa et al., 2009).

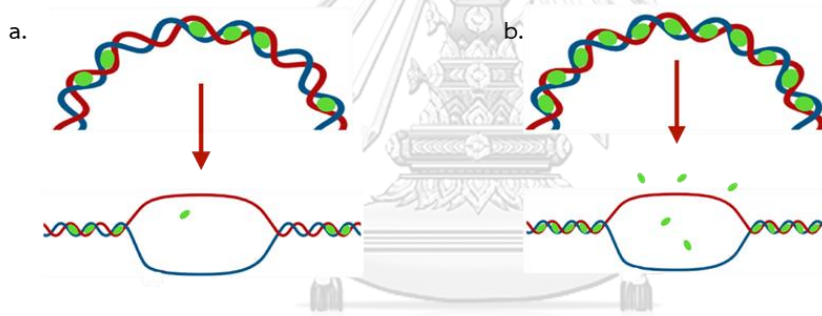


Figure 8 Intercalating dyes.

a, Nonsaturated intercalating dyes, e.g., SYBER Green I<sup>®</sup>; some dye molecules relocate as melting begins. b, Saturated intercalating dyes, e.g., EvaGreen<sup>®</sup>, the dye saturation leaves no room for relocation during melting.

Besides, HRM is also applied in veterinary medicine; it has been published the use of HRM for simultaneous detection and identification of Bovine herpesvirus type 1 (BoHV-1) and 5 (BoHV-5) both *in vivo* and clinical samples (Marin et al., 2016). Furthermore, Vaz et al. (Vaz et al., 2019) have applied this technique in a molecular

epidemiological study of 810 koalas. Two Koala gammaherpesviruses, phascolarctid gammaherpesviruses 1 and 2 ( PhaHV-1 and PhaHV-2 ), had been detected, discriminated, and shown viral prevalence and clinical association in this study (Vaz et al., 2019). Moreover, this application is also utilized in companion animals for detection and differentiation between canine parvovirus and feline parvovirus (Sun et al., 2019). In addition, HRM seems likely simplicity, rapid, inexpensive closed-tube format, satisfying sensitivity, and specificity. Thus, this technique is a proper method for diagnosis and molecular epidemiological study of feline upper respiratory viruses.

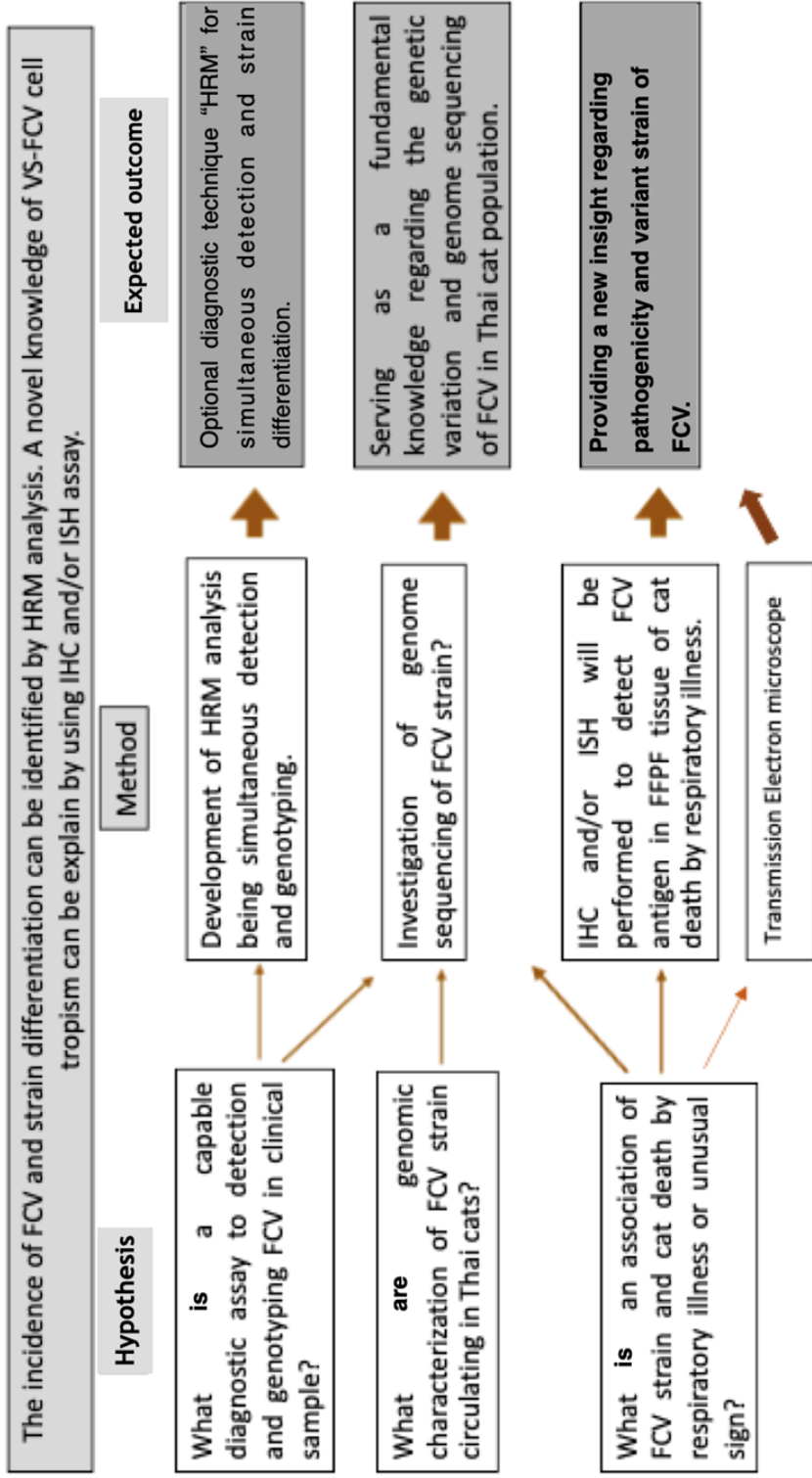
#### Objectives of the study

1. To determine the incidence of feline calicivirus circulating in Thai cats during 2016-2021.
2. To investigate the molecular characterization and diversity of circulating FCV strains in Thai cats and identify the strain variability between FCV-TH strains and previously known sequence strains deposited in the database.
3. To establish HRM assay for concurrent diagnosis and strain differentiation, either FCV vaccine strain (FCV-Vac) and wild-type FCV-THs and between wild-type FCV-THs from a clinical sample.
4. To localize viral protein, genomic antigen, and virion for determination cell tropism of VS-FCV circulating in Thai cats using immunohistochemistry (IHC), *in situ* hybridization (ISH), and transmission electron microscopy (TEM).

#### Hypothesis

FCV circulating in Thai cats can be simultaneously detected and differentiated strain using a high-resolution melting analysis application. In addition, a novel knowledge of cell tropism of VS-FCV can be disclosed by using IHC, ISH, and TEM assay.

Conceptual Framework



### Advantages of the study

1. Establishment of HRM assay as rapid, simultaneous detection and differentiated strain typing of FCV circulation in Thai cats.
2. Serving as a fundamental knowledge regarding the genetic variation and whole-genome sequence of FCV in Thailand.
3. Acquirement of the current epidemiological and genetic diversity of FCV in Thai cats.
4. Establish ISH techniques to understand better cell tropism of VS-FCV infection in Thai cats.



## CHAPTER II

Molecular Epidemiology and Strain Diversity of Circulating Feline Calicivirus in  
Thai Cats**Authors**

Kannika Phongroop, Chutchai Piewbang, Somporn Techangamsuwan

Department of Pathology, Faculty of Veterinary Science, Chulalongkorn University,  
Pathumwan, Bangkok 10330 Thailand, Animal Virome and Diagnostic Development  
Research Group, Faculty of Veterinary Science, Chulalongkorn University, Bangkok  
10330, Thailand

Anudep Rungsipipat

Department of Pathology, Faculty of Veterinary Science, Chulalongkorn University,  
Pathumwan, Bangkok 10330 Thailand

Jatuporn Rattanasrisomporn

Companion Animal Clinical Sciences, Faculty of Veterinary Medicine, Kasetsart  
University, Bangkok 10900, Thailand

Sahatchai Tangtrongsup

Department of Companion Animal and Wildlife Clinic, Faculty of Veterinary Medicine,  
Chiang Mai University, Chiang Mai 50100, Thailand

Publication status: in preparation

## Abstract

Feline calicivirus (FCV) is one of the major viral pathogens causing upper respiratory tract and oral diseases in cats. Virulent systemic feline calicivirus (VS-FCV) variant has been consistently reported worldwide in the last decade. This study aimed to determine molecular epidemiology, characterization, and diversity of circulating FCV strains in Thai cats. Nasal, oropharyngeal, and rectal swabs from 184 cats from various regions were collected to investigate the incidence of FCV and feline herpesvirus-1 (FHV-1) infection from 2016 to 2021 using reverse transcription real-time polymerase chain reaction. The overall incidence of FCV, FHV-1, and co-infection of both viruses was 46.7% (86/184), 65.8% (121/184), and 31.5% (58/184), respectively. The association between singly FCV infection and the presentation of gingivostomatitis lesion was shown with an odds ratio (OR) of 9.02 (95% CI: 2.61-30.46;  $p < 0.001$ ). Moreover, the vaccination displayed well protectability to only FCV infection (OR: 0.31, 95% CI: 0.10-0.93;  $p = 0.036$ ). Amino acid sequence analysis of the VP1 major capsid protein of 14 FCV-Thai (FCV-TH) strains revealed that they could be segregated as 14 strains with a genetic distance between 0 – 86.6%. The evidence of physicochemical amino acid criteria like VS-FCV strain was recognized from three samples (KP100, KP103, and KP105) derived from kittens with mild respiratory illness, which was incompatible with the previous report. Interestingly, one FCV-TH strain (KP339) showed phylogenetically related to vaccine strains based on full-length VP1, P2 subdomain, and hypervariable region E. So, the geographic region where the high number of circulating FCV detected might result in their rapid response to selective environmental force. Lastly, the evolutionary vaccine strain for FCV protection should be further investigated in Thai cats to find the most effective FCV prevention and control protocol.

**Keywords:** Cats, Feline calicivirus, Phylogenetic analysis, Physicochemical property, Strain diversity, Thailand

## Introduction

Feline calicivirus (FCV) is one major viral pathogen causing feline upper respiratory tract disease (FURTD) and oral disease in cats. The typical clinical signs of FCV infection are sneezing, nasal and ocular discharge, conjunctivitis, and oral diseases, such as tongue ulceration, glossitis, gingivostomatitis, and faucitis. Although FCV-infected cats generally reveal a mild to a moderate symptom and can be self-limiting, FCV infection associated with severe pneumonia, abortion, and acute febrile lameness syndrome has been occasionally noticed (Dawson et al., 1994; Gaskell et al., 2012). Furthermore, the lethal form of severe systemic FCV infection, named virulent systemic FCV (VS-FCV), has been consistently reported worldwide (Hurley et al., 2004; Pesavento et al., 2004; Abd-Eldaim et al., 2005; Coyne et al., 2006b; Guo et al., 2018; Caringella et al., 2019). The target cells of VS-FCV are both epitheliotropic and endotheliotropic, which commonly induce epithelial cytolysis and systemic vascular disruption and result in the clinical presentations of severe generalized edema and ulcerative dermatitis with a high mortality rate (Hurley et al., 2004; Vinje et al., 2019).

FCV belongs to the family *Caliciviridae*, which comprises seven genera that infect mammals, including *Lagovirus*, *Norovirus*, *Nebovirus*, *Recovirus*, *Sapovirus*, *Valovirus*, and *Vesivirus* (Vinje et al., 2019). FCV is a member of the genus *Vesivirus*; its genome is characterized as a positive-sense, single-stranded, non-enveloped RNA virus with approximately 7.6-7.7 kb (Prikhodko et al., 2014; Vinje et al., 2019; Cubillos-Zapata et al., 2020). FCV genome contains three major open reading frames (ORFs); ORF1 encodes the nonstructural protein, ORF2 encodes for the leader capsid (LC) and VP1 major capsid protein, and ORF3 encodes for the VP2 minor capsid protein.

The ORF1 is located at the 5' end of the genome. It mainly encodes a polyprotein that has undergone post-translational cleavage into six nonstructural

proteins (p5.6, p32, 2C-like helicase (NTPase), p30, 3C-like protease (Pro), and RNA dependent RNA polymerase (RdRp)), and a viral protein (VPg, for “virion protein, genome-linked”) (Smertina et al., 2019). The RdRp plays a primary role as a protein being accountable for viral replication and can also drive viral evolution owing to its error-prone nature (Smertina et al., 2019). In FCV, sequence identity between the RdRp and structural protein-coding region (ORF2) is also focused as a majority recombinant hot spot site (Symes et al., 2015).

As a unique genetic feature of *Vesivirus* members, the ORF2 predominantly encodes a unique VP1 protein that is translated as a precursor protein and then cleaved by viral protease, resulting in LC protein and VP1 major capsid protein (Sosnovtsev et al., 1998; Abente et al., 2013; Urban and Luttermann, 2020). Following the amino acid and antigenic analyses, the ORF2 can be divided into six distinct regions (A to F), in which region A corresponds to the LC protein (Cubillos-Zapata et al., 2020). The LC protein functionally acts as a crucial element in viral spread by associated with a cytopathic effect. Meanwhile, the VP1 is accountable for capsid formation and has been shown to correlate with the replication complex (Urban and Luttermann, 2020). Regions B, D, and F are relatively conserved, whereas regions C and E are highly divergent among FCV isolates. Region E is an immunodominant region where further differentiated into 5' (5' HVR-E) and 3' hypervariable regions (3' HVR-E), split by a conserve central region (Cons-E) (Radford et al., 1999; Neill et al., 2000).

On the other hand, the VP1 monomer is composed of three structural domains, including an N-terminal arm (NTA), a shell domain (S), and a protrusion domain (P) (Neill et al., 2000). The P domain is further divided into P1 and P2 subdomains, by the latter subdomain located as a surface-exposed region of viral capsid (Cubillos-Zapata et al., 2020). Likewise, two distinct linear epitopes that have



been recognized by neutralizing and non-neutralizing monoclonal antibodies were discovered at the outermost capsid surface (P2 subdomain) of VP1 within the 5' HVR-E region (Cubillos-Zapata et al., 2020). Recently, the physicochemical properties of amino acid residue at positions 438, 440, 448, 452, and 492 of the HVR-E regions had been significantly disclosed to be associated with VS-FCV pathotype variance (Brunet et al., 2019). The last FCV genome component, VP2 minor capsid protein, can form a channel in the capsid via a portal-like assembly to transport the viral genome to the host cell's cytoplasm (Conley et al., 2019).

FCV has continuously been mentioned being a highly variable RNA virus possessing genetic heterogeneity (Coyné et al., 2012; Hou et al., 2016). Nevertheless, it has still been declared that having a single diverse serotype (Ohe et al., 2007; Afonso et al., 2017). Furthermore, although many publications have represented vaccine cross-reactivity (Kalunda et al., 1975; Povey and Ingersoll, 1975; Poulet et al., 2000; Smith et al., 2020), commercial vaccines are widely available in several different strains (Addie et al., 2009), and the broader use of vaccines worldwide raises the hypothesis about the evolution of vaccine-resistant strain (Afonso et al., 2017). While some studies show the contrary idea (Smith et al., 2020), some reports also display evidence of vaccination failure (Radford et al., 1997; Ohe et al., 2007). In Thailand, feline vaccination protocol commonly follows the American Animal Hospital Association (AAHA) and the American Association of Feline Practitioners (AAFP) guideline (Stone et al., 2020), and both inactivated and attenuated live forms of feline rhinotracheitis virus (caused by FCV and feline herpesvirus type-1 (FHV-1)) vaccine are available. However, although those vaccines are widely used in Thai cats, the detection rate of FCV is still higher than 50% (Phongroop et al., 2018b). In addition, molecular characterization of circulating FCV strains in Thailand is relatively limited (Phongroop et al., 2018a). Therefore, this study aimed to determine molecular epidemiology, genetic and amino acid characterizations, and diversities of

circulating FCV strains in Thai cats. Moreover, identification of genetic variability and relationship between FCV Thai strains (FCV-TH) and other strains deposited in the database, including vaccine strains, were also inspected.

## Materials and Methods

### Sample collection

The experiment was designed as a cross-sectional study with convenient randomized sampling in 184 feline patients, either clinically healthy (n= 53) or with clinical signs (n= 131) of FURTD and oral diseases, from different regions in Thailand during 2016-2021. Signalments including age, vaccination history within one year, and presented respiratory and oral clinical signs were recorded for further analysis. Nasal swab, oropharyngeal swab, and rectal swab were collected individually from each cat, immersed separately in 1% sterile phosphate buffer saline (PBS), and then stored at  $-80^{\circ}\text{C}$  until processing. All procedures were authorized by the Chulalongkorn University Animal Care and Use Committee (No. 1631002).

### Nucleic acid extraction and complementary DNA (cDNA) construction

QIAamp<sup>®</sup> *cador* Pathogen Mini Kit (Qiagen GmbH, Germany) was used for viral genomic extraction. Briefly, the mixture of 200- $\mu\text{l}$  sample solution, 100- $\mu\text{l}$  buffer VXL and 20- $\mu\text{l}$  proteinase K was prepared and incubated for 15 min at room temperature. Afterward, the protocol was conducted following the manufacturer's recommendation. The concentration of extracted nucleic acid was quantified and qualified using a NanoDrop Lite Spectrophotometer (Thermo Fisher Scientific Inc., Waltham, MA, U.S.A.) and then kept at  $-80^{\circ}\text{C}$  until used. For reverse transcription (RT), cDNA was constructed using an Omniscript<sup>®</sup> RT Kit (Qiagen GmbH, Hilden,

Germany) according to manufacturer's guidelines, and cDNA products were stored at  $-20^{\circ}\text{C}$  until assayed (Chaiyasak et al., 2020).

### **FCV and FHV-1 detection using real-time polymerase chain reaction (qPCR)**

cDNA products (for FCV) and extracted nucleic acids (for FHV-1) were investigated using qPCR and specific primers that were self-designed by targeting the ORF1 gene (FCV\_NS F2/R2 for FCV) and glycoprotein B (gB) gene (FHV-gB F/R for FHV-1) (Table 1). The qPCR reaction was conducted using KAPA SYBR<sup>®</sup> FAST qPCR Master Mix (2X) KIT (KAPA BIOSYSTEM, Sigma-Aldrich<sup>®</sup>, Modderfontein, South Africa) according to manufacturer's instruction. All samples were run in duplicate operating by Rotor-Gene<sup>®</sup> Q (Qiagen GmbH, Manheim, Germany). The cycling conditions were composed of an initial denaturation at  $95^{\circ}\text{C}$  for 3 min, 40 cycles at  $95^{\circ}\text{C}$  for 3 sec,  $60^{\circ}\text{C}$  for 20 sec, and  $64^{\circ}\text{C}$  for 20 sec. The melting analysis was further analyzed using Rotor-Gene Q software version 2.3.1 (Qiagen GmbH, Manheim, Germany). Moreover, a limit of detection (LoD) of the qPCR assay was determined by employing a 10-fold serial dilution of string DNA fragment synthesis as a template (Thermo Fisher Scientific<sup>®</sup>, MA, USA) with the concentration ranging from  $6.2 \times 10^1$  to  $6.2 \times 10^8$  copies/ $\mu\text{l}$ . Other known feline viral pathogens, including feline morbillivirus (FeMV), feline bocavirus (FBoV), feline leukemia virus (FeLV), and feline immunodeficiency virus (FIV), were also tested to validate the specificity of the qPCR (Chaiyasak et al., 2020; Chaiyasak et al., 2021; Wardhani et al., 2021).

According to the qPCR result, the positive samples of FCV and FHV-1 (amplicon sizes as 121 bp and 176 bp, respectively) were resolved in 2% (w/v) gel electrophoresis, purified using NucleoSpin Extract II kit (Macherey Nagel, Düren,

Germany) and submitted for commercial bi-directional Sanger's sequencing (Macrogen Inc., Incheon, South Korea) to verify the presence of FCV and FHV-1.

**Table 1** Primer sequences for feline calicivirus (FCV) and feline herpesvirus type-1 (FHV-1) detection and full-length FCV genome amplification

<b>Primer name</b>	<b>Direction</b>	<b>Primer Sequence (5'- 3')</b>	<b>Nucleotide position<sup>1</sup></b>
FCV_NS F1	Forward	GTAAAAGAAATTTGAGACAATGTCT	1
FCV_NS R1	Reverse	TGTTGATTGGCGGGTAG	2439
FCV_NS F2	Forward	GAACTACCCGCCAATCA	2429
FCV_NS R2	Reverse	AGCACRYCATATGCGGC	2550
FCV_NS F3	Forward	TGGTGYAAGGAGTATGTC	1931
FCV_NS R3	Reverse	TCCACCATGATCTAAATTTTACTGCA	3098
FCV_NS F4	Forward	TGCAGTAAAATTTAGATCATGGTGGA	3073
FCV_RdRp F1	Forward	TATGGTGATGATGGWGTKTAYATGTT	4778
FCV_RdRp F2	Forward	GGYGTGGAGGCGCGGWC	5237 <sup>2</sup>
FCV_VP1 F1	Forward	ATGTGCTCAACCTGCGCTAACG	5314
FCV_RdRp R	Reverse	CGTHAGCGCAGGTTGAGCACAT	5335 <sup>2</sup>
FCV_VP1 F2	Forward	CCCTCAYGTTCTATTTGATGCT	6066
FCV_VP2 R	Reverse	TGTRTATGAGTAAGGGTCAACC	7568
FHV_gB F	Forward	CTCGATGGCCCTAGAACGTC	60008 <sup>2</sup>
FHV_gB R	Reverse	AGTCATTGAGGGCACGGAAG	60183 <sup>2</sup>

<sup>1</sup> Nucleotide position based on Accession no. L40021 (for FCV) and MH070336 (for FHV-1)

<sup>2</sup> Primers used for FCV and FHV-1 detection

### FCV genetic sequencing

Selected FCV positive samples were subsequently conducted for multiple RT-PCR amplification to obtain the full-length genome sequence (n= 1), partial RdRp gene sequences (n= 13), full-length VP1 major capsid protein gene (n= 13), and VP2 minor capsid protein gene (n= 13). Degenerated primer sets were designed based on multiple alignments of various global strains of the FCV genome published on the GenBank database (Table 1). Briefly, the RT-PCR reactions were processed employing Qiagen<sup>®</sup> OneStep RT-PCR kit (Qiagen, Hilden, Germany) in a reaction volume of 50  $\mu$ l, constituting of a mixture of QIAGEN OneStep RT-PCR Enzyme Mix, 10mM of dNTP in 5x QIAGEN OneStep RT-PCR Buffer, 10  $\mu$ M final concentration of each primer and 10  $\mu$ l of the template. Thermocycler conditions included 50<sup>o</sup>C for 30 min for the RT step, and an initial denaturation at 95<sup>o</sup>C for 15 min, followed by 40 cycles of 94<sup>o</sup>C for 10 sec, 58<sup>o</sup>C for 1 min and 72<sup>o</sup>C for 2 min, then a final extension at 72<sup>o</sup>C for 10 min. The PCR products were visualized using 1% (w/v) gel electrophoresis, purified and submitted for Sanger sequencing as mentioned above.

### Genetic characterization and phylogenetic analysis

The acquired nucleotide sequences of FCV-TH strains were assembled and compared with former published FCV strains retrieved from the GenBank database, including Urbana strain (Accession no. L40021) as a reference strain using BioEdit Sequencing Alignment Editor Version 7.2.5. The evolutionary analysis and pairwise genetic distance were estimated by MEGA X (Kumar et al., 2018) and inferred using the maximum likelihood (ML) method. The dendrogram of genetic relationship was established according to the Bayesian information criterion with 1000 bootstrapped replicates, and bootstrap values were significantly considered when greater than 70. Substitution models of the evolutionary tree were selected based upon the best fit

model of both substitution types; nucleotide or amino acid sequence, and sequence regions, including whole genome sequence, partial RdRp gene, full-length VP1 gene, P2 subdomain, HVR-E region, and VP2 gene. Derived dendrograms were drawn using FigTree v. 1. 4. 4. Twenty percent genetic distance threshold between capsid sequences was consumed to define the distinct strains (Radford et al., 2001b; Prikhodko et al., 2014; Hou et al., 2016)

### **Recombination and selective pressure analyses**

The capability of recombination site in full-length VP1 gene of FCV-TH strains was identified using the Recombination Detection Program (RDP) version 4.0. Any analytical methods, including RDP, GENECONV, BootScan, MaxChi, Chimaera, SiScan, and 3Seq, had proceeded with default setting on the alignment of full-length VP1 gene of FCV sequence. The significant recombination events were noted when more than four positive analytical methods were illustrated. To determine the mechanism underlying the genetic diversity of the FCV-TH strain, the evidence of positive selection was authenticated using the codon-based approach in the Datamonkey webserver (Pond and Frost, 2005). Single-likelihood ancestor counting (SLAC), Fixed-effects likelihood (FEL), Mixed Effect Model Evolution (MEME), and Fast Unconstrained Bayesian AppRoximation (FUBAR) algorithms were applied with accepted significance at the  $p$ -value  $\leq 1$ .

### **Statistical analysis**

Overall incidences of FCV and FHV-1 detection on each region in Thailand were demonstrated as descriptive analysis. In addition, the association between FCV and FHV-1 detection and clinical presentations (respiratory and oral diseases) and vaccination history was evaluated using Fisher's exact or Pearson chi-square test. The

multinomial logistic regression model was used to estimate odds ratios (OR) and 95% confidence intervals (95% CI) of associated variables. The statistical significance was set as  $p < 0.05$  for considerable variables related to FCV and FHV-1 detection. All statistical analyses were performed using STATA statistical software release 16.1 (Stata Corp., College Station, Texas, USA).

## Results

### Incidence of FCV and FHV-1 detection circulating in Thai cats

The specimens were derived from 184 cats from various provinces, including healthy cats at 28.8% (53/184), cats with respiratory illness 60.3% (111/184), and gingivostomatitis lesion at 22.8% (42/184), in which 12% (22/184) of ill cats presented both clinical signs.

Of 184 cats, the incidence of FCV detection was found at 46.72 (85/184) of FHV-1 at 65.8% (121/184) and co-detection at 31.5% (58/184) utilizing qPCR assays determining at Ct value less than 35 (Table 2). From all 184 cats, the samples consisted of 138 samples of the nasal swab (NS), 159 samples of the oropharyngeal swab (OS), 36 samples of the rectal swab (RS), 1 sample of pleural effusion (PE), and 21 fresh tissue samples (FTS) (Supplementary Table S1). FCV had shown positive results from NS, OS, RS, PE, and FTS as 35.51% (49/138), 46.54% (74/159), 5.56% (2/36), 0 (0/1), and 19.05% (4/21) respectively. Besides, FHV-1 also presented positive from NS, OS, RS, PE, and FTS as 42.03% (58/138), 57.23% (91/159), 33.33% (12/36), 0 (0/1), and 61.9% (13/21) respectively. The age of studied cats ranged from 1–154-month-old. Cats receiving the vaccination against FCV and FHV-1 within a year at sampling time were accounted for 50.5% (93/184) (Supplement Table S1). The distribution of FCV detection from each region in Thailand was shown in Table 2.

Interestingly, a FCV PCR-positive cat (no. 158) showed clinical signs like the VS-FCV infection, including generalized edema, ulcerative dermatitis at the upper lip, and severe acute respiratory illness (Supplement table S1, Supplementary figure S1).

**Table 2** Incidence of feline calicivirus (FCV), feline herpesvirus type-1 (FHV-1), and co-detection from 184 cats from different regions in Thailand during 2016-2021

Region / Province	% FCV positive (n)	% FHV-1 positive (n)	% Co-detection (n)
<b>North (n = 33)</b>			
- Chiang Mai			
- Tak	24.2% (8)	69.7% (23)	21.2% (7)
- Phayao			
- Nakhon Sawan			
- Uttaradit			
<b>Northeast (n = 17)</b>			
- Khon Kaen	35.3% (6)	94.1% (16)	29.4% (5)
- Sakon Nakhon			
<b>East (n = 4)</b>			
- Chonburi	25% (1)	25% (1)	0 (0)
<b>South (n = 11)</b>			
- Phuket	100% (11)	81.8% (9)	81.8% (9)
<b>Central (n = 119)</b>			
- Bangkok and vicinity	49.58% (59)	60.5% (72)	31.1% (37)
- Saraburi			
<b>Overall incidence</b>	46.2% (85)	65.8% (121)	31.5% (58)

#### Associations between FCV, FHV-1, and co-detection with clinical variables

The associations between viral detection and clinical variables, including signs of oral and respiratory diseases and vaccination history against FCV and FHV-1 within a year before sampling, were analyzed. A significant correlation was observed only between single FCV detection and oral sign presenting gingivostomatitis ( $p < 0.001$ ). The multinomial logistic regression result indicated that the singly FCV detected cats had a higher risk for developing gingivostomatitis lesion (OR = 9.02, 95% CI: 2.67-30.46) than either only FHV-1 or FCV/FHV-1 detected cats. Meanwhile, the presented respiratory sign was not associated with either single or double viral detection; nonetheless, the co-detection of FCV/FHV-1 was prone to induce the respiratory illness cats (Table 3).



Besides, the significant correlation was evident between previous vaccination status and the positive detection of FCV and FCV/FHV-1 ( $p < 0.05$ ). Cats receiving vaccination showed significantly well protectability in both FCV-positive cats (OR = 0.31, 95% CI: 0.10-0.93) and FCV/FHV-1 positive cats (OR = 0.21, 95% CI: 0.08-0.54); meanwhile this correlation was absent in singly FHV-1 positive cats (Table 3).

### Sequencing and phylogenetic analysis

One complete whole genome sequence, thirteen partial RdRp (aa354–502), full-length VP1, and VP2 coding sequences were achieved (Supplementary Table S1) from self-designed specific primers. In addition, the 7,671 nucleotides (nt) complete coding sequence of KP361/THA/2021 FCV-TH strain (Cat no. 158; Accession no. MZ542330) was accomplished. Overall, the nt identity of the KP361/THA/2021 FCV-TH strain ranged from 39.1-79.3% compared to the other 32 available FCV whole genome sequences in GenBank. The highest identity (79.3%) was closed to two vaccine strains (Accession no. MC177175 and LP834111). Phylogenetic analysis based on the complete genome coding sequence of FCV found that KP361/THA/2021 strain also gathered with other five vaccine strains with nucleotide distance at 49.3-55.6% (Figure 9).

**Table 3** The multinomial logistic regression analysis of variables associated with feline calicivirus (FCV) and feline herpesvirus-1 (FHV-1) detection from 184 cats in Thailand during 2016-2021

Variables <sup>1</sup>	Non-detection	FCV (n =27)			FHV-1 (n=63)			Co-detection (n=58)		
		Odds ratios	95% CI	p value	Odds ratios	95% CI	p value	Odds ratios	95% CI	p value
Oral sign (n = 42/184)	Ref	<b>9.02*</b>	<b>2.67 – 30.46</b>	<b>&lt; 0.001*</b>	1.46	0.47 – 4.54	0.514	1.14	0.35 – 3.17	0.829
Respiratory sign (n = 111/184)	Ref	1.00	0.37 – 2.73	~1.000	0.88	0.39 – 2.00	0.761	2.29	0.95 – 5.54	0.065
Vaccination (n=77/162)	Ref	<b>0.31#</b>	<b>0.10 – 0.93</b>	<b>0.036#</b>	1.69	0.59 – 4.88	0.328	<b>0.21#</b>	<b>0.08 – 0.54</b>	<b>0.001#</b>

\*,# p value < 0.05

<sup>1</sup> Variables of clinical presentations: oral sign showed gingivostomatitis; respiratory sign displayed

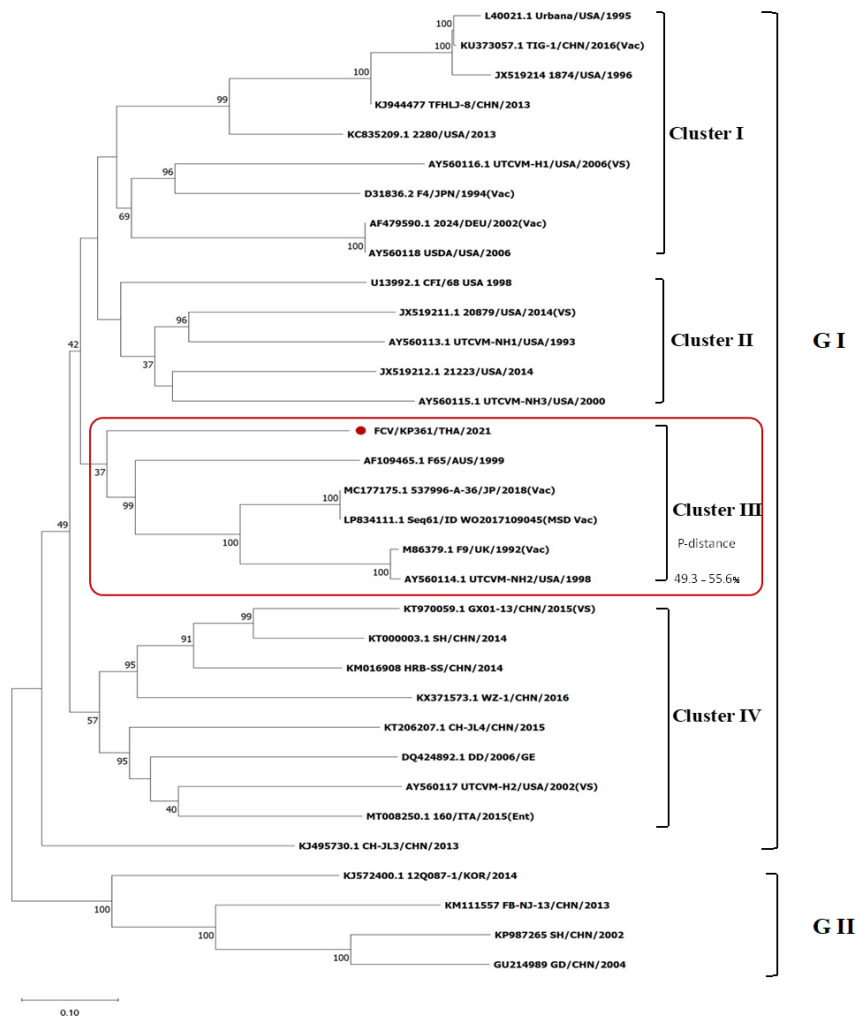


Figure 9 Phylogenetic tree is constructed based on 33 complete nucleotide sequences of feline calicivirus (FCV).

The tree is created using the maximum likelihood method with General Time Reversible (GTR) model. The phylogeny test is encouraged by 1,000 bootstrapped replicates and bootstrap value is significantly considerate when greater than 70. FCV-TH strain is labeled with red circle. Interclade divergence of FCV-TH to others is represented by p-distance threshold limited as < 20 percent divergence for single strain.

Deduced amino acid identity of 14 full-length VP1 sequences from this study was compared with other 43 available sequences in GenBank and showed the homology as 79.0-96.4% . Likewise, amino acid sequence identities were further determined separately on two regions: P2 subdomain region (aa 382-550) and HVR-E region (aa 426-520) by showing as 66.6-90.5% and 60-84.3%, respectively. The highest identical numbers calculated from the deduced amino acid sequence of either full-length VP1, P2 subdomain region, or HVR-E region were similarly suggested to the vaccine strain. The full-length VP1 sequence among FCV-TH strains derived from this study shared amino acid identity between each other at 84-99.8% (Table 4).

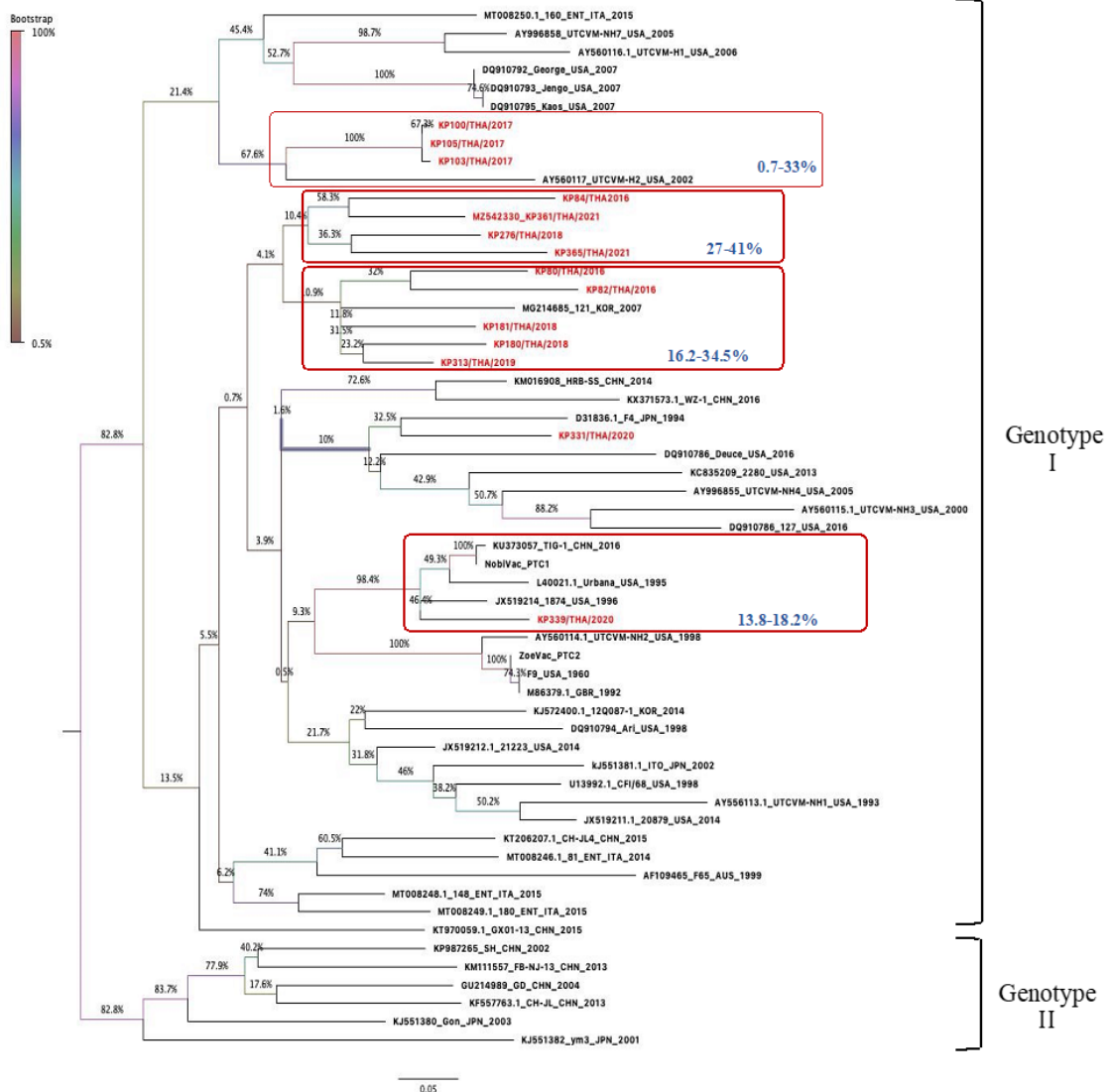
The phylogenetic trees of the full-length VP1, P2 subdomain, and HVR-E were constructed based on 57 amino acid sequences retrieved from 14 FCV-TH strains from this study and the other 43 sequences from GenBank (Figure 10 to 12). As the result of phylogenetic construction, all FCV-TH strains were filled in genotype I. Interestingly, one of FCV-TH strain (KP339/THA/2020) reveal the phylogenetic related to commercially available vaccine strain (NobiVac<sup>®</sup> PTC1), as among amino acid divergent between KP339/THA/2020 and vaccine strain (NobiVac<sup>®</sup> PTC1) is computed according to VP1 capsid protein, P2 subdomain, and HVR-E region as 4.8% , 13.8% , and 20.8% , respectively. Moreover, the FCV-TH stain acquired from three cats (KP100/THA/2017, KP103/THA/2017, and KP105/THA/2017) presented the amino acid homology as 99.7-99.8% , so we assumed that it was the same strain. Besides, this strain always shared a common ancestor with one published VS-FCV strain (UTCVM-H2; Accession no. AY56117), whether evolutionary trees were constructed with any phylogenetic model (Figure 10 to 11).

**Table 4** Deduced amino acid identity between 14 feline calicivirus Thai (FCV-TH) strains and other 43 FCV strains deposited in GenBank database

	<b>Full-length VP1</b>	<b>P2 domain (aa 382-551)</b>	<b>HVR-E (aa 426-520)</b>
Between FCV-TH strain and other strains in GenBank	79.0 - 96.4 %	66.6 – 90.5%	60.0 – 84.3%
Within group (FCV-TH strain)	84.0 - 99.8 %	70.7 - 99.4%	63.5 - 100%

In addition to the statistical association between amino acid residues in the HVR-E region, including amino acid position 438, 440, 448, 452, 455, 465, and 492, and the pathotype identification either VS-FCV pathotype or classical (CLD) pathotype (Brunet et al., 2019). The amino acid alignment and visual assessment on this region of our retrieved VP1 sequences had shown that three from fourteen FCV-TH strains (KP100/THA/2017, KP103/THA/2017, and KP105/THA/2017) were displayed physicochemical properties associated with the VS-FCV pathotype (Table 5), even though those cats did not present any severe respiratory symptom. Nevertheless, one of the sequences of FCV-TH strain (KP361/THA/2021; Accession No. MZ542330) that conspicuously showed typical clinical sign of VS-FCV pathotype never owned any related remarkable residue positions as followed by pathotype differentiated criteria (Table 5)





Figure

### 11 Phylogenetic trees of P2 subdomain.

The trees were constructed based on deduced amino acid using the maximum likelihood method with Whelen and Goldman model. The statistical support supplied with bootstrapping of 1,000 replicates and significantly considerate when bootstrap value greater than 70. FCV-TH strains were presented as red bold letters. Pairwise p-distance of each group was shown in each box by limited threshold as < 20 percent divergence for single strain.

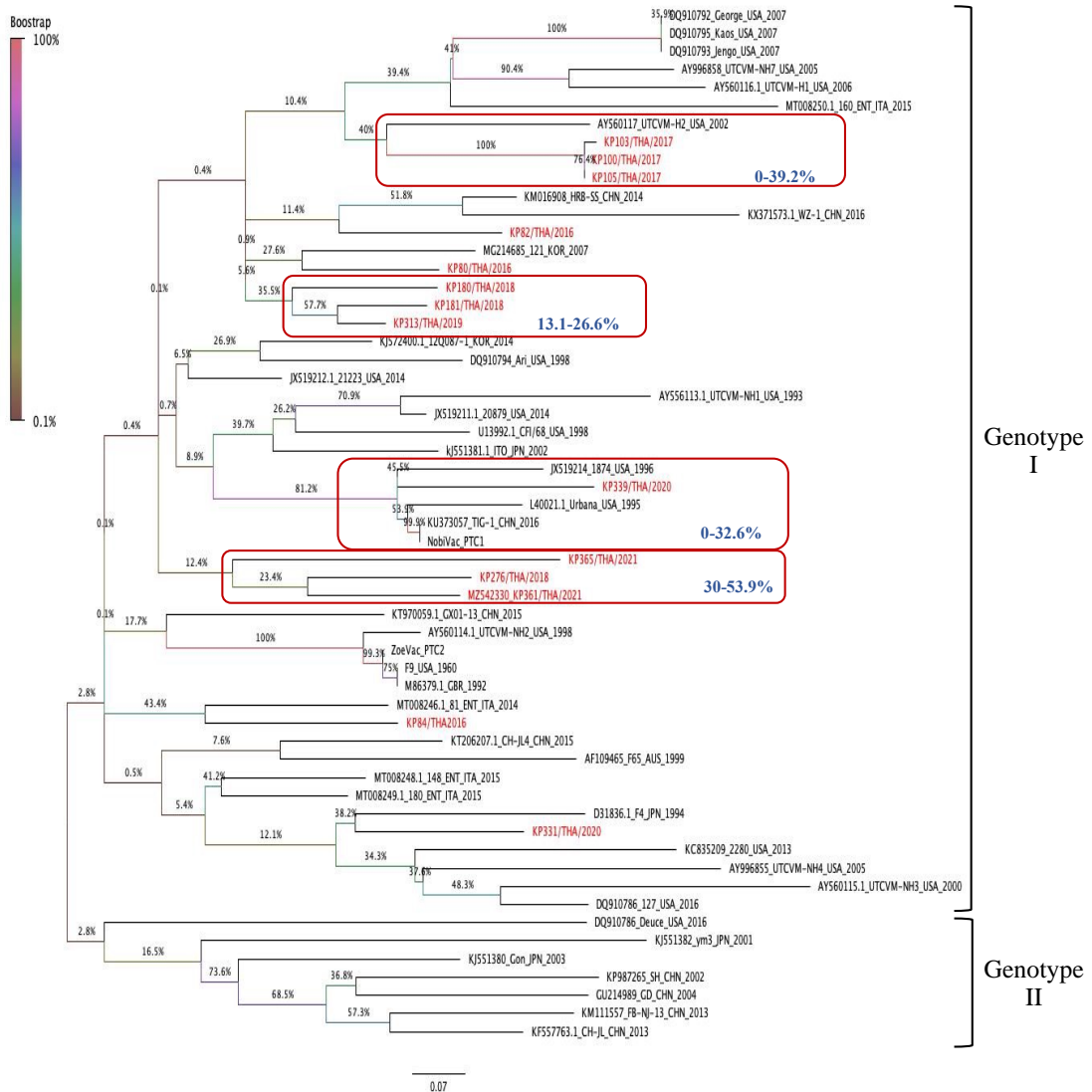


**Figure 12** Phylogenetic trees of Hypervariable E region (HVR-E).

The trees were constructed based on deduced amino acid using the maximum likelihood method with Le Gascuel 2008 model. The statistical support supplied with bootstrapping of 1,000 replicates and significantly considerate when bootstrap value greater than 70. FCV-TH strains were presented as red bold letters. Pairwise p-distance of each group was shown in each box by limited threshold as < 20 percent divergence for single strain.



### Recombinant and selective pressure analysis

The dN/dS ratio was acquired from the full-length VP1 gene and partial RdRp gene of various available FCV strains using a codon-based analysis implemented in Datamonkey web service. The result of negative selective pressure of VP1 gene presented mainly on all tested algorithm of evolutionary mechanism including SLAC, FEL, and MEME with dN/dS ratio <1. In addition, the MEME test revealed potential evidence of 24 amino acid sites of VP1 that were undergone episodic positive selection. Three locations of amino acid residues that demonstrated the positive selection evidence by MEME stood on 3 of 7 remarkable amino acid residues (448, 455, and 492) with a *p-value* threshold of 0.1 (Table 6). Likewise, the partial RdRp gene sequence (aa 1615-1737) exhibited positive episodic selection by MEME on four deduced amino acid sites (1675, 1701, 1708, and 1728). Additionally, some amino acids represented the characteristic display of FCV-TH strain at 3' end of ORF1 by the visualized discovery (Figure 13), including deduced amino acid Q1728, Y1733, T1745, A1750, A1754.

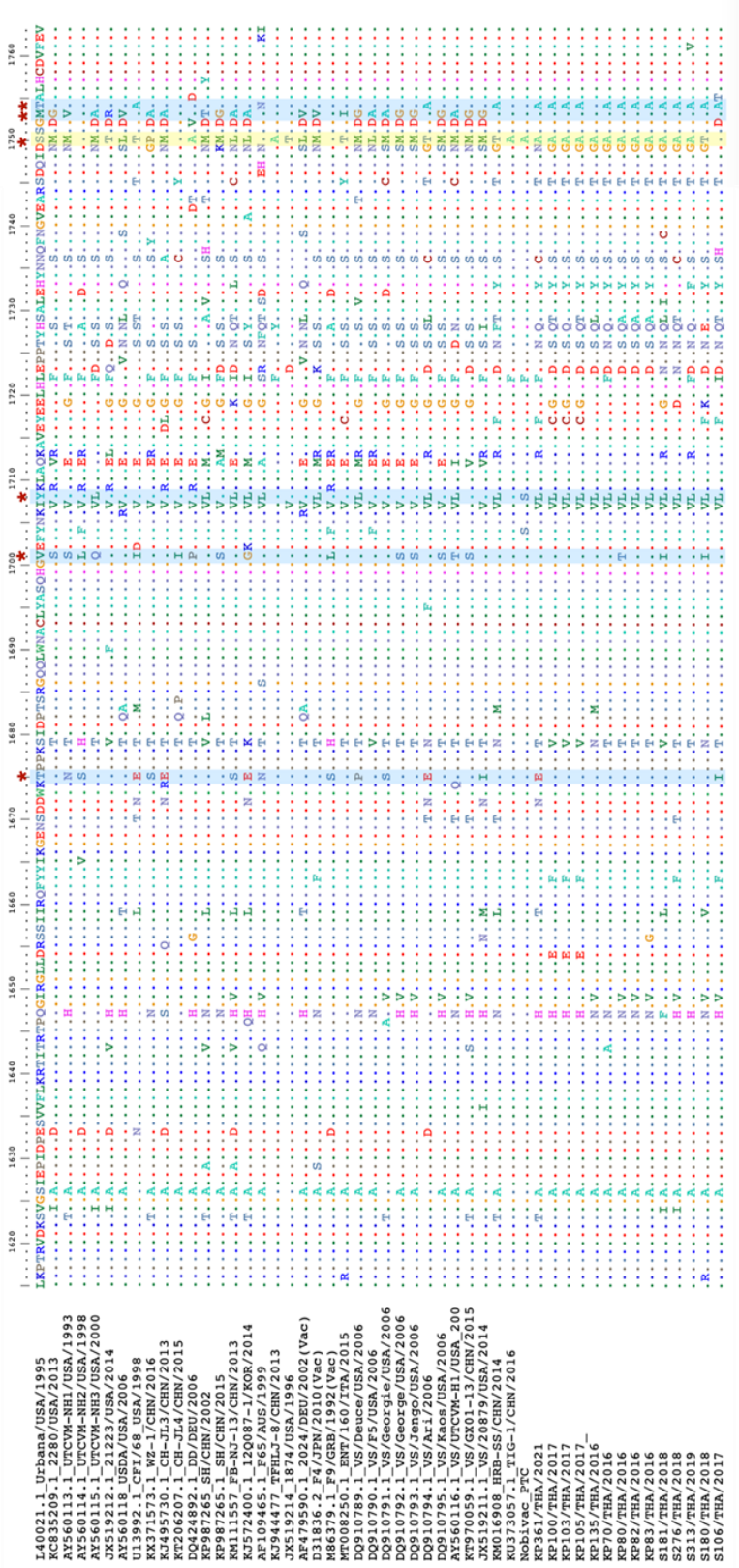


Figure 13 The multiple deduced amino acid sequence alignment of partial RNA polymerase (RdRp) protein (aa1615-1763).

The sequence composed of total 49 sequences including 14 FCV-TH strains and 35 sequences from GenBank database. The seven positions (asterisk) of evidentially positive episodic selection and one positive (yellow strip) pervasive/purifying selection were shown as bold asterisk

Table 5 Physicochemical property of remarkable amino acid residue position on hypervariable region E (HVR-E) of VP1 major capsid protein gene hypothesized to differentiate between classical FCV and VS-FCV pathotype

Strains	aa 438	aa 440	aa 448	aa 452	aa 455	aa 465	aa 492
	Hydrophilic aliphatic	Not small	Polar positive charge	Not small	Not negative charge	Polar	Small
VS-FCV* (21 sequences)	V <sub>10</sub> , T <sub>11</sub>	S <sub>3</sub> , K, E <sub>4</sub> , Q <sub>6</sub> , G <sub>7</sub>	A <sub>3</sub> , P <sub>2</sub> , G <sub>2</sub> , R, K <sub>11</sub> , E, G	D <sub>7</sub> , E <sub>14</sub>	E, D <sub>6</sub> , N, T <sub>7</sub> , I <sub>2</sub> , M <sub>3</sub> , S	S <sub>16</sub> , G <sub>5</sub>	V <sub>19</sub> , R, I
CLD-FCV# (26 sequences)	T <sub>21</sub> , V <sub>3</sub> , A <sub>2</sub>	S <sub>8</sub> , Q <sub>3</sub> , D, K, G <sub>13</sub>	A <sub>19</sub> , R <sub>3</sub> , P <sub>2</sub> , G, K	D <sub>20</sub> , E <sub>2</sub>	D <sub>13</sub> , S <sub>2</sub> , T <sub>5</sub> , A <sub>2</sub> , G <sub>2</sub> , V, I	S <sub>8</sub> , G <sub>18</sub>	V <sub>13</sub> , K <sub>5</sub> , R <sub>6</sub> , L <sub>2</sub> , I <sub>2</sub>
KP80/THA/2016	T	G	A	D	D	G	V
KP82/THA/2016	T	G	A	D	D	G	I
KP84/THA/2016	T	E	A	D	D	G	V
KP100/THA/2017	T	E	R	E	T	S	V
KP103/THA/2017	T	E	R	E	T	S	V
KP105/THA/2017	T	E	R	E	T	S	V
KP180/THA/2018	T	G	A	D	E	G	V
KP181/THA/2018	T	G	P	D	D	G	V
KP276/THA/2018	T	G	A	D	D	G	V
KP313/THA/2019	T	D	A	D	D	G	V
KP331/THA/2020	T	G	A	D	T	S	V
KP339/THA/2020	T	R	A	D	H	G	V
KP361/THA/2021	T	G	A	D	D	G	I
KP365/THA/2021	T	S	S	N	D	G	V

\*VS-FCV refer to Virulent systemic feline calicivirus, #CLD-FCV refer to classical feline calicivirus

Table 6 Evidence of positive and negative selection using various detection methods

FCV genome	Selection pressure analysis	SLAC	FEL	MEME
VP 1 gene	Positive selection	0	0	24 <sup>a</sup>
	Negative selection	593	616	-
	Overall dN/dS	0.058	0.058	0.058
Partial RdRp (aa 1615-1737)	Positive selection	0	1 <sup>b</sup>	7 <sup>c</sup>
	Negative selection	110	113	-
	Overall dN/dS	0.065	0.054	0.054

#### Amino acid diversifying selection site

<sup>a</sup> MEME: 7, 29, 31, 82, 91, 120, 366, 396, 400, 408, 411, 441, 448, 455, 483, 492, 497, 500, 502, 506, 507, 542, 625, 637

<sup>b</sup> FEL: 1750

<sup>c</sup> MEME: 1675, 1701, 1708, 1728, 1750, 1753, 1754

#### Discussion

Feline viral upper respiratory tract infection, mainly caused by FCV and FHV-1, is commonly diagnosed in Thai cats in practice. Although the commercially available vaccines derived from various FCV strains, including F9, FCV-255, and FCV-G1, are widely used in Thailand; the relatively high incidence of FCV (46.2%) circulating in Thai cats was detected in this study

The result has also shown a statistically significant correlation between only FCV detection and gingivostomatitis lesion likely the previous studies (Coyne et al., 2012; Hou et al., 2016), by only 22.8% of the recruited sample became from gingivostomatitis cats. In addition, the good protectability of vaccination to singly FCV

detection and co-detection of FCV and FHV had statistically significant demonstrated in this study. However, our study found that one FCV-TH strain (KP339/THA/2020) reveals the phylogenetic related to the commercially available vaccine strain. According to the medical history, this cat did not receive any vaccine within three months before sampling collection, and the cat always had chronic respiratory tract disease problems. Previously, few studies reported the occurrence of vaccine strain (F9)-like viruses in the cat population (Radford et al., 2001a; Coyne et al., 2007b; Coyne et al., 2012). However, those detections might be the vaccine-derived viruses because all those cats received vaccination within 90-day before sample collection. Following our finding, we suggest that the persistence duration of vaccine shedding in an unhealthy cat should be more observed. Moreover, the evolution of vaccine-derived FCV causing vaccine-related respiratory tract disease should be more concerned and investigated in the future.

The analysis of amino acid physicochemical properties of HVR-E of VP1 capsid region based on the previous study that has illustrated the statistically significant of seven notable residues in which potentially segregate between classical and VS-FCV ( Brunet et al. , 2019) , remarkably, three sequences ( KP100/ THA/ 2017, KP103/THA/2017, KP105/THA/2017) in this study dramatically discloses incompatible result to the previous report. However, all those sequences have shown homology across their VP1 capsid protein amino acid sequence with the identical score of 99.7% - 99.8%, so it can be assumed that they are the same strain. Moreover, those sequences share a common ancestor with the VS-FCV UTCVM-H2 strain (Accession No. AY560117) from the evolutionary analysis. Although their seven amino acid residue markers associated with VS-FCV criteria and phylogenetic tree also reveal sharing a common ancestor with other notable VS-FCV strain, all those three sequences (KP100/THA/2017, KP103/THA/2017, and KP105/THA/2017) were delivered

from stray unvaccinated kittens that reside in the same area and they presented only mild clinical respiratory symptom.

On the other hand, one of the FCV-TH sequences (KP361/THA/2021) was acquired from a kitten exhibiting associated clinical signs with VS-FCV symptoms such as facial edema and epidermal ulceration, glossitis, acute respiratory tract infection, and death. In evolutionary analysis, it shares a common ancestor with other circulating FCV-TH strains constructed based on sequence on VP1 gene by genetic distance within the group as 8.3-21.3% . Nevertheless, the phylogenetic tree was created based on the whole-genome coding nucleotide sequence, FCV/ KP361/ THA/ 2021 had grouped with other five vaccine strains with genetic divergence as between 49.4% - 55.6% . Besides, seven remarkable amino acid residues for pathotype differentiation of KP361/ THA/ 2021 are indeed not characterized by any physicochemical criteria of the VS-FCV pathotype. However, this study has found that 3 of 7 remarkable amino acid residues (448, 455, and 492) that have been noticed to be statically significant associated with pathotype differentiated (Table 5) (Brunet et al., 2019) are driven undergone episodic positive selection.

Moreover, one of them is also shown in the immunogenicity dominance domain; aa448. As besides, three amino acid positions (441, 448, 455) that became evidence of episodic positive selection have ever been identified as Monoclonal antibodies (MAb) escaped point mutation (Tohya et al., 1997). Likewise, the previous study has investigated the evolutionary mechanism by emphasizing on persistence and diversification of FCV. Furthermore, they have annotated the association between positive selection and immune-mediated mechanism of viral evolution (Coyne et al., 2007b). Moreover, another study has also indicated regions that frequently identified as antibody evasion point mutations locating at amino acid

position 441, 448, 449, and 455 (Tohya et al., 1997), by aa 445–451 have been proved to be the neighborhood of neutralizing epitope (Cubillos-Zapata et al., 2020). In addition, this study demonstrates the multiple variances of FCV circulating in Thai cats and seem likely to evolve undergone positive selection.

RNA-dependent RNA polymerases ( RdRp) play a role as mainly essential proteins accountable for viral replication. In *Caliciviridae*, RdRp encodes the sequence of viral protease at the 3' end of ORF1 (Smertina et al., 2019), in which function to cleave VP1 leader capsid protein producible the mature VP1 (Penaflor-Tellez et al., 2019). According to the character as an error-prone enzyme of RdRp, many studies have suggested about higher mutation rate of several viruses of *Caliciviridae* (Bull et al., 2010; Bull et al., 2011). Besides, FCV has demonstrated the recombination hot spot site at the 3' end of ORF1, the junction between ORF1/ORF2 (Symes et al., 2015). Although this study does not find any recombination evidence in our Thai variance, some amino acid residues demonstrated the unique divergence of amino acids residue, particularly in FCV-TH strains. Moreover, the pressure analysis has also found evidence of both episodic positive/ diversifying selection on aa position S1750 by mostly FCV-TH strain reveal amino acid residue as Ala in this position. This situation has also related to a previous study that notifies the higher mutation rate of RdRp capable of increasing genetic diversity and can influence viral populations fitness undergone selective pressures (Mahar et al., 2013).

### Conclusion

This study demonstrates the first report of molecular characterization of FCV circulation in Thai cats. Besides, some FCV-TH strains revealed the amino acid physicochemical properties on the capsid hypervariable region contrasted to the previous hypothesis. Therefore, it can be suggested that in the geographic region in

which there is a high number of FCV circulating, the high genomic plasticity of FCV results in their rapid response to environmental selective force (Radford et al., 2007). Furthermore, the enhancing amino acid diversity in a gene at numerous phylogenetic levels, either within or among species, reflects their adaptive ability. Lastly, the question about FCV vaccine breakdown strain and evolutionary of vaccine strain related to FURTD should be more investigated in Thailand to find the most effective FCV prevention and control protocol.

### **Acknowledgment**

KP was granted by Chiang Mai University for Ph.D. Program. CP was supported by the Ratchadapisek Somphot Fund for Postdoctoral Fellowship, Chulalongkorn University. This study was supported by the 90<sup>th</sup> Anniversary of Chulalongkorn University Fund (Rachadaphiseksomphot Endowment Fund). The Chulalongkorn Academic Advancement into Its 2<sup>nd</sup> Century Project, Faculty of Veterinary Science, Chulalongkorn University is also acknowledged

### **Ethics Statement**

All experimental protocols were approved by the Chulalongkorn University Animal Care and Use Committee (No. 1631002). All procedures were done following the relevant guidelines and regulations.

### **Data accessibility**

All the data supporting our findings is contained within the manuscript. One full-length coding Feline calicivirus sequence has been deposited in NCBI GenBank under accession MZ542330.



### Declaration of competing interest

The authors have declared no competing financial or non-financial interests.



## CHAPTER III

### Simultaneous Detection and Differentiation between Feline Calicivirus Vaccine and Wild-type Thai Strain in Clinical Samples Using High-Resolution Melting Analysis

#### Authors

Kannika Phongroop, Chutchai Piewbang, Somporn Techangamsuwan

Department of Pathology, Faculty of Veterinary Science, Chulalongkorn University, Bangkok, 10330, Thailand and Animal Virome and Diagnostic Development Research Group, Faculty of Veterinary Science, Chulalongkorn University, Bangkok 10330, Thailand

Anudep Rungsipipat

Department of Pathology, Faculty of Veterinary Science, Chulalongkorn University, Bangkok, 10330, Thailand

Jatuporn Rattanasrisomporn

3Companion Animal Clinical Sciences, Faculty of Veterinary Medicine, Kasetsart University, Bangkok 10900, Thailand

Sahatchai Tangtrongsub

Department of Companion Animal and Wildlife Clinic, Faculty of Veterinary Medicine, Chiang Mai University, Chiang Mai 50100, Thailand

Publication status: in preparation



## Abstract

High-resolution melting (HRM) technology overcomes limitations of classical viral detection and genome identification such as viral isolation and genome sequencing by providing less complexity and enhancing greater sensitivity and specificity. HRM analysis is an innovation of post-polymerase chain reaction (PCR) application that advantage the most straightforward method for simultaneous detection, genotyping, and mutation scanning. This study aimed to establish reverse transcription-quantitative PCR (RT-qPCR) and HRM assay for concurrent diagnosis and genome typing of feline calicivirus (FCV) using clinical samples derived from nasal and oropharyngeal swabs. This study used RT-qPCR to amplify a 99-base pair target segment between open reading frame 1 (ORF1) and open reading frame 2 (ORF2) of FCV. Subsequently, HRM assay was promptly applied as a post-PCR application using Rotor-Gene Q® Software 2.3.1.49. The results successfully showed detection and genome differentiation between two commercially available FCV vaccine strains and five wild-type FCV Thai strains within a single PCR reaction. There was no cross-reactivity with other viruses in cats, including feline herpesvirus-1, feline infectious peritonitis virus, feline leukemia virus, feline immunodeficiency virus, and feline morbillivirus. The detection limit of the assay was  $6.18 \times 10^1$  copies/ $\mu$ l. The linear regression analysis revealed a statistically significant correlation between the % C:G component and melting temperature shift of each strain typing pattern at 0.25°C to 1% C:G alteration. Thus, this study is the first demonstration of the benefits of HRM assay for spontaneous detection, strain differentiation, and mutation scanning of FCV on clinical samples.

**Keywords:** Feline calicivirus, High resolution melting analysis, Simultaneous detection, Strain differentiation

## Introduction

Feline calicivirus (FCV) is non-enveloped, single-stranded, positive-sense RNA virus (Weiblen et al., 2016; Pereira et al., 2018). The virus belongs to the family *Caliciviridae*, which currently includes eleven viral genera: *Lagovirus*, *Nebovirus*, *Norovirus*, *Sapovirus*, *Vesivirus*, *Bavorirus*, *Nacovirus*, *Recovirus*, *Salovirus*, *Valovirus*, and *Minovirus* (Vinje et al., 2019), and FCV is the member of genus *Vesivirus*. FCV is commonly the causative agent of feline upper respiratory tract disease and stomatitis in cats. The virus was discovered in 1957 (Fastier, 1957), then now widely spread in European, American, and Asian countries (Bannasch and Foley, 2005; Coyne et al., 2007b; Hou et al., 2016; Afonso et al., 2017; Zhou et al., 2021). Formerly, FCV-infected cats are suggested to be self-limited infections with either mild respiratory symptoms or oral disease (Gaskell et al., 2012). Meanwhile, other symptoms, including chronic gingivostomatitis, abortion, ulcerative dermatitis, severe pneumonia, acute febrile lameness syndrome, and acute jaundice, were also found (Schorr-Evans et al., 2003; Hurley et al., 2004). In the last decade, the emergence of highly virulent systemic FCV, called VS-FCV, has been pointed out as the cause of the severe and acute virulent systemic disease (VSD), resulting in a higher mortality rate even in FCV-vaccinated cats (Hurley et al., 2004; Reynolds et al., 2009; Battilani et al., 2013). Indeed, the lack of proofreading of the RNA viral polymerase gene is the essential factor that makes the RNA virus prone to possess a high evolution rate (Coyne et al., 2012). In FCV, it has been stated that the majority of recombination event occurs at the "hot spot" between open reading frame 1 (ORF1) and ORF2, both *in vitro* (Symes et al., 2015) and in natural evidence (Zhou et al., 2021). Therefore, the efficiency and broadly acting of the FCV vaccine are currently interested and challenged. At present, two types of FCV vaccine are commercially available in Thailand, consisting of (1) inactivated vaccine, either single strain (FCV-255) or double strains (FCV-431 and FCV-G1), and (2) modified live attenuated vaccine (FCV-F9). The FCV vaccine

preferably reduces the severity of clinical signs rather than promotes sterilizing immunity in cats (Radford et al., 2006). A study has presented the potency of the modified live vaccine to reduce the duration of RNAemia and lower the number of viral load shedding after secondary infection (Spiri et al., 2021). On the other hand, some studies proposed the possibility of prolonged use of the modified live vaccine could not provide enough cross-protection to wild-type FCV strain in some countries (Zhou et al., 2021), and it also might capably drive the evolution of circulating FCV strain turning to vaccine-resistant variants (Lauritzen et al., 1997; Addie et al., 2008). Moreover, the evidence of the genetic relationship between epidemic FCV strain and vaccine strain was also notable in the previous study (Zhou et al., 2021).

Although traditional cell culture is still a standard gold method for viral identification, molecular techniques such as conventional polymerase chain reaction (PCR), quantitative PCR (qPCR), or probe-based qPCR have been concurrently developed, providing a faster and specific viral detection. Additionally, the application of genome sequencing is still required for genetic analysis and strain identification. While sequencing is a reliable method, it is also unwieldy and time-consuming. In the last decade, high resolution melting (HRM) assay has been widely utilized in several manners both in human and veterinary medicine (Chua et al., 2015; Sun et al., 2019; Vaz et al., 2019) for mutation scanning, repeat typing, genetic variant scanning, and genotype differentiation (Reed et al., 2007). Following the principle of saturated fluorescent dye, alteration of the fluorescent signal after PCR amplification is assembled by qPCR machine, then data are calculated afterward with the appropriate software. In addition, HRM assay turns into a new trendy method that seems likely simple, quick, inexpensive, and effective for scanning and monitoring initially genetic variants from clinical samples (Toi and Dwyer, 2008b; Tajiri-Utagawa et al., 2009; Marin et al., 2016). Therefore, this study established a HRM assay for concurrent diagnosis and discrimination of either FCV-vaccine strain (FCV-

Vac) and wild-type FCV-Thai strains (FCV-TH) and between wild-type FCV-TH strains from clinical samples of infected cats.

## Materials and Methods

### Sample collection, RNA extraction, and complementary DNA (cDNA) synthesis

Nasal (NS) and oropharyngeal swabs (OS) were collected from 184 cats with and without an upper respiratory symptom or oral disease between 2016 and 2021. The owner signed a consent form before performing sample collection from each cat. All procedures were approved by the Chulalongkorn University Animal Care and Use Committee (No. 1631002). The NS and OS were obtained using an individual sterile cotton swab, then were kept in 1% sterile phosphate buffer saline (PBS) and stored at  $-80^{\circ}\text{C}$  until used.

QIAamp<sup>®</sup> cador<sup>®</sup> Pathogen Mini Kit (QiagenGmbH, Hilden, Germany) was used for RNA extraction by adding 100- $\mu\text{l}$  of Buffer VXL and 20- $\mu\text{l}$  of proteinase K in a 200- $\mu\text{l}$  of the sample (in 1% PBS). After incubating the mixture at room temperature ( $20-25^{\circ}\text{C}$ ) for 15 min, the extracted procedure was performed following the manufacturer's instructions. Then reverse transcription (RT) was employed using Omniscript<sup>®</sup> RT Kit (QiagenGmbH, Hilden, Germany), and cDNA products were stored at  $-20^{\circ}\text{C}$  until analysis (Chaiyasak et al., 2020).

### Primer design

Full-length genomes of global FCV strains, including classical, virulent, and commercial vaccine strains, were retrieved from the GenBank database. Those strains were aligned with 14 sequences of partial RNA dependent RNA polymerase (RdRp)

and full-length VP1 major capsid protein sequences of FCV-TH strains using BioEdit Sequencing Alignment Editor Version 7.2.5. Primers for HRM assay were initiated at the location between ORF1 and ORF2 where nucleotide sequence demonstrated significantly different between available FCV-Vac, wild-type FCV-TH, and other global FCV strains (Figure 14). The nucleotide sequence of all primers used in this study was shown in Table 7

#### **FCV screening detection**

cDNA products derived from cats' NS and OS were amplified for FCV screening using conventional RT-PCR. The specific primers for FCV screening were designed for this study (Table 1). The RT-PCR was operated as follows; briefly, each 25- $\mu$ l reaction contained 3  $\mu$ l cDNA, 12.5  $\mu$ l GoTaq<sup>®</sup> Green Master Mix (2X) (Promega, USA), 7.5  $\mu$ l nuclease-free water and 1  $\mu$ l each forward and reverse primers (ORF1 For and ORF1 Rev). The thermal cycling started with an initial denaturation (95°C, 5 min), followed by 40 cycles of denaturation (95°C, 30 sec), primer annealing (59°C, 30 sec), and primer extension (72°C, 1 min). Then, a final extension was continuously run at 72°C for 5 min. The RT-PCR products were inspected for positive results using capillary electrophoresis (QIAxcel DNA Screening Kit, Qiaxcel<sup>®</sup>, Qiagen GmbH, Germany). Then, the amplicons were purified using a commercial kit (NucleoSpin<sup>®</sup> Extract II kit, Macherey Nagel, Germany) according to the manufacturer's instructions. Nucleotide sequencings were operated by MacroGen<sup>®</sup> (Incheon, South Korea).



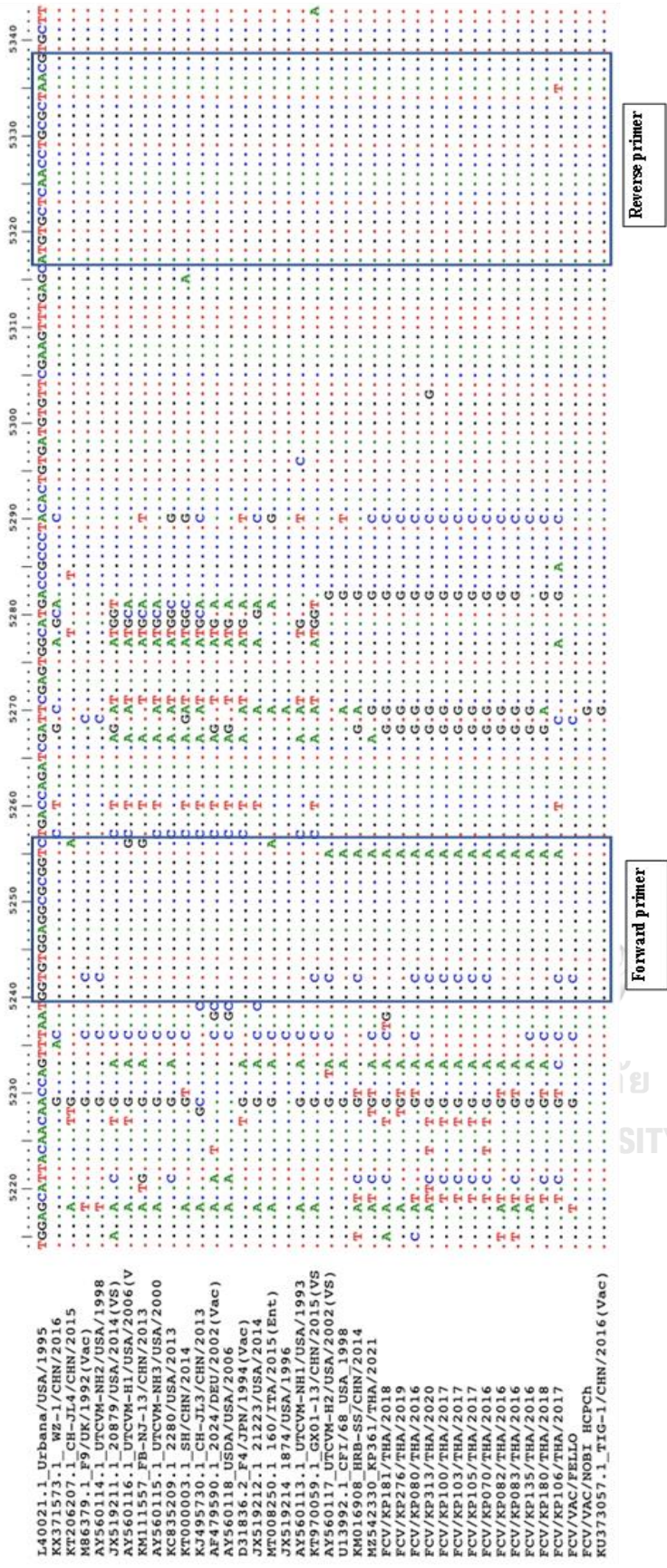


Figure 14 The multiple nucleotide alignment of partial RNA dependent RNA polymerase (RdRp) sequence (nucleotide position 5214-5343).

The forward and reverse primers for HRM assay flanked on the junctional region of ORF1 and ORF2.

Table 7 Nucleotide sequence, position, and amplicon size of primers used in this study

Assay	Primer name	Sequence 5'to3'	Position <sup>a</sup>	Amplicon size (bp)
Screening RT-PCR	ORF1 For	GTAAGAAGAAATTGAGACAATGTCT	1-25	414
	ORF1 Rev	GTGAGCTGTTCTTTGCACAT	414-394	
Conventional RT-PCR	RdRp For	TATGGTGATGATGGWGTKTAYATGTT	4778-4805	696
	RdRp Rev	AATCCACACAGTGCCAAAT	5473-5454	
HRM assay	HRM For	GGYGTGGAGGCGGGWC	5240-5256	99
	HRM Rev	CGTHAGCCAGGTTGAGCACAT	5338-5317	

<sup>a</sup> Primer position was quoted to the sequence of FCV strain Urbana (GenBank accession number L40021)

### **FCV vaccine strain preparation**

FCV-Vac template received from commercially available vaccines in Thailand (Nobivac<sup>®</sup>1- HCPCh ). cDNA of FCV-Vac templates was amplified for sequence verification using self-designed primers (RdRp For and RdRp Rev) (Table 7). The RT-PCR was operated using GoTaq<sup>®</sup> Green Master Mix and similar thermal cycling conditions mentioned above except for the primer annealing temperature (60°C). Then, the derived FCV-Vac amplicons were resolved by 2% (w/v) agarose gel electrophoresis, purified, and submitted for sequencing as mentioned above.

### **Standard reference synthesis of FCV strains**

Nucleotide sequences of various FCV strains were selected and ordered to synthesize the string DNA fragments for the HRM assay optimization (Table 8). String DNA fragments at the region between 3'-terminal of RdRp gene and 5'-terminal of VP1 major capsid protein gene with a 150-base pair (bp)-product length were commercially synthesized by Invitrogen<sup>™</sup> GeneArt<sup>™</sup> Strings<sup>™</sup> DNA Fragments (ThermoFisher Scientific<sup>®</sup>, MA, USA).

Two VS-FCV strains consisting of UTCVM-H2 strain (Accession no AY560117) and GX01-13 strain ( Accession no KT970059) and possessing a phylogenetic relationship with FCV-TH strains from our previous study (unpublished data) were included as the virulent reference strains in this study. Additionally, one selected known sequence of FCV-TH and a commercial FCV-Vac (Nobivac<sup>®</sup> 1-HCPCh) were also synthesized for string DNA template to determine the HRM efficacy for strain differentiation of mimetically mixed infection.

Table 8 List of synthetic reference strains and wild-type Thai strain of feline calicivirus (FCV)

FCV strain	Accession no.	Sequence	Position	Base pair
Reference strain GX01-13	KT970059	TGGAACATTACAACAGCCAGTTCAATGGCGGTGGAGGCGGGTCCGATCAGATCAATATGAGTGAT GGTACCGCCCTACACTGTGATGTTTGAAGTTTGAGCATGTGCTCAACCTGGCTAACCGTGCTA AAATACTATGATTGGGACCC	5192 - 5341	150
Reference strain UTCVM-H2	AY560117	TGGAGCATTACAACAGCCTATTCAATGGCGTGGAGGCGGGACTGACCAGATCGATTCGAGTGG CATGGCCGCCCTACACTGTGATGTTTGAAGTTTGAGCATGTGCTCAACCTGGCTAACCGTGCT TAAATACTATGATTGGGATCC	5208 - 5357	150
Reference strain TIG-1 (FCV-Vac, Nobivac® 1- HCPCh)	KU373057	TGGAGCATTACAACAGCAGTTTAATGGGTGGAGGCGGGTCTGACCAAGATCGATGCGAGTGG CATGACCGCCCTACACTGTGATGTTTGAAGTTTGAGCATGTGCTCAACCTGGCTAACCGTGCT TAAATACTATGATTGGGACCC	5211 - 5360	150
Wild-type Thai strain: FCV-TH/KP313	-	TGGAAATCTATAATAGCCAAATTAATGGCGTGGAGGCGGGACTGACCAGATCGGTGCGAGTGG CATGGCCGCCCTCCACTGTGATGTTTGAAGTTTGAGCATGTGCTCAACCTGGCTAACCGTGCT TAAACACTATGATTGGGACCC	5214-5363 <sup>a</sup>	150

<sup>a</sup> Reference position from FCV strain Urbana (GenBank accession number L40021)

### RT-qPCR and HRM assay

RT-qPCR was employed to amplify the 99-bp fragment product of FCV, and then HRM application was subsequently analyzed using Rotor-Gene<sup>®</sup> Q (Qiagen GmbH, Hilden, Germany). Template amplification was generated using the Type-it<sup>®</sup> HRM<sup>™</sup> PCR kit (Qiagen GmbH, Hilden, Germany), in which EvaGreen<sup>®</sup> was applied as an intercalating fluorescent dye. The reaction was conducted in the final volume of 25  $\mu\text{l}$  containing 2x HRM PCR Master Mix, 0.5  $\mu\text{M}$  degenerated primers each (HRM For and HRM Rev), and 2  $\mu\text{l}$  of either cDNA from clinical samples or synthesized string DNA fragment as the template. The qPCR reaction was carried in duplication in all samples to assure reproducibility of intra-assay. FCV-Vac (Nobivac<sup>®</sup> 1- HCPCh), FCV-TH/KP367, and FCV-TH/KP361 (Accession no MZ542330) were incorporated into each run verify the reproducibility of inter-assay. The thermal cycling condition was run as follows: initial PCR denaturation at 95°C for 5 min, then 40 cycles of PCR at 95°C for 10 sec, 60°C for 30 sec, and 72°C for 10 sec. Then, the fragments were ramped from 65°C to 95°C, incrementing at 0.1°C by holding 2 secs at each step. The data analysis was run on Rotor-Gene Q Software 2.3.1.49 (Qiagen GmbH, Hilden, Germany) with a generated report.

### Sensitivity and specificity evaluation of HRM assay

Ten-fold serial dilutions of reference synthesized string DNA (FCV strain TIG-1), ranging from  $6.18 \times 10^0$  to  $6.18 \times 10^8$  copies/ $\mu\text{l}$ , were used as templates for measurement the limitation of detection of HRM assay. In addition, the cross-reactivity between FCV and other feline viral pathogens, including feline herpesvirus-1 (FHV-1), feline infectious peritonitis virus (FIPV), feline leukemia virus (FeLV), feline immunodeficiency virus (FIV), and feline morbillivirus (FeMV), were also investigated.

### **Efficacy to detect a mixed infection**

Mimetically mixed infection was manufactured at  $6.18 \times 10^5$  copies/ $\mu$ l concentration of synthesized string DNA of FCV-Vac strain, synthesized string DNA of FCV-TH strain (FCV-TH/KP313), and clinical samples (unknown concentration). The samples were paired for two different strains in one mixture with altered concentration ratio ranging from 1:4 to 4:1 (v/v). The sample mixture was conducted undergone RT-qPCR and HRM assay. Then, the efficacy of the lineage detection on each concentration was determined as representative of a mixed infection.

### **Data analysis and interpretation**

Normalized and different graph plots of HRM assay were constructed to determine the sample deviation related to FCV strain typing by generating on the Rotor-Gene Q Software 2.3.1.49. Linear regression analysis was calculated to identify the correlation between the % C:G component and melting temperature ( $T_m$ ) of each strain typing pattern. STATA statistical software release 16.1 (Stata Corp., College Station, Texas, USA) was used for all statistical analyses.



## **Result**

### **FCV screening by RT-PCR**

From clinical specimens retrieved from 184 cats, only 86 cats showed positive FCV detection by screening RT-PCR. Due to the limitation of sample quantity, 44 out of 184 samples could be used for HRM assay measurement in which positive FCV RT-PCR was shown in 31 cats and the negative result presented in 13 cats. Among FCV-positive cats, 14 of 31 samples acquired nucleotide sequence between ORF1 and ORF2 region, which covered the partial RdRp gene (Figure 14). In addition, one

retrieved sequence of FCV-TH strain (FCV-TH/KP313) was synthesized as string DNA for being a known concentration template in a mimetically mixed infection model.

### RT-qPCR and HRM assay

The RT-qPCR and HRM assay in this study exhibited the successful differentiation of all 11 FCV templates, including FCV-Vac (n= 1), VS-FCV reference strains (n=2), and FCV from clinical samples (n=8). Furthermore, following the results of HRM melting analysis, both normalized and difference melt plots demonstrated seven different strain typing patterns in which eight FCV-TH strains deriving from clinical samples could be distinguished into five strain typing patterns with confidence percentage over 90% (Figure 15). Besides, the correlation between % C:G of PCR product sequence in each strain typing pattern and their  $T_m$  revealed conspicuously significant by linear regression model (Figure 16). As shown, we found that either 1% C:G alteration could significantly encourage 0.25°C of  $T_m$  modification with  $p$ -value = 0.000 and  $R^2$  as 0.9954 (Table 9).

Table 9 Linear regression model showing the relationship between % C:G of PCR product sequence and melting temperature deriving from HRM assay.

Temp	Coef.	Std. Err.	t	P >  t	[95% Conf. Interval]
CG	0.2529	0.0070	35.93	0.000	0.2356 – 0.2701
_Cons	71.3463	0.3836	186.00	0.000	70.4077 – 72.2849

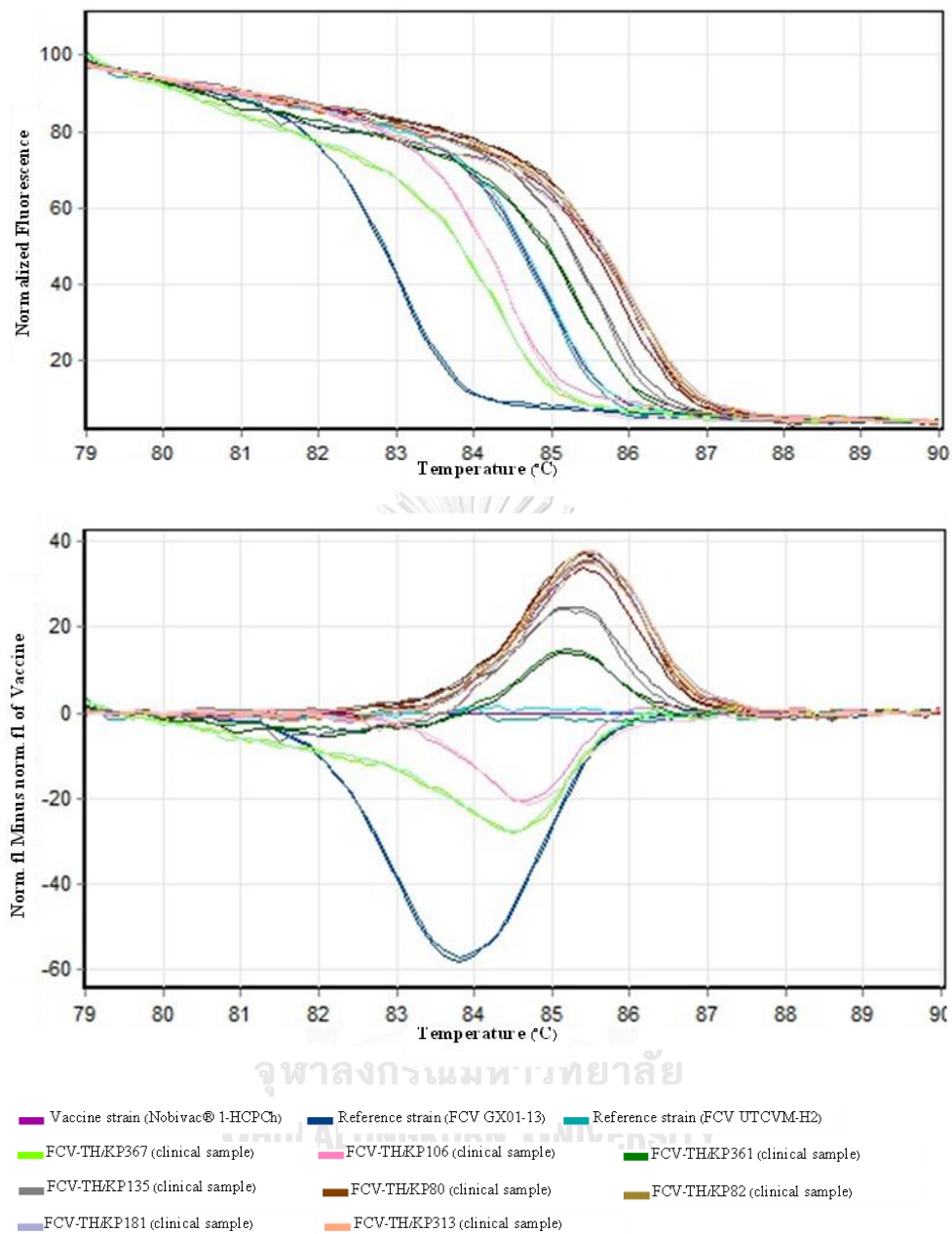


Figure 15 Feline calicivirus (FCV) strain differentiation by melt curve analysis. (A) HRM analysis normalized graph. (B) HRM analysis difference graph. Both HRM normalized, and difference graphs could distinguish seven FCV strain typing patterns from 11 strain template



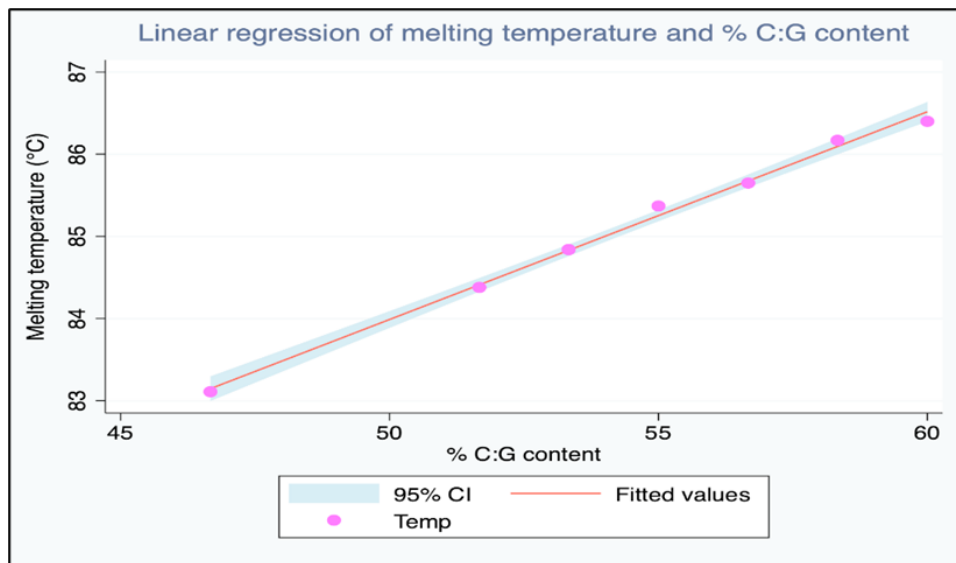


Figure 16 Linear regression analysis of the relationship between % C:G content of PCR product and  $T_m$  value.

#### Sensitivity and Specificity evaluation

HRM assay's sensitivity was evaluated using a ten-fold serial dilution of synthesized strings DNAs (FCV strain TIG-1), ranging concentration between  $10^{-1}$  and  $10^{-8}$  ng/ $\mu$ l ( $6.18 \times 10^1$  to  $6.18 \times 10^8$  copies/ $\mu$ l). As a result, the detection limit of assay indeed represented as  $6.18 \times 10^1$  copies/ $\mu$ l with cycle threshold (Ct) value lower than 35 (Figure 17a) and all dilution placed as the same melt curve alignment in normalized plot curve (Figure 17b). Additionally, the assay efficacy displayed a strong linear correlation between  $10^1$  and  $10^8$  copies/ $\mu$ l by the slope value as -3.418, coefficients of correlation ( $R^2$ ) as 0.998, and reaction efficient as 0.96 (Figure 17c).

To evaluate the specificity of HRM assay, the result highly revealed specificity to commercially available FCV-Vac (Nobivac<sup>®</sup> 1-HCPCh) and FCV-TH strain from the clinical sample. On the other hand, the emerging fluorescent caused by FIV, FeLV, FHV-1, FIP, and FeMV could not be detected before the positive cut-off value at Ct 35 (Figure 18).

### Efficiency in detecting the FCV mixed infection

The developed HRM assay successfully demonstrated the ability to distinguish the mock double FCV strains mixed infection in various concentrations ratio (1:4 to 4:1). Both normalized and difference HRM graph plots exhibited strain typing patterns in the same direction by the melt graph plot deviated along with a higher concentration template (Figure 19a, 19b). Meanwhile, the melt curve peaks also corresponded to  $T_m$  of each FCV strain and appeared on the different plots (Figure 19c).

### Determination of the clinical sample

Thirty-three of 44 clinical samples could be segregated the strain typing pattern by HRM assay in which known nucleotide sequences of the region between ORF1 and ORF2 ( nt 5214-5343) were derived from 14 samples. The qPCR amplification of all 33 samples revealed  $C_t$  value at less than 30, and the amplicons contributed to the sufficient quality of signals that could differentiate the strain typing patterns. Interestingly, two of 33 samples, a previously shown negative result from RT-PCR, revealed FCV positive with HRM assay and could further differentiate strain pattern. However, 11 of 44 clinical samples remained to show FCV negative with HRM assay in which the detectable  $C_t$  values showed between 33-35 (n = 6) and over 35 (n = 5).

After HRM analysis of 33 FCV-positive samples, seven different strain typing patterns of HRM melt plot curve were evident based on the  $T_m$  shift of altered C:G content. Those seven strains patterns consisted of two associated FCV-Vac typing patterns and five wild-types FCV-TH typing patterns by standard deviation on each group presenting between  $0^\circ\text{C}$  to  $0.099^\circ\text{C}$  (Table III-4). Interestingly, nine wild-type FCV-TH strains showed melt curve patterns related to two vaccine strains that are

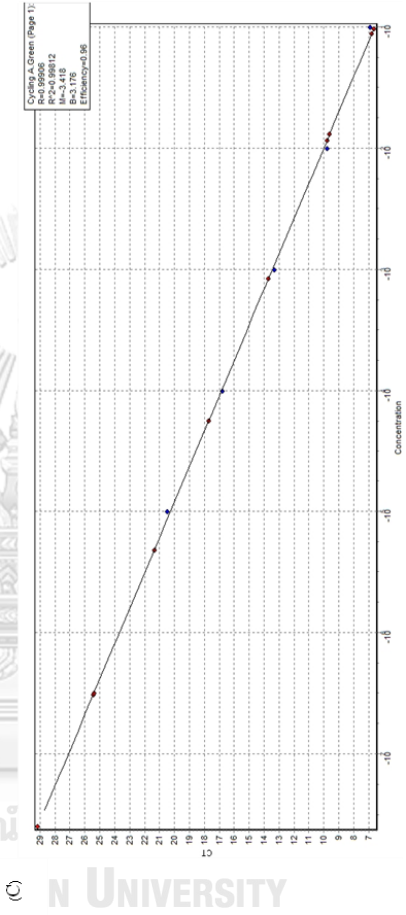
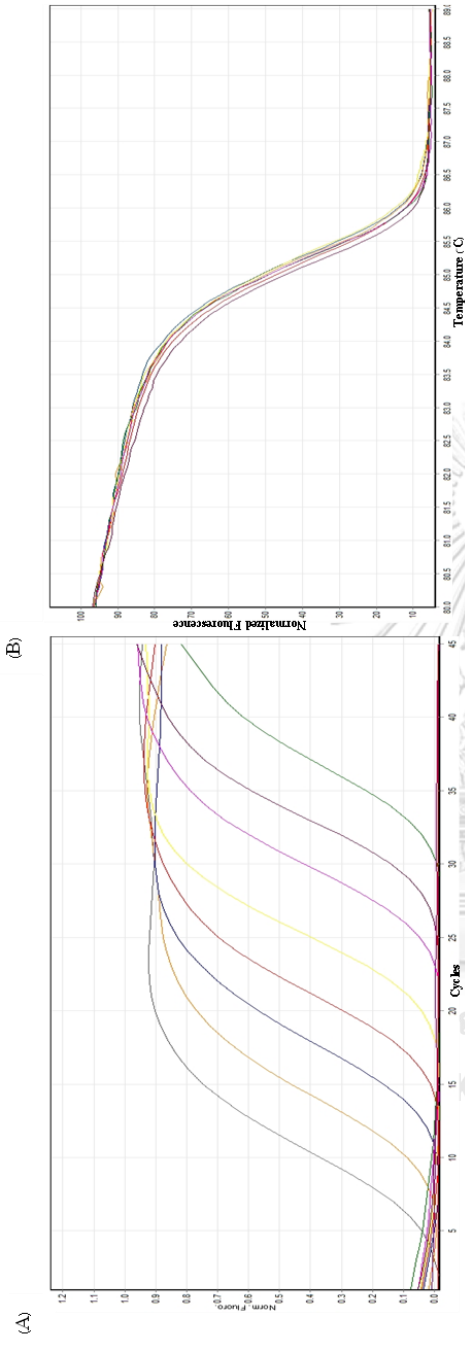
commercially available in Thailand. Additionally, all cats were healthy on the sampling date. Meanwhile, five cats had been vaccinated over three months before sample collection, and the other four cats did not receive any vaccination against the feline rhinotracheitis virus.

**Table 10** Mean melting temperature ( $T_m$ ) and standard deviation (SD) within the group of each feline calicivirus (FCV) strain detected from clinical samples

Strain typing	Number of samples	Mean $T_m$	SD
FCV-TH wild-type pattern 1	3	84.34	$\pm 0.023$
FCV-Vac related pattern 1 <sup>a</sup>	6	84.74	$\pm 0.018$
FCV-Vac related pattern 2 <sup>b</sup>	3	84.99	$\pm 0.099$
FCV-THA wild-type pattern 2	3	85.46	$\pm 0.094$
FCV-TH wild-type pattern 3	5	85.77	$\pm 0.074$
FCV-TH wild-type pattern 4	12	86.11	$\pm 0.068$
FCV-TH wild-type pattern 5	1	86.40	0

<sup>a</sup> FCV-Vac (Nobivac<sup>®</sup> 1-HCPCh)

<sup>b</sup> FCV-Vac (Felocell CVR<sup>®</sup>)



- Conc. 6.18 x 10<sup>8</sup> copies/μl
- Conc. 6.18 x 10<sup>7</sup> copies/μl
- Conc. 6.18 x 10<sup>6</sup> copies/μl
- Conc. 6.18 x 10<sup>5</sup> copies/μl
- Conc. 6.18 x 10<sup>4</sup> copies/μl
- Conc. 6.18 x 10<sup>3</sup> copies/μl
- Conc. 6.18 x 10<sup>2</sup> copies/μl
- Conc. 6.18 x 10<sup>1</sup> copies/μl

**Figure 17** Analytical sensitivity of HRM assay.

(A) The quantitative assessment in various concentrations of FCV-synthesis string DNA ( $6.18 \times 10^1$  and  $6.18 \times 10^8$  copies/ $\mu\text{l}$ ) was evaluated using qPCR and analyzed by HRM software. (B) The normalized graph of HRM analysis revealed the normalization region between 80-89 °C with a confidential threshold of 95%. The cut-off  $C_t$ -value of the positive sample was decided at  $C_t < 35$ . (C) The standard curve for indicating the efficiency of qPCR detection assay by x-axis referred to the ten-fold dilution of FCV-synthesis string DNA (ng/ $\mu\text{l}$ ), whereas the y-axis referred to the corresponding  $C_t$  values. The assay was linear in the range of  $6.18 \times 10^1$  to  $6.18 \times 10^8$  template copies/ $\mu\text{l}$  with a determination coefficient ( $R^2$ ) at 0.998 and reaction efficiency at 96.13%



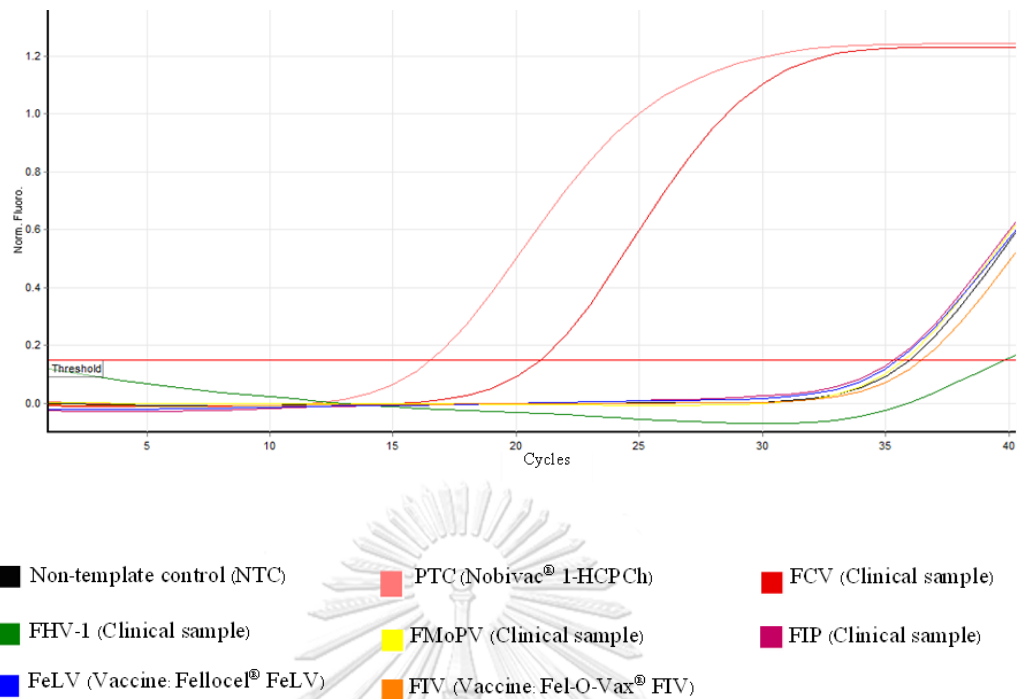


**Figure 18 Analytical specificity of HRM assay.**

The result showed HRM specific to both positive control (synthesis string DNA with concentration as  $6.2 \times 10^5$  copies/ $\mu$ l) and positive clinical sample. Non-template control and other virus templates, including FHV-1, FIV, FeLV, FIP, and FeMV, showed amplification over positive cut-off values (Ct > 35 cycles).

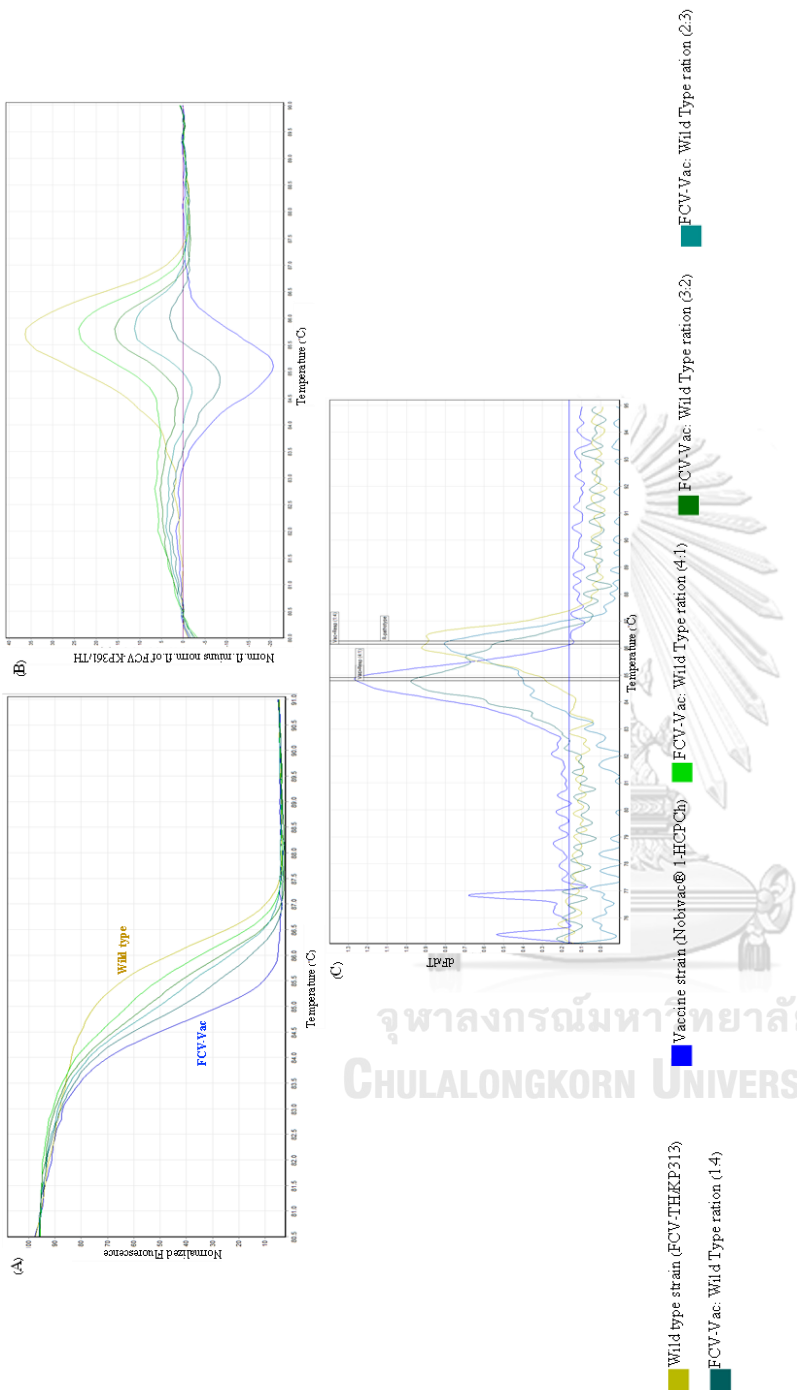


Figure 19 Analytical HRM assay of the mimetically mixed-infection model of FCV-TH strain (Wild type) and vaccine strain (FCV-Vac).

The pattern of HRM normalized graph (A) and HRM difference graph (B) demonstrated detectability patterns on each various concentration ratio. Melt curve analysis from HRM assay (C) represented the derivative melt peak patterns that seem likely to correspond to the divergence ratio of the strained mixture

## Discussion

Feline calicivirus (FCV) is still one common pandemic respiratory pathogen in cats, even though the vaccination is regularly applied. Meanwhile, driving to emerge the vaccine-resistance strain from long-term using of modified-lived vaccine is ongoingly concerned (Afonso et al., 2017; Smith et al., 2020). Moreover, FCV is regarded as a highly genetic diversity RNA virus, in which evolutionary mechanism usually results from either genetic drift or recombination (Coyne et al., 2006a; Coyne et al., 2006c; Coyne et al., 2007a). So, identifying genetic markers for differentiation, either genotype or pathotype, especially between virulent FCV and classical FCV, is still challenging (Brunet et al., 2019). Thus, a classical method as genome sequencing is still necessary for strain identification.

The junction between ORF1 and ORF2 has been noticed as a hot-spot recombination site of some *Caliciviridae* viruses, including Human Norovirus and FCV (Katayama et al., 2002b; Tajiri-Utagawa et al., 2009; Symes et al., 2015). Furthermore, this region has been noticed as a suitable region for genotyping Norwalk-like viruses (Katayama et al., 2002a). On the other hand, the remarkable region for genotyping of FCV is uncertainly caught. Hence, our study designed a pair of primers that flanks the junctional region of ORF1 and ORF2 for targeting to amplify a 99-bp product, which obviously differs between FCV-TH, vaccine, and other global strains for detection and strain differentiation. In addition, this study developed a functional diagnosis and differentiation method in which rapid, inexpensive, sensitive, and specific for FCV within a closed tube system.

High resolution melting (HRM) assay has been recognized as the simplest method for genotyping and mutation scanning that can identify a single base change in short fragments up to 400 bp (Reed and Wittwer, 2004; Tamburro and Ripabelli, 2017). Usually, changing the number of hydrogen bonds makes it easy to indicate a



purine to pyrimidine sequence modification because the temperature will be altered by about 1°C (Sun et al., 2019). Nonetheless, the transformation of C/G or A/T is hard to distinguish due to a slight alteration of  $T_m$  (Liew et al., 2004). In this study, our designated primer targeting to amplify a 99-bp segment revealed the capability to discern between wild-type FCV-TH and between other FCV global and FCV-Vac strains. Furthermore, the primers could also segregate between two commercially available FCV vaccines containing single nucleotide polymorphism (SNP) at T5269C (Felocell CVR®) and T5270G (Nobivac® 1-HCPCh).

The developed HRM assay in this study demonstrated that this technique could identify strain differentiation in terms of different strain co-infection by showing double peaks on melt peak analysis and shifting to the higher concentration template's side. Despite this, this mimetic mix-infection model could not be used to represent the recombination evidence that seems possible to emerge in long-term co-infection. However, we assure that the HRM assay can distinguish the new recombinant strain if the recombination event occurs at the amplification region.

The developed HRM assay had a detection limit at  $6.18 \times 10^1$  copies/ $\mu$ l and delicate as 0.25°C  $T_m$  shift in 1% C:G modification. The quality of the DNA template is also necessary for the optimal potential of HRM analysis (Toi and Dwyer, 2008b). According to the result of detection and strain typing of 44 clinical samples in this study, we found six clinical samples in which the viruses were detected between  $C_t$  value at 33-35 and unable to segregate HRM melt curve plot; they presented relatively faint amplified PCR bands when determined by agarose gel electrophoresis. Hence, the result should be interpreted cautiously when the late amplification ( $C_t$  values are higher than 30) occurs because it is usually accountable for a low amount of starting template and/or a high degree of sample degradation. On the other hand, two of 33 clinical samples showed FCV positive results by HRM assay, and even they

previously showed negative results from conventional RT-PCR. So, it could refer that HRM assay had more detectability potential than classical molecular technique. As following nucleotide sequence alignment, the result showed six alignment patterns of wild-type FCV-TH (Figure 1), while only four melt patterns were demonstrated by HRM assay (Figure 2). However, one known template sequence (FCV-TH/KP180) was excluded from the validation due to a depletion of the sample. The other FCV-TH sequence (FCV-TH/KP313) presented SNP at T5303G but displayed the same melt curve pattern with others. The mis-sequencing process probably causes it.

HRM analysis of 33 FCV positive samples demonstrated seven melt curve patterns, two of them referring to FCV-Vac. Additionally, this finding reported nine wild-type variants presenting the melt curve patterns like vaccine strain. Hence, expansion sequencing on the VP1 region may be needed to determine whether there is some FCV-Vac-related strain circulating in Thai cats. Besides, five melt curve patterns of wild-type FCV-TH revealed a conspicuously different pattern to vaccine strain in both the normalized melt curve graph and difference graph.

In conclusion, our results indicated that HRM assay is helpful for simultaneous detection and strain differentiation between the vaccine and wild-type FCV-TH strain. Moreover, the HRM assay developed in this study can also distinguish between the virulent FCV-TH (FCV-TH/KP361) and other wild-type FCV-TH strains.

### **Acknowledgment**

KP was granted by Chiang Mai University for Ph.D. Program. CP was supported by the Ratchadapisek Somphot Fund for Postdoctoral Fellowship, Chulalongkorn University. This study was supported by the 90<sup>th</sup> Anniversary of Chulalongkorn University Fund (Ratchadaphiseksomphot Endowment Fund). The Chulalongkorn

Academic Advancement into Its 2<sup>nd</sup> Century Project, Faculty of Veterinary Science, Chulalongkorn University is also acknowledged

### **Ethics Statement**

All experimental protocols were approved by the Chulalongkorn University Animal Care and Use Committee (No. 1631002). All procedures were done following the relevant guidelines and regulations.

### **Data accessibility**

All the data supporting our findings is contained within the manuscript. One full-length coding Feline calicivirus sequence has been deposited in NCBI GenBank under accession MZ542330.

### **Declaration of competing interest**

The authors have declared no competing financial or non-financial interests.

## CHAPTER IV

### Pathological Identification of Virulent Systemic Feline Calicivirus in Naturally Infected Cat revealed Neurotropism Aspect

#### Authors

Kannika Phongroop, Chutchai Piewbang, Somporn Techangamsuwan

Department of Pathology, Faculty of Veterinary Science, Chulalongkorn University, Pathumwan, Bangkok 10330 Thailand, Animal Virome and Diagnostic Development Research Group, Faculty of Veterinary Science, Chulalongkorn University, Bangkok 10330, Thailand

Anudep Rungsipipat, Sitthichok Lacharoje

Department of Pathology, Faculty of Veterinary Science, Chulalongkorn University, Pathumwan, Bangkok 10330 Thailand

จุฬาลงกรณ์มหาวิทยาลัย

Publication status: in preparation

CHULALONGKORN UNIVERSITY

## Abstract

Feline calicivirus (FCV) is a widespread contagious viral pathogen commonly causing mild self-limiting upper respiratory tract disease and oral disease in cats. In the last decade, highly virulent FCV strains, known as virulent systemic feline calicivirus (VS-FCV), had widely emerged and raised the mortality rate of infected cats. This study aimed to investigate the pathological change of naturally VS-FCV infected cats and localize the tissue tropism in various affected organs. Twenty-two necropsied cats with respiratory-associated symptoms were included in this study. Different tissue samples were collected for both molecular and pathological investigations for FCV and other feline pathogens. As a result, the molecular analysis showed three FCV-positive cats in which a cat (KP361) revealed RT-PCR positive in numerous organ tissues. In addition, full-length genome sequencing of this cat was conducted, and it showed nucleotide homology at 79.3% to FCV vaccine strains. Histopathology findings demonstrated interstitial pneumonia, hydropic degeneration of epidermal epithelial cells in ulcerative skin lesion, and degeneration of cryptal cells in the small intestine. Interestingly, the cerebrum and cerebellum represented lesions of vasogenic edema, gliosis, satellitosis, and apoptosis of neuronal cells. Immunohistochemistry and *in situ* hybridization were performed parallelly and showed immunoreactivity of protein and genomic antigen of FCV in both intracytoplasmic and intranuclear of the various cell types. Additionally, the transmission electron microscopy also indicated FCV viral particles in the intranuclear brain's neuronal cells. In conclusion, this is the first discovery of VS-FCV circulating in Thai cats. Although FCV is not a neurotropic virus, various cell types in the brain have shown the existence of FCV, both intranuclear and intracytoplasmic. So, further insight study about FCV-associated neuropathy should be emphasized.

**Keywords:** brain, ISH, neurotropism, pathology, TEM, VS-FCV

## Introduction

Feline calicivirus (FCV) is a non-enveloped, single-stranded, positive-sense RNA virus and belongs to genus *Vesivirus*, family *Caliciviridae* (Weiblen et al., 2016). FCV is a small RNA virus with approximately 7.7 kilobases (kb) that can be separated into three open reading frames (ORFs) (Symes et al., 2015; Pereira et al., 2018). FCV is recognized as a common causative viral pathogen of feline upper respiratory tract disease (FURTD). Classical clinical signs of FCV infection mainly compose ulcerative glossitis, gingivitis, conjunctivitis, rhinitis, and pneumonia (Hurley and Sykes, 2003; Radford et al., 2007; Gaskell et al., 2012). Although the mortality rate of FCV infection is usually low, fatal pneumonia can occasionally be developed in kittens (Monne Rodriguez et al., 2014). Furthermore, due to the virus's high genetic variability and variable cell tropism, pathogenesis and virulence are shown in various clinical manifestations (Monne Rodriguez et al., 2014), like self-limiting, lameness due to acute synovitis (Dawson et al., 1994), and systemic disease. A few decades ago, emerging of highly virulent FCV strains, known as virulent systemic FCV (VS-FCV), was widespread noticed in many countries (Pedersen et al., 2000a; Hurley et al., 2004; Coyne et al., 2006b; Schulz et al., 2011). The typical clinical signs of VS-FCV infection usually represent cutaneous edema (mostly on head and limb) and mucosa and skin ulceration (mainly at oral cavity, nares, pinnae, and footpads).

Moreover, multiorgan necrosis is occasionally revealed where the most commonly affecting organs are liver, spleen, pancreas, and lungs (Pedersen et al., 2000a; Pesavento et al., 2004; Coyne et al., 2006b). Interestingly, although the common clinical sign and detection of FCV are associated with the respiratory tract, there is a publication showing the FCV detection in feces of shelter cats (Zhang et al., 2014). Accordingly, the replication ability in the enteric tract of some FCV strains has been reported (Mochizuki, 1992; Radford et al., 2007), and there are some suggestions that some FCVs strains may promote enteric tropism and ultimately

serve as enteric pathogens (Di Martino et al., 2020). Thus, FCV should be considered as a causative viral pathogen in the diagnostic algorithm of feline viral enteric diseases.

Genetic diversity leads to quasispecies virus evolution, especially RNA virus. Besides, the mortality rate of FCV infection is previously recognized as low (1-2% ) (Wong et al., 2013). However, a severe clinical sign and a higher mortality rate raising to 60% have been published several times in the last ten years (Hurley et al., 2004; Prikhodko et al., 2014). Although the FCV vaccine seems likely to reduce the severity of classical signs of FCV infection, it does not show potency to protect animals from either infection or virulent form (Radford et al., 2007; Caringella et al., 2019). Due to the genetic instability of FCV, it is being a motivative force to the further investigation for more understanding the pathogenesis and tissue interaction and searching the preferable effective disease prevention still challenges.

The traditional and gold standard viral identification method is still a cell culture technique, but it is time-consuming, laborious, and high cost. Therefore, molecular techniques, such as reverse transcription polymerase chain reaction (RT-PCR) (Wilhelm and Truyen, 2006), nested RT-PCR (Marsilio et al., 2005), and quantitative RT-PCR (qRT-PCR) (Abd-ElDaim et al., 2009), have been developed for rapid detection and are helpful for clinical diagnosis. Immunohistochemistry (IHC), *in situ* hybridization (ISH), and transmission electron microscope (TEM) are the additional viral identification techniques in tissues and cells. Currently, the identification effort of FCV in many tissues has been represented continuously (Pesavento et al., 2004), but it still limits and focuses mainly on the respiratory system (Monne Rodriguez et al., 2014). Hence, investigation of FCV associated with tissue localization in multiple organ involvement will advantage and result in more understanding of FCV cell tropism.

In this study, we mainly focused on necropsied cats with the respiratory associated clinical feature. We performed an RT-PCR assay to detect genomic FCV and conducted IHC, ISH, and TEM for FCV localization in various tissue tropisms of a VS-FCV infected cat. Our findings also proposed information on the molecular characterization of the detected FCV strain.

## **Materials and Methods**

### **Necropsied cats and sample collection**

Samples were received from 22 cats that died with clinical signs associated with respiratory problems and submitted to the Department of Pathology, Faculty of Veterinary Science, Chulalongkorn University for routine necropsy between 2020-2021. Postmortem workups were performed, and macroscopic lesions were recorded systematically. Tissue samples were duplicated collected for histopathological study as formalin-fixed tissues and molecular analysis as fresh frozen tissues. FCV was detected using self-designed primers (Phongroop et al., 2018a). In addition, other feline viral pathogens such as feline herpesvirus-1 (FHV-1), feline panleukopenia virus (FPLV), feline leukemia virus (FeLV), feline immunodeficiency virus (FIV), feline coronavirus (FCoV), feline morbillivirus (FeMV), and feline bocavirus (FBoV) were screened using primer set from previous publications (Mochizuki et al., 1996; Ksiazek et al., 2003; Piewbang et al., 2019; Chaiyasak et al., 2020).

### **Samples preparation and feline viral detection by molecular technique**

The fresh frozen tissues were homogenized in 1% sterile phosphate-buffered saline (PBS) and centrifuged at 6000 g for 1 min, and then the supernatants were collected in a 1.5 ml microcentrifuge tube. Both DNA and RNA nucleic acid were extracted using QIAamp<sup>®</sup> cadior Pathogen Mini Kit (Qiagen GmbH, Germany). In brief,



the mixture of 200  $\mu\text{l}$  sample solution, 100  $\mu\text{l}$  of buffer VXL and 20  $\mu\text{l}$  of proteinase K was prepared and incubated for 15 min at room temperature. Afterward, the protocol was conducted following the manufacturer's recommendation. The concentration of extracted nucleic acid was quantified and qualified using a NanoDrop Lite Spectrophotometer (Thermo Fisher Scientific Inc., USA) and then kept at  $-80^{\circ}\text{C}$  until used.

The genomic extracted samples were used for screening the FCV and other feline viruses as mentioned above using Qiagen<sup>®</sup> OneStep RT-PCR Kit (Qiagen GmbH, Germany) for conventional RT-PCR and GoTaq Green Master Mix (Promega, USA) for conventional PCR. The primers used for FCV detection were FCV\_1F (5' - GTAAAAGAAATTTGAGACAATGTCT-3'), and FCV\_414R (5' -GTGAGCTGTTCTTTGCACAT-3'), which amplified 414 base pair (bp) fragments consistent to the conserve region on the ORF-1. The amplification process was run following the manufacturer's protocol. Briefly, a total reaction volume of 25  $\mu\text{l}$  consisting of a mixture of QIAGEN OneStep RT-PCR Enzyme Mix, 10mM of dNTP in 5x QIAGEN OneStep RT-PCR Buffer, 0.6  $\mu\text{M}$  final concentration of each primer, and 3  $\mu\text{l}$  of the template. The cycling condition was initially started with a reverse transcription step at  $50^{\circ}\text{C}$  for 30 min, then an initial denaturation at  $95^{\circ}\text{C}$  for 15 min, followed by 40 cycles of  $94^{\circ}\text{C}$  for 30 sec,  $59^{\circ}\text{C}$  for 30 sec and  $72^{\circ}\text{C}$  for 1 min, then a final extension at  $72^{\circ}\text{C}$  for 10 min. The PCR products were visualized using capillary electrophoresis (Qiaxcel<sup>®</sup>, Qiagen GmbH, Germany). Positive amplicons were purified and submitted for commercial bi-directional Sanger's sequencing (Macrogen Inc., South Korea) to verify the presence of FCV.

### Sequencing and phylogenetic analysis

To investigate the genetic correlation of identified FCV strain in this study, multiple RT-PCR amplifications for whole-genome sequencing were consequently proceeded in the positive sample using a self-designed primer. Briefly, the RT-PCR reactions were processed employing Qiagen® OneStep RT-PCR kit in a reaction volume of 50  $\mu$ l, constituting of a mixture of QIAGEN OneStep RT-PCR Enzyme Mix, 10mM of dNTP in 5x QIAGEN OneStep RT-PCR Buffer, 10  $\mu$ M final concentration of each primer and 10  $\mu$ l of the template. Thermocycler conditions included 50°C for 30 min for the RT step, and an initial denaturation at 95°C for 15 min, followed by 40 cycles of 94°C for 10 sec, 60.5°C for 45 sec and 68°C for 2 min, then a final extension at 72° C for 10 min. The PCR products were visualized using 1% (w/v) gel electrophoresis, purified, and submitted for bi-directional Sanger sequencing as mentioned above.

The obtained sequences were assembled and compared with published FCV genome retrieving from the GenBank database, including Urbana strain (Accession no. L40021) as a reference strain using BioEdit Sequencing Alignment Editor Version 7.2.5. The phylogenetic analysis was carried out on the whole genomic nucleotide sequence by MEGA X (Kumar et al., 2018) and inferred using the maximum likelihood (ML) method. Dendrogram of genetic relationship was constructed according to the Bayesian information criterion with 1000 bootstrapped replicates. The bootstrap values were significantly considered when more than 70. Substitution models of the evolutionary tree were selected based upon the best fit model. Twenty percent genetic distance threshold between sequences was consumed to define as the distinct strains (Radford et al., 2001b; Prikhodko et al., 2014; Hou et al., 2016).

### **Histopathology**

Formalin-fixed paraffin-embedded (FFPE) tissues from various organs, including skin, trachea, lung, mesenteric lymph node, small intestine, and brain were cut at 3- $\mu$ m thickness and stained with hematoxylin and eosin (H&E) following the standard protocol for histopathological examination. In addition, consecutive sections for IHC and ISH were also cut and placed on positively charged slides.

### **Immunohistochemistry (IHC)**

Various tissue sections, including lung, trachea, facial skin, intestine, and brain in which FCV positive by RT-PCR were immunohistochemically stained to confirm and determine cell tropism and FCV localization pattern. Then, horseradish-peroxidase (HRP) method was applied using the Dako REAL EnVision Detection System (Dako, Glostrup, Denmark) for detection of the positive antigen-antibody signal according to the previous description (Wardhani et al., 2021).

Briefly, after the deparaffinization and rehydration of the FFPE sections, they were washed with 1x PBS before performing the antigen retrieval step by autoclaving at 121°C for 15 min in citrate buffer pH 6.0. Then, blocking endogenous peroxidase activity was conducted by soaking the slides in 3% (v/v) hydrogen peroxide (H<sub>2</sub>O<sub>2</sub>) for 15 min at room temperature. Also, the immersion in 5% (w/v) skim milk at 37°C for 60 min was employed to block non-specific reactions. Next, the primary monoclonal anti-FCV antibody (dilution 1:100; Abcam, ab33990, UK) was applied and incubated the slide overnight at 4°C. Subsequently, the anti-mouse/rabbit secondary antibody (Dako REAL EnVision Detection System) was applied and followed by labeling with 3,3'-diaminobenzine (DAB). Lastly, hematoxylin was used as a counterstain, then cover slides was applied and determined under the light microscope.

### Riboprobe preparation and *in situ* hybridization (ISH)

To detect the FCV mRNA *in situ*, a DNA probe was prepared from the amplification region of the conserved site on ORF1 (nt 1 to 414) of the FCV genome. The PCR product amplified from the RNA extracted sample was resolved in 2% (w/v) gel electrophoresis, then purified using Monarch<sup>®</sup> DNA Gel Extraction Kit (New England BioLabs Inc, USA). According to the product's instructions, a DNA probe covering 414 bp of the ORF1 gene of FCV was synthesized using a PCR DIG Probe Synthesis Kit (Roche Diagnostics, Switzerland). The PCR reaction was performed under the same thermal cycling conditions described above, except using the digoxigenin (DIG)-labeled oligonucleotides instead of the normal oligonucleotides. In addition, the hybridization probe was evaluated by size resolution on 2% (w/v) agarose gel electrophoresis.

Examined tissues (included the organs parallel to IHC) were prepared for ISH procedure. The ISH with chromogenic DNA was performed as previously reported (Piewbang et al., 2019) with some modifications. Briefly, each 3- $\mu$ m-thick FFPE slide was deparaffinized, rehydrated, and subsequently rinsed in deionized water (DI). After that, the slides were treated by incubation in citrate buffer pH 6.0 in 95°C for 20 min. Slides were then washed three times in DI for 5 min each. Next, cold 3% (v/v) H<sub>2</sub>O<sub>2</sub> in absolute methanol was applied on each slide for 10 min to eliminate the endogenous alkaline phosphatase. Then, the slides were soaked with DI thrice for 5 min each. Then, slides were prehybridized in prehybridization buffer 50% (v/v) formamide, 4X sodium SSC at 37°C for 10 min, followed by incubation with hybridization buffer containing 5X SSC, 5X Denhardt's solution, 100  $\mu$ g/mL sperm DNA, and 0.5% (w/v) sodium dodecyl sulfate, and 10 ng/ $\mu$ l of the synthesized FCV probe at 50°C for overnight in a moist chamber.

Meanwhile, a hybridization buffer containing a DIG-labeled FCV probe was also placed on each FCV negative slide as an additional negative control. Then slides were soaked in the series of buffer standard saline citrate, including 2X SSC at pH 7.0–7.4 at 37°C for 15 min, 1X SSC at 42°C for 15 min, and 0.5X SSC at 42°C for 15 min. For blocking non-specific binding, all slides were immersed with a blocking solution mixture composed of 5% (w/v) bovine serum albumin in blocking solution, then were incubated at room temperature for 1 hr. After non-specific blocking, 100 µl of anti-DIG-AP Fab fragments (Roche Diagnostics, Switzerland) (dilution 1:200 in 1X Blocking solution) were applied on each slide and further incubated in the moist chamber for 1 hr at room temperature. After thrice washes with DI for 5 min each, Liquid permanent red (LPR) (Dako, Denmark) was applied in the dark chamber at room temperature for 20 min. Slides were then counterstained with hematoxylin and wright green, dehydrated, and mounted with coverslips.

### **Transmission electron microscopy (TEM)**

TEM technique was used to elucidate the FCV viral particles in selected positive tissue to support RT-PCR, IHC, and ISH. All TEM procedures were performed by pop-off technique according to previously described (Piewbang et al., 2020; Piewbang et al., 2021a; Piewbang et al., 2021b) and FCV virions were inspected at 80 kV by HT7800 (Hitachi, Japan).

## **Results**

### **Sample collection and FCV molecular screening**

Twenty-two necropsied cats with major history of acute respiratory distress were included. After performing feline viral molecular screening, Four of twenty-two cats (18.18% ) were positive for FCV. However, all of them were co-detected with

FHV-1 (cat no.1) and FBoV (cat no.6, 11, 13) (Table 11). In addition, cat no.1, who presented clinical signs likely VS-FCV infection, demonstrated a strongly positive RT-PCR reaction in several organs (lung, spleen, facial skin, tongue, mediastinal lymph node) (Figure 20).



Table 11 Molecular screening result of feline viral pathogen and organs of detection

Cat No.	Molecular screening of Feline viral detection.					Organs of FCV detection
	FCV	FHV	FBoV	FPLV	FCoV	
1	+	+	-	-	-	Lung, Trachea, Spleen, Cerebellum, Cerebrum, Heart, Stomach, Duodenum, Jejunum, Ileum, Kidney, Pancrease, Mesenteric lymph node
2	-	-	-	N/A	N/A	
3	-	-	-	N/A	N/A	
4	-	-	-	N/A	N/A	
5	-	-	-	N/A	N/A	
6	+	-	+	-	-	Cheek, tongue, tonsil, eyelid, trachea
7	-	-	-	N/A	N/A	
8	-	-	-	N/A	N/A	
9	-	-	-	N/A	N/A	
10	-	-	+	N/A	N/A	
11	-	-	+	N/A	N/A	Lung (weak signal)
12	-	-	+	-	N/A	
13	+	-	+	-	-	Lung (weak signal)
14	-	+	-	N/A	N/A	
15	-	+	-	N/A	N/A	
16	-	+	-	N/A	N/A	
17	-	+	-	N/A	N/A	
18	-	-	-	N/A	N/A	
19	-	-	+	N/A	N/A	
20	-	-	-	N/A	N/A	
21	-	-	-	N/A	N/A	
22	-	-	+	N/A	N/A	

<sup>a</sup> N/A (not applicable)

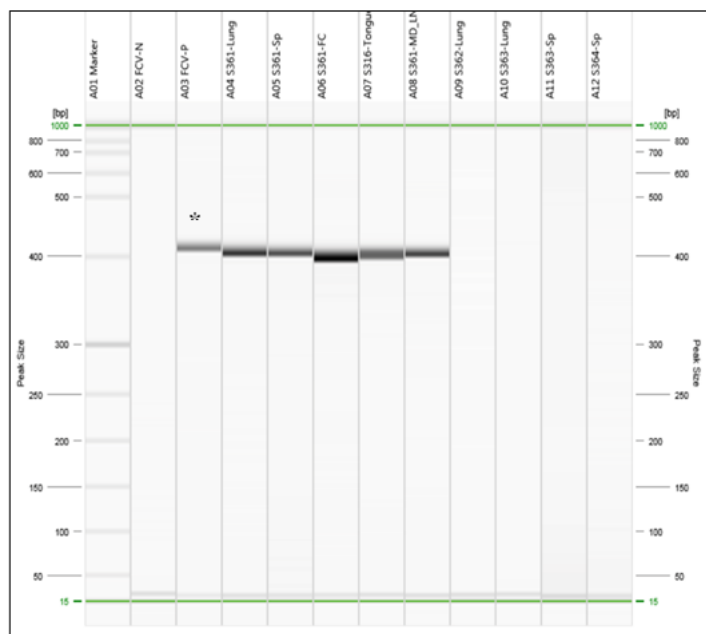


Figure 20 RT-PCR results of Feline calicivirus (FCV) were determined using capillary electrophoresis (Qiaxcel®).

The positive control was demonstrated as \*. Derived nucleic acids from fresh tissue extractions including lung, spleen (Sp), facial skin (FC), tongue, and mediastinal lymph node (MD LN) were investigated for FCV.

จุฬาลงกรณ์มหาวิทยาลัย  
CHULALONGKORN UNIVERSITY

#### Sequencing and phylogenetic analysis

The complete coding sequence from cat no.1 was obtained with 7671 nucleotides (nt). Phylogenetic analysis of various whole-genome FCV strains could divide FCV into two genogroups (genogroup I and II) in which the genogroup I composed of four clusters (Figure 21). In addition, cat no.1's strain (KP361) was filled in genogroup I in the same cluster with other vaccine strains by sharing 72.7 – 79.3% nucleotide homology to different strains in the cluster.



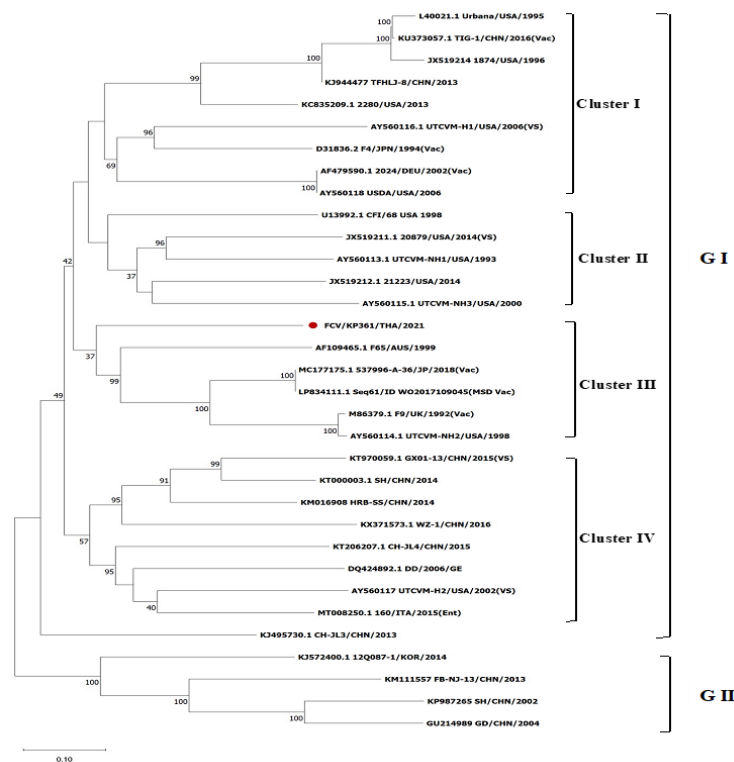


Figure 21 Phylogenetic correlation of FCV from cat. no.1 (red circle) with distinct strains from the GenBank database.

The phylogeny was constructed based on whole-genome nucleotide sequence using MEGA X software by maximum likelihood method with 1000 bootstrap values

### Gross lesion and histopathology

Twenty one of twenty-two cats did not present any abnormality of external appearance except one cat. Interestingly, one kitten (cat no.1: KP361) showed gross lesions similar to the VS-FCV infection, including facial edema, conjunctivitis, skin ulceration at the nostril, and sudden death. Cat no.1 (KP361) is a 6-month-old, non-vaccinated, female, domestic short hair cat. She was brought to a private clinic with clinical signs of subcutaneous edema at face, conjunctivitis, epiphora, respiratory distress, and acute death. The gross findings revealed pulmonary edema, mild congestion and grey hepatization at left caudal lobe. In brain, mild congestion was

observed in the cerebral area ( Figure 22) . Surprisingly, other organs showed unremarkable lesions on gross.



**Figure 22** Gross lesion of cat no.1.

Displaying facial edema, mild skin ulceration of nostril, mild congestion in the cerebral and cerebellum, and red hepatization in the right caudal area of a caudal lung lobe.

The histopathological findings revealed the desquamation of bronchiole and alveolar epithelial cells, some bronchiole epithelial cell also demonstrated karyolysis and pyknotic nuclei. Mild interstitial pneumonia with type II pneumocyte hyperplasia was also demonstrated ( Figure 23a) . Moreover, some alveolar macrophages also infiltrated in the alveolar space ( Figure 23b) . The skin lesion revealed the diffuse ballooning degeneration and subepidermal cleft of basal epithelial cells with subepidermal clefts. The infiltration of neutrophils, lymphocytes, and mononuclear cells were found in the epidermal and dermal layers ( Figure 23c) . Intestinal epithelial cells showed the degeneration of cryptal cells and collapsed villi ( Figure 23d) . In

brain, both cerebrum and cerebellum notably presented the histopathological change. Cerebral grey matter revealed diffuse gliosis ( Figure 23e) , whereas perineuronal satellitosis and some dark neurons are also presented in the cerebral parenchyma (Figure 23f)

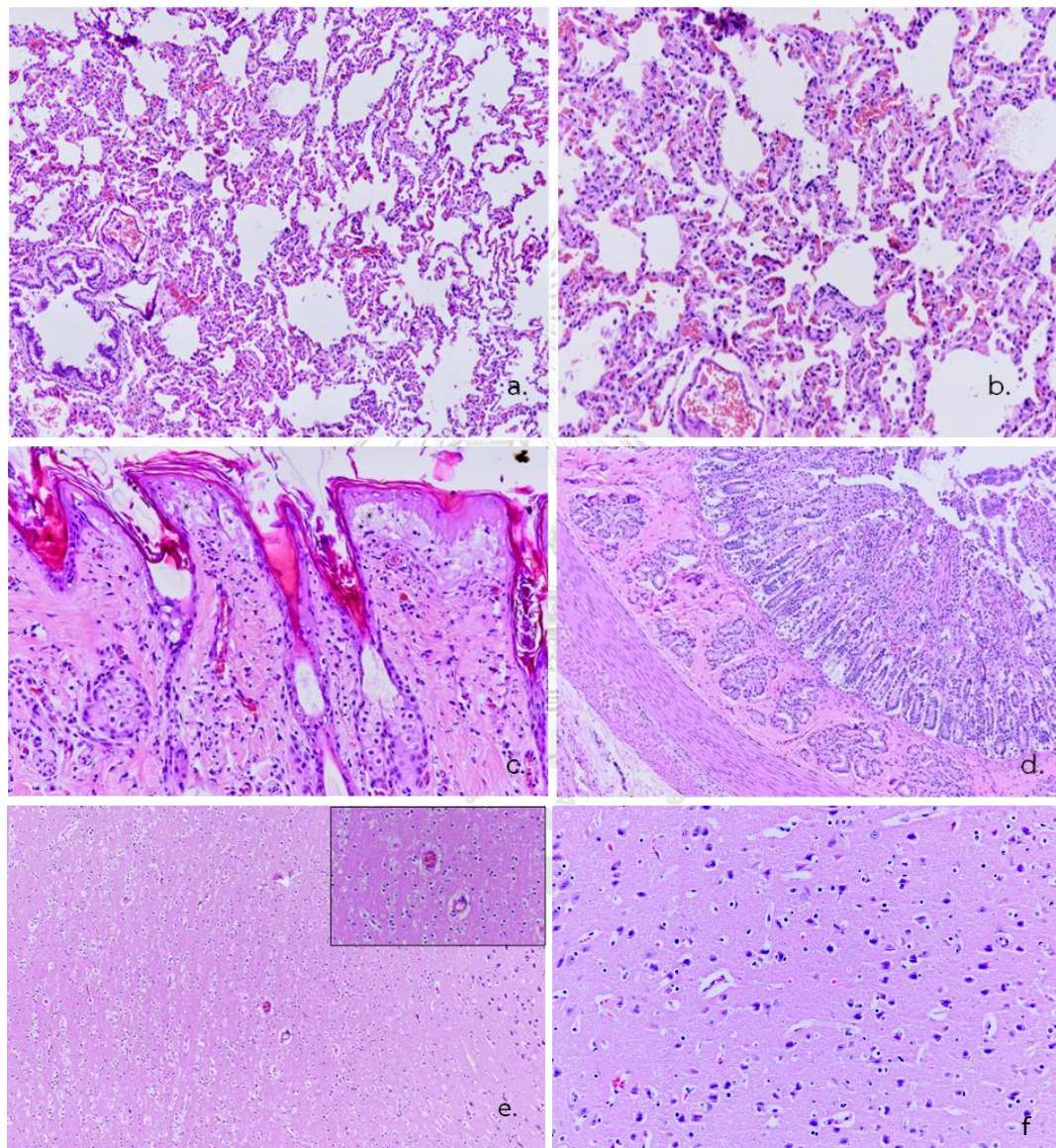


**Figure 23** Histological features of FCV were associated with numerous affected tissues by Hematoxylin & eosin staining (H&E).

(a) Lung; Interstitial pneumonia with type II pneumocytes hyperplasia and desquamation of bronchiole and alveolar epithelium cell (100x). (b) Lung; a



moderate number of alveolar (200x). (c) Skin; ballooning degeneration of basal epithelium cell with subepidermal clefts (asterisks). Infiltration of inflammatory mononuclear cells and some neutrophils in effected epidermis and dermis (400x). (d) Duodenum; degenerated cryptal cells and collapsed (100x). (e) Cerebrum; Presentation of widening space around blood vessel in cerebral grey matter (vasogenic edema) (inset: 400x) and diffuse gliosis in cerebral parenchyma (100x). (f) Cerebrum; Demonstration of mild perineuronal satellitosis and some of dark neuron in cerebral parenchyma. (200x)

### **Immunohistochemistry**

The representation of viral protein antigen in the affected tissue, including skin, tongue, lung, trachea, intestinal, and brain (Figure 24), displayed immunoreactivity in various cells. Strong immunoreactivity of epithelial cells in the lesion of skin epithelial necrosis was shown, and intracytoplasmic immunoreactivity was also demonstrated in the inflammatory mononuclear cells in the dermis (Figure 24a). Moreover, immunoreactivity to FCV protein antigen was presented intracytoplasmic of vascular endothelial cell of skin. Tracheal epithelial cells and epithelial cells lining of the tracheal gland displayed a strong intracytoplasmic immunoreactivity (Figure 24b). In small intestine, antigen-antibody complex also strongly presented in the cytoplasm of enterocyte and in the nucleus of submucosal nerve cells (Figure 24c and 24d). Meanwhile, intranuclear and intracytoplasmic immunoreactivity to FCV viral protein antigens were also found in neuronal cells and glial cells in brain tissue (Figure 24e and 24f).

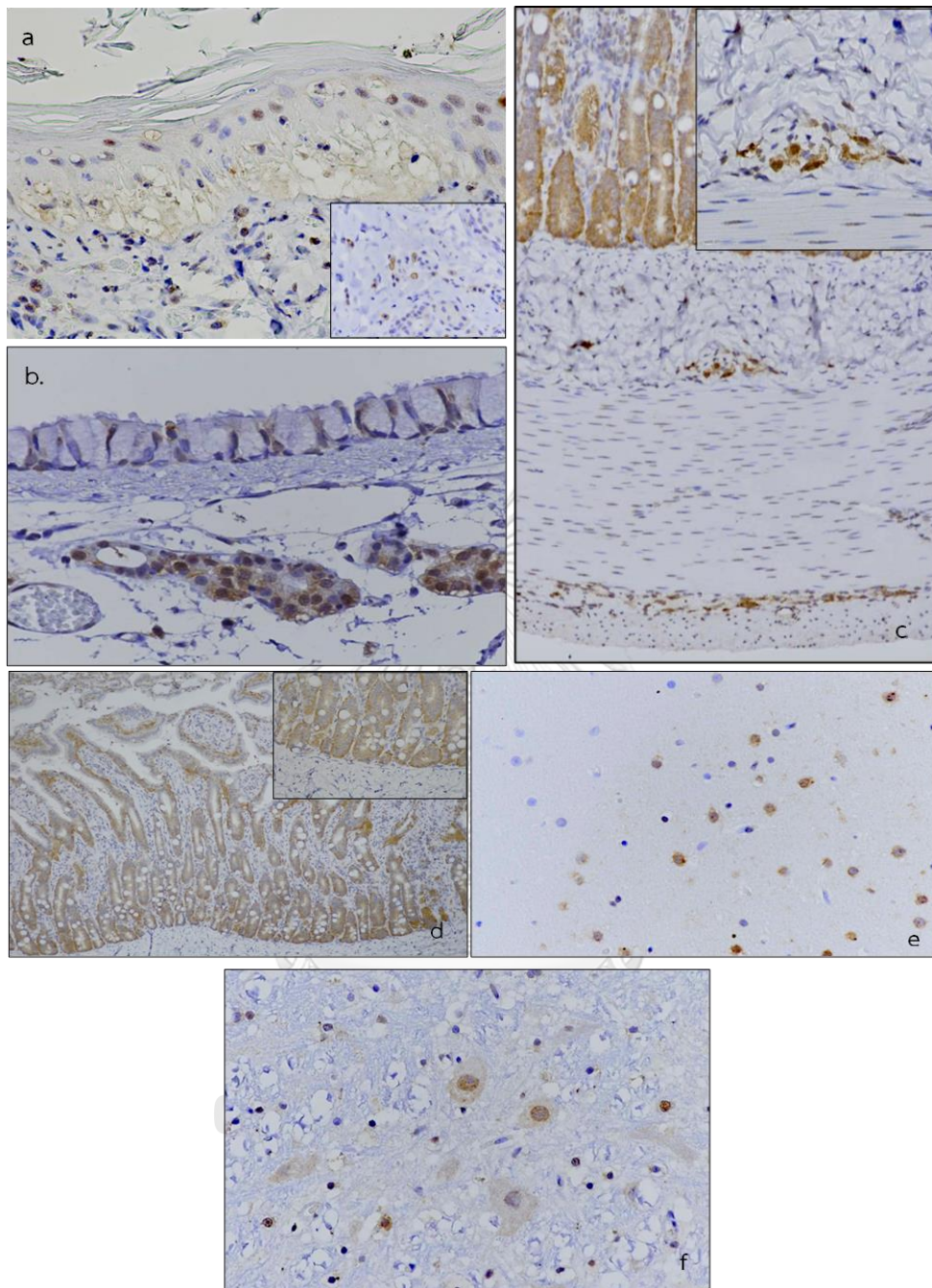


Figure 24 Feline calicivirus protein antigen was revealed by immunohistochemical (IHC) stain in various organs of cat no.1.

(a) **Skin**; immunoreactivity was showed in the epithelial cell in the lesion of the epithelial necrosis and intracytoplasm of diffuse dendritic cells (DCs) in the dermis (inset) (200x). (b) **Trachea**; strong immunoreactivity in the intracellular ciliated

epithelium of trachea and epithelium cell lining of the bronchiolar gland (400x). **(c) Small intestine;** strong intranuclear immunoreactivity at submucosal nerve ganglion (inset) (100x). **(d) Small intestine;** diffuse of strongly immunopositivity of enterocyte and goblet cell in the mucosal layer (200x). **(e) Brain;** immunoreactivity of FCV viral protein antigen was diffusely demonstrated in neuronal cells located in the cerebellar cortex (200x). **(f) Brain;** strong intranuclear immunoreactivity in the neuronal cell (arrowhead) and intracytoplasmic of glial cells (arrow)(400x)

#### ***In situ* hybridization**

Along with the demonstration of FCV protein antigen by IHC, genomic mRNA of FCV was also displayed by RNA-ISH in various tissue samples of cat no.1. The respiratory epithelial cells exhibited diffuse intracytoplasmic FCV genomic signal in bronchiolar epithelial cells (Figure 25). Moreover, the viral nucleic signals also localized in the intracytoplasmic dermal epithelial cells and necrotic follicular epithelial cells (Figure 26b). Moreover, the ISH signals were also exhibited within the intracytoplasmic of various intestinal cells, including intestinal cryptal cells and stromal supporting cells in villi (Figure 26a). In brain, the positive signal represented in neuronal cells and glial cells in cerebral parenchyma (Figure 26c and 26d).

#### **Transmission electron microscopy**

Two sizes of viral particles, approximately 80 nm, and 40 nm, were localized in the nucleus of neuronal cells of cerebral tissue (Figure 27). The smaller viral particle measuring about 40 nm displayed icosahedral capsid structure and surface indentations typical of *Caliciviridae*.

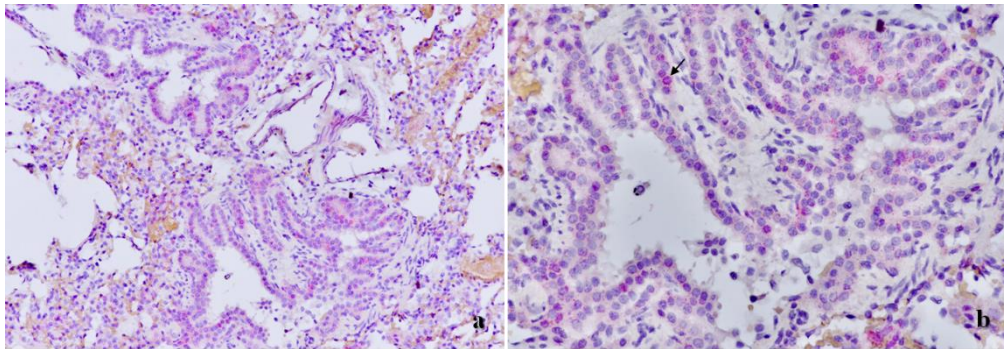


Figure 25 In situ hybridization (ISH) identified FCV genomic antigen in respiratory epithelial cells.

(a) Bronchiolar epithelial cells diffusely presented the ISH signal; (100x) (b) High magnification displayed intracytoplasmic strong genomic signal of FCV antigen in bronchiolar epithelial cell (arrow); (400x).

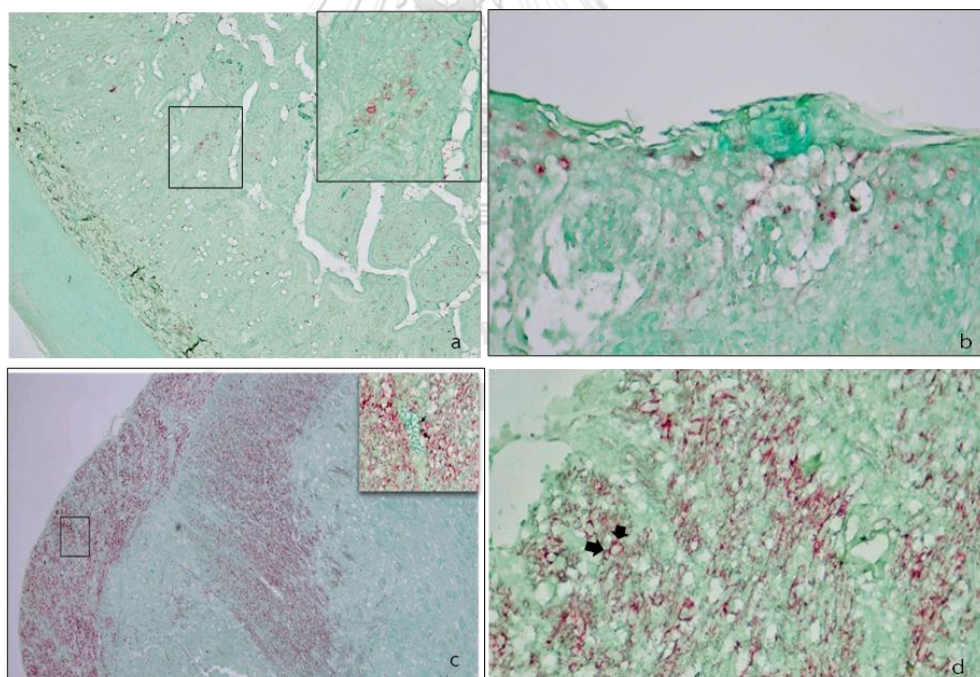
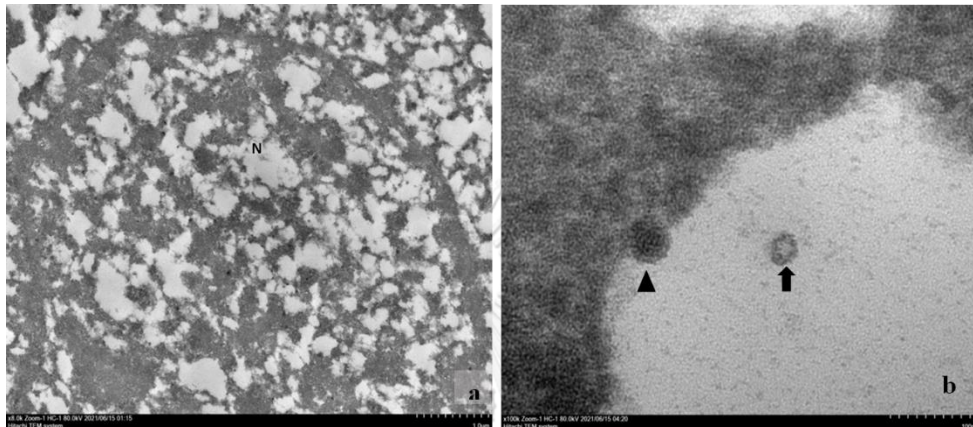


Figure 26 *In situ* hybridization (ISH) signals indicated the FCV genome in various cells.

(a), The nucleic signals were displayed in the intracytoplasmic of intestinal cryptal cells and stromal supporting cells of the small intestine (100x). (b) The strong genomic signals were identified at the intracytoplasmic of various skin epithelial cells



(400x). (c) The strong signals were showed in a wide area of the cerebral cortex and presented the signal in endothelial cell of the blood vessel (arrow in insert) (200x). (d) The brain tissue revealed the genomic signal of FCV in neuronal cells (arrow) (400x).



**Figure 27** The ultrastructure of the mixed infected brain of cat no 1.

(a) TEM revealed a neuronal cell containing viral particle within the nucleus (N); scale bars as 1.0  $\mu\text{m}$ . (b) Two sizes of viral particles were identified. The larger viral particle (arrowhead) displayed size approximately 2 times compare with the smaller. The smaller viral particle (arrow), measuring size about 40 nm, displayed an icosahedral capsid structure and surface indentations typical of Caliciviridae; scale bars as 100 nm.

### Discussion

This study demonstrated the first evidence of VS-FCV infection in a Thai cat. There were three cats whose tissue samples were positive for FCV from RT-PCR. In addition, one cat (Cat no.1) revealed positive results in numerous tissue samples by showing clinical signs resembling the previously described VS-FCV cases in several countries (Pedersen et al., 2000a; Schorr-Evans et al., 2003; Coyne et al., 2006b; Battilani et al., 2013). Furthermore, this finding revealed the remaining FCV genome in various tissue samples of cat no.1, especially the skin, lung, intestine, and brain. As



known that the typical cell tropism of FCV is the epithelial cells in which the viral antigen frequently presents in the cytoplasm of epithelial lining cells of mouth and tongue (Pesavento et al., 2004). Besides, the molecular detection of viral antigens in VS-FCV affected cats is also positive in various cell types such as epithelial cells and endothelial cells in organs (Mochizuki, 1992; Truyen et al., 1999). The finding of mature viral particles has also been documented within the nucleus of epithelial cells by TEM (Pesavento et al., 2004). FCV passes into the host cell via feline junctional adhesion molecule A (fJAM-A) receptor, which presents on the surface of the epithelial and endothelial cells.

Additionally, fJAM-A is also expressed on the surfaces of erythrocytes, platelets, and leukocytes (Lu et al., 2018). Besides the epithelial lining of the skin, intestinal, and lung tissue, the result of this study also displayed FCV antigen expression in the cytosol of the inflammatory mononuclear cells, as likely have stated by former studies (Wobus et al., 2004; Monne Rodriguez et al., 2014). Likewise, our finding presents remarkable detection of both FCV protein antigen and genomic signal remaining within neuronal cells in various organ tissues, including skin, tongue, muscular layer of the intestine, and brain. Interestingly, even though FCV is not a neurotropic virus, the publications to locate FCV in the various neurotropism cells, including neurons, glial cells, and pericyte, have occasionally been shown (Sato et al., 2004; Battilani et al., 2013; Wardhani et al., 2021). However, the explanation for the detection of FCV within neurotropism is still unclear.

On the other hand, *Caliciviridae* including within the same order as *Piconarviridae*; Order *Piconavirales*, in which blood-brain barrier (BBB) and neuromuscular junctions (NMJs) are mainly entry routes to the central nervous system (Koyuncu et al., 2013). Thus, we hypothesize that the infected leukocytes may transport the virus pass BBB, which comprises the brain microvascular

endothelium cells (BMVECs) with specialized tight junctions, into the brain parenchyma and other surrounding cells such as microglia, neuron, and pericyte. So, this is supposed to be the point of interest for further investigating the nervous system infection of FCV.

In conclusion, this study provides interesting insight into VS-FCV tropism, especially in neurotropism. Furthermore, our data on viral localization discloses the potential of VS-FCV to infect brain. Thus, more information about the distribution of fJAM-A receptors in brain tissue may need in a future study.

#### **Acknowledgment**

Chiang Mai University granted KP for Ph.D. Program. CP was supported by the Ratchadapisek Somphot Fund for Postdoctoral Fellowship, Chulalongkorn University. This study was supported by the 90<sup>th</sup> Anniversary of Chulalongkorn University Fund (Ratchadaphiseksomphot Endowment Fund). The Chulalongkorn Academic Advancement into Its 2<sup>nd</sup> Century Project, Faculty of Veterinary Science, Chulalongkorn University is also acknowledged.



#### **Ethics Statement**

All experimental protocols were approved by the Chulalongkorn University Animal Care and Use Committee (No. 1631002). Furthermore, all procedures were done following the relevant guidelines and regulations.

### Data accessibility

All the data supporting our findings is contained within the manuscript. One full-length coding Feline calicivirus sequence has been deposited in NCBI GenBank under accession MZ542330.

### Declaration of competing interest

The authors have declared no competing financial or non-financial interests.



## CHAPTER V

### DISCUSSION AND CONCLUSION

#### General discussion

Feline calicivirus (FCV) was noticed as one of the key players in feline upper respiratory tract disease (FURTD) for over 40 years (Caringella et al., 2019). Although the primary symptoms of FCV-infected cats are oral diseases and the upper respiratory tract, some strains could cause of raising in mortality rate up to 50% (Pesavento et al., 2008) by known as virulent systemic feline calicivirus (VS-FCV). While the prevalence and molecular characterization of both classic FCV and VS-FCV is documented worldwide (Sato et al., 2002; Afonso et al., 2017; Zhao et al., 2017; Caringella et al., 2019), the information of these viruses circulating in Thailand is entirely limited (Phongroop et al., 2018a; Phongroop et al., 2018b). Thus, this is the first study enclosing the molecular epidemiology and genetic characterization of FCV wild-type strains circulating in Thai cats (FCV-THs) from 2016 to 2021. Moreover, we also established and validated recent diagnostic techniques that could simultaneously diagnose and differentiate the strain using a clinical sample. Finally, we identified the localization of VS-FCV's cell tropism, causing acute death in a kitten in various organ tissues.

In the aspect of FCV-THs molecular characterization, our findings indicated that all circulating FCV-TH strains clustered in genogroup I compared with the deduced amino acid sequence of full-length VP1 with other 43 global strains. Moreover, the diversity of FCV-TH strains did not associate with geographic distribution. Interestingly, although the previous report had published the association between the amino acid physicochemical property of HVR-E and potentially differentiated the classical FCV and VS-FCV pathotype (Brunet et al., 2019), our study

represented incongruous results that seem likely other (Bordicchia et al., 2021). Additionally, this study noticed that some FCV-TH strains revealed closely phylogenetic related to vaccine strain with the low number of amino acid divergence. Besides, the cat never got any vaccination in nearly a period. Hence, although our research did not find any recombination evidence of FCV-TH strains in the study period, we should keep monitoring the event, especially the recombination between the vaccine strain and some wild-type strains.

According to our molecular study, we found some amino acid residual showing the particularly disclosure of Thai strain at 3' end of ORF1, which is the junction between ORF1 and ORF2 that had ever caution for being a hot spot recombination site of FCV (Symes et al., 2015). So, we decided to initiate and validate a fashionable technique named high-resolution melting analysis (HRM) that could concurrently detect and strain typing. Additionally, this technique could differentiate between FCV-TH strains and commercial vaccine strains; likewise, our validated design could also distinguish between FCV-TH strains at the delicate of detection as  $0.25^{\circ}\text{C}$   $T_m$  shift in 1% C:G contain alteration. However, our validated HRM technique could detect only a short nucleotide sequence and a snapshot event, so extended nucleotide sequencing is still required to confirm the definite strain.

Based on the fact that the VS-FCV infected cat had never been officially reported in Thailand. Thus, we attempted to investigate it from the necropsy cats submitted to the Pathology Unit of the Department of Pathology at Faculty of Veterinary Science, Chulalongkorn University, during 2020-2021. The inclusion criteria included cats that died from a respiratory-associated illness. Thereby, our last chapter represented the various cell tropism of the dead cat caused by VS-FCV using numerous identification methods, including molecular technique,

immunohistochemistry (IHC), *in situ* hybridization (ISH), and transmission electron microscopy (TEM). Our general findings revealed the cell tropism of VS-FCV circulating in Thai cats related to the previous publications (Pesavento et al., 2004; Monne Rodriguez et al., 2014; Monne Rodriguez et al., 2018). Of note, we distinctly displayed both immunoreactivity of FCV protein antigen and FCV genomic signal in various neurotropic cell types. Moreover, we also identified intranuclear FCV particles in brain tissue using TEM.

Although some publications reported the evidence of FCV antigen in neurotropic cells (Battilani et al., 2013; Wardhani et al., 2021), the understanding of their pathogenesis is still poorly understood. However, *Caliciviridae* is the member within the same order as *Piconarviridae*; Order *Piconavirales*, that blood-brain barrier (BBB) and neuromuscular junctions (NMJs) are mainly entry routes of the virus to the central nervous system (Koyuncu et al., 2013). Thus, we hypothesize that the infected leukocytes, macrophages, or dendritic cells (DCs), may transport the virus pass the BBB, which comprises the brain microvascular endothelium cells (BMVECs) with specialized tight junctions, into the brain parenchyma and other surrounding cells such as microglia, neuron, and pericyte.

#### **Limitation of the study and suggestion for the further study**

The animal scale of this survey from each region in Thailand is quite limited to both live and dead animals. Thus, the expansion of sample size on each geographical area in Thailand should be considered in the future study. Additional techniques such as viral isolation may be needed for the investigation of whole-genome sequencing.

## Conclusion

This thesis provides the picture regarding FCV-TH strains circulating in Thai cats in many aspects, including overall incidence since 2016-2021, molecular characterization, and deeply in cell tropism vision. Moreover, we also contribute a beneficial diagnostic technique for screening FCV infection from clinical samples and strain-typing in the only one-step closed-tube system.

## APPENDIX

### Supplementary data of Chapter II

**Supplementary Table S1** Demographic data of age, vaccination history, clinical presentation, and molecular detection of feline calicivirus (FCV) and feline herpesvirus-1 (FHV-1) with route of detection of 184 studied cats





17	48	Yes	No	No	Neg	Neg	Neg	N/A	Pos	Neg	Pos	N/A
18	48	Yes	No	No	Neg	Neg	Neg	N/A	Pos	Neg	Pos	N/A
19	84	Yes	No	No	Neg	Neg	Neg	N/A	Pos	Neg	Pos	N/A
20	3	No	No	Yes	Neg	Neg	Neg	N/A	Pos	Neg	Pos	N/A
21	3	No	No	Yes	Neg	Neg	Neg	N/A	Pos	Neg	Pos	N/A
22	71	No	Yes	Yes	Pos	Neg	Pos	N/A	Pos	Neg	Pos	N/A
23	36	Yes	No	No	Neg	Neg	Neg	N/A	Pos	Neg	Pos	N/A
24	N/A	Yes	Yes	Yes	Neg	Neg	Neg	N/A	Pos	Neg	Pos	N/A
25	N/A	Yes	Yes	Yes	Neg	Neg	Neg	N/A	Pos	Pos	Neg	N/A
26	N/A	No	Yes	Yes	Neg	Neg	Neg	N/A	Pos	Pos	Neg	N/A
27	N/A	Yes	Yes	No	Neg	Neg	Neg	N/A	Pos	Pos	Pos	N/A
28	N/A	Yes	Yes	Yes	Neg	Neg	Neg	N/A	Pos	Pos	Neg	N/A
29	N/A	Yes	Yes	Yes	Pos	Pos	Pos	N/A	Pos	Pos	Pos	N/A
30	N/A	No	No	Yes	Pos	Neg	Pos	N/A	Pos	Pos	Pos	N/A
31	N/A	Yes	Yes	Yes	Pos	Pos	Pos	N/A	Pos	Pos	Pos	N/A
32	N/A	Yes	No	Yes	Neg	Neg	Neg	N/A	Pos	Neg	Pos	N/A
33	N/A	Yes	Yes	Yes	Neg	Neg	Neg	N/A	Pos	Pos	Pos	N/A
34	N/A	Yes	Yes	No	Neg	Neg	Neg	N/A	Neg	Neg	Neg	N/A
35	N/A	Yes	Yes	No	Neg	Neg	Neg	N/A	Pos	Neg	Pos	N/A

36	N/A	Yes	Yes	No	Neg	Neg	Neg	N/A	Pos	Neg	Pos	N/A
37	N/A	Yes	Yes	No	Pos	Neg	Pos	N/A	Pos	Pos	Pos	N/A
38	N/A	Yes	Yes	No	Neg	Neg	Neg	N/A	Pos	Pos	Pos	N/A
39	N/A	Yes	No	No	Neg	Neg	Neg	N/A	Pos	Pos	Pos	N/A
40	12	Yes	No	Yes	Pos	Pos	Neg	N/A	Pos	Pos	Neg	N/A
41	36	Yes	No	No	Pos	Neg	Pos	N/A	Pos	Neg	Pos	N/A
42	12	No	No	No	Pos	Neg	Pos	N/A	Pos	Pos	Pos	N/A
43 <sup>b,c</sup>												
44	2	No	Yes	Yes	Pos	Pos	Pos	N/A	Pos	Pos	Neg	N/A
45	N/A	No	No	Yes	Pos	Neg	Pos	N/A	Neg	Neg	Neg	N/A
46	N/A	No	No	No	Neg	Neg	Neg	N/A	Neg	Neg	Neg	N/A
47	N/A	No	No	Yes	Pos	Pos	Pos	N/A	Pos	Neg	Pos	N/A
48	N/A	No	No	Yes	Pos	Pos	Pos	N/A	Pos	Neg	Pos	N/A
49 <sup>a,b,c</sup>												
50	N/A	No	No	Yes	Pos	Pos	Pos	N/A	Pos	Neg	Pos	N/A
51 <sup>a,c</sup>												
52	N/A	No	No	Yes	Pos	Neg	Pos	N/A	Pos	Neg	Pos	N/A
53	N/A	No	No	Yes	Pos	Pos	Pos	N/A	Pos	Neg	Pos	N/A
54	N/A	No	No	Yes	Pos	Pos	Pos	N/A	Pos	Neg	Pos	N/A
55	N/A	No	No	Yes	Pos	Pos	Pos	N/A	Pos	Neg	Pos	N/A
56	N/A	No	No	Yes	Pos	Pos	Pos	N/A	Pos	Neg	Pos	N/A
57	N/A	No	No	Yes	Pos	Pos	Pos	N/A	Pos	Neg	Pos	N/A
58	N/A	No	No	Yes	Pos	Pos	Pos	N/A	Pos	Neg	Pos	N/A
59	N/A	No	No	Yes	Pos	Pos	Pos	N/A	Pos	Neg	Pos	N/A
60	N/A	No	No	Yes	Pos	Pos	Pos	N/A	Pos	Neg	Pos	N/A
61	N/A	No	No	Yes	Pos	Pos	Pos	N/A	Pos	Neg	Pos	N/A
62	N/A	No	No	Yes	Pos	Pos	Pos	N/A	Pos	Neg	Pos	N/A
63	N/A	No	No	Yes	Pos	Pos	Pos	N/A	Pos	Neg	Pos	N/A
64	N/A	No	No	Yes	Pos	Pos	Pos	N/A	Pos	Neg	Pos	N/A
65	N/A	No	No	Yes	Pos	Pos	Pos	N/A	Pos	Neg	Pos	N/A
66	N/A	No	No	Yes	Pos	Pos	Pos	N/A	Pos	Neg	Pos	N/A
67	N/A	No	No	Yes	Pos	Pos	Pos	N/A	Pos	Neg	Pos	N/A
68	N/A	No	No	Yes	Pos	Pos	Pos	N/A	Pos	Neg	Pos	N/A
69	N/A	No	No	Yes	Pos	Pos	Pos	N/A	Pos	Neg	Pos	N/A
70	N/A	No	No	Yes	Pos	Pos	Pos	N/A	Pos	Neg	Pos	N/A
71	N/A	No	No	Yes	Pos	Pos	Pos	N/A	Pos	Neg	Pos	N/A
72	N/A	No	No	Yes	Pos	Pos	Pos	N/A	Pos	Neg	Pos	N/A
73	N/A	No	No	Yes	Pos	Pos	Pos	N/A	Pos	Neg	Pos	N/A
74	N/A	No	No	Yes	Pos	Pos	Pos	N/A	Pos	Neg	Pos	N/A
75	N/A	No	No	Yes	Pos	Pos	Pos	N/A	Pos	Neg	Pos	N/A
76	N/A	No	No	Yes	Pos	Pos	Pos	N/A	Pos	Neg	Pos	N/A
77	N/A	No	No	Yes	Pos	Pos	Pos	N/A	Pos	Neg	Pos	N/A
78	N/A	No	No	Yes	Pos	Pos	Pos	N/A	Pos	Neg	Pos	N/A
79	N/A	No	No	Yes	Pos	Pos	Pos	N/A	Pos	Neg	Pos	N/A
80	N/A	No	No	Yes	Pos	Pos	Pos	N/A	Pos	Neg	Pos	N/A
81	N/A	No	No	Yes	Pos	Pos	Pos	N/A	Pos	Neg	Pos	N/A
82	N/A	No	No	Yes	Pos	Pos	Pos	N/A	Pos	Neg	Pos	N/A
83	N/A	No	No	Yes	Pos	Pos	Pos	N/A	Pos	Neg	Pos	N/A
84	N/A	No	No	Yes	Pos	Pos	Pos	N/A	Pos	Neg	Pos	N/A
85	N/A	No	No	Yes	Pos	Pos	Pos	N/A	Pos	Neg	Pos	N/A
86	N/A	No	No	Yes	Pos	Pos	Pos	N/A	Pos	Neg	Pos	N/A
87	N/A	No	No	Yes	Pos	Pos	Pos	N/A	Pos	Neg	Pos	N/A
88	N/A	No	No	Yes	Pos	Pos	Pos	N/A	Pos	Neg	Pos	N/A
89	N/A	No	No	Yes	Pos	Pos	Pos	N/A	Pos	Neg	Pos	N/A
90	N/A	No	No	Yes	Pos	Pos	Pos	N/A	Pos	Neg	Pos	N/A
91	N/A	No	No	Yes	Pos	Pos	Pos	N/A	Pos	Neg	Pos	N/A
92	N/A	No	No	Yes	Pos	Pos	Pos	N/A	Pos	Neg	Pos	N/A
93	N/A	No	No	Yes	Pos	Pos	Pos	N/A	Pos	Neg	Pos	N/A
94	N/A	No	No	Yes	Pos	Pos	Pos	N/A	Pos	Neg	Pos	N/A
95	N/A	No	No	Yes	Pos	Pos	Pos	N/A	Pos	Neg	Pos	N/A
96	N/A	No	No	Yes	Pos	Pos	Pos	N/A	Pos	Neg	Pos	N/A
97	N/A	No	No	Yes	Pos	Pos	Pos	N/A	Pos	Neg	Pos	N/A
98	N/A	No	No	Yes	Pos	Pos	Pos	N/A	Pos	Neg	Pos	N/A
99	N/A	No	No	Yes	Pos	Pos	Pos	N/A	Pos	Neg	Pos	N/A
100	N/A	No	No	Yes	Pos	Pos	Pos	N/A	Pos	Neg	Pos	N/A

KP70/THA2016

KP80/THA2016

KP82/THA2016

52 <sup>c</sup>	N/A	No	Yes	Pos	Pos	Pos	N/A	Neg	Neg	N/A
KP83/THA/2016										
53 <sup>a,b</sup>	N/A	No	Yes	Pos	Pos	Pos	N/A	Neg	Pos	N/A
KP84/THA/2016										
54	N/A	No	Yes	Pos	Pos	Pos	N/A	Pos	Pos	N/A
55 <sup>a,c</sup>	N/A	No	Yes	Pos	Pos	Pos	N/A	Pos	Pos	N/A
KPI05/THA/2017										
56 <sup>a,c</sup>	N/A	No	Yes	Pos	Pos	Pos	N/A	Pos	Pos	N/A
KPI06/THA/2017										
57	N/A	No	Yes	Pos	Pos	Pos	N/A	Neg	Pos	N/A
58	N/A	No	Yes	Pos	Pos	Pos	N/A	Neg	Pos	N/A
59 <sup>a,b,c</sup>	N/A	No	Yes	Pos	Pos	Pos	N/A	Neg	Pos	N/A
KPI00/THA/2017										
60	N/A	No	Yes	Pos	Pos	Pos	N/A	Pos	Pos	N/A
61	N/A	No	Yes	Pos	Pos	Pos	N/A	Pos	Pos	N/A
62 <sup>a,c</sup>	N/A	No	Yes	Pos	Pos	Pos	N/A	Pos	Pos	N/A
KPI03/THA/2017										
63	N/A	No	Yes	Pos	Neg	Pos	N/A	Pos	Pos	Neg
64	N/A	No	No	Neg	Neg	Neg	N/A	Neg	Neg	N/A
65	N/A	No	No	Neg	Neg	Neg	N/A	Neg	Neg	N/A







101	94	N/A	No	Yes	Neg	Neg	Neg	Neg	N/A	Pos	Pos	Neg	N/A
102	12	N/A	No	Yes	Neg	Neg	Neg	Neg	N/A	Pos	Pos	Pos	N/A
103	11	N/A	No	Yes	Neg	Neg	Neg	Neg	N/A	Pos	Pos	Pos	N/A
104	N/A	Yes	No	Yes	Neg	Neg	Neg	Neg	N/A	Neg	Neg	Neg	N/A
105	120	Yes	No	Yes	Neg	Neg	Neg	Neg	N/A	Pos	Pos	Pos	N/A
106	N/A	Yes	No	Yes	Pos	Pos	Pos	Pos	N/A	Neg	Neg	Neg	N/A
107	6	No	Yes	No	Neg	Neg	Neg	Neg	N/A	Neg	Neg	Neg	N/A
108	N/A	No	No	No	Pos	Pos	Pos	Pos	Neg	Pos	Pos	N/A	Pos
109	N/A	Yes	No	Yes	Neg	Neg	Neg	Neg	Neg	Pos	Pos	N/A	Pos
110	N/A	Yes	No	Yes	Neg	Neg	Neg	Neg	Neg	Pos	Pos	N/A	Pos
111	N/A	Yes	No	Yes	Neg	Neg	Neg	Neg	Neg	Pos	Pos	N/A	Pos
112	N/A	Yes	No	Yes	Pos	Pos	Pos	Pos	Neg	Neg	Neg	Neg	Neg
113	N/A	Yes	No	Yes	Neg	Neg	Neg	Neg	Neg	Pos	Pos	N/A	Pos
114	N/A	Yes	No	Yes	Neg	Neg	Neg	Neg	Neg	Pos	Pos	N/A	Pos
115	N/A	Yes	No	Yes	Neg	Neg	Neg	Neg	Neg	Neg	Neg	Neg	Neg
116	N/A	Yes	No	Yes	Neg	Neg	Neg	Neg	Neg	Pos	Pos	Pos	Pos
117	1	Yes	No	No	Neg	Neg	Neg	Neg	Neg	Pos	Pos	N/A	Pos
118	N/A	Yes	Yes	Yes	Neg	Neg	Neg	Neg	Neg	Neg	Neg	Neg	Neg
119	N/A	Yes	No	Yes	Pos	Neg	Neg	Neg	Neg	Pos	Pos	Pos	Pos



120	N/A	No	No	Yes	Neg	Neg	Neg	Pos	Pos	Pos	Pos	Pos
121	N/A	Yes	No	Yes	Pos	N/A	Pos	Pos	N/A	Pos	Pos	Pos
122	N/A	Yes	Yes	No	Pos	Neg	Pos	Pos	Pos	Pos	Pos	N/A
123 <sup>a,b,c</sup>												
KP276/THA./2018												
	1	N/A	Yes	No	Pos	N/A	Pos	Pos	Pos	Neg	Neg	Neg
124	N/A	N/A	Yes	No	Pos	Neg	Pos	Pos	Neg	Neg	Neg	Neg
125	N/A	N/A	Yes	Yes	Pos	Pos	Neg	Neg	N/A	Pos	Pos	N/A
126	N/A	No	Yes	Yes	Pos	Neg	Pos	Pos	N/A	Neg	Neg	N/A
127 <sup>b</sup>												
KP285/THA./2018												
	N/A	Yes	No	No	Pos	N/A	Pos	Pos	Pos	Neg	Neg	Neg
128	N/A	Yes	No	Yes	Pos	N/A	Pos	Pos	Neg	Neg	Neg	Neg
129	N/A	Yes	No	No	Neg	N/A	N/A	N/A	Neg	Neg	N/A	Neg
130	N/A	Yes	No	Yes	Neg	Neg	Neg	Neg	Neg	Neg	Neg	Neg
131	N/A	Yes	Yes	No	Pos	Neg	Pos	Pos	Neg	Neg	Neg	Neg
132	1	Yes	No	Yes	Neg	Neg	Neg	Neg	Neg	Neg	Neg	Neg
133	N/A	Yes	No	No	Neg	Neg	Neg	Neg	Neg	Neg	Neg	Neg
134	N/A	Yes	No	Yes	Neg	Neg	Neg	Neg	Neg	Neg	Neg	Neg
135	N/A	Yes	No	No	Neg	N/A	Neg	Neg	N/A	Pos	Pos	N/A
136	N/A	No	No	Yes	Neg	Neg	Neg	Neg	N/A	Neg	Neg	N/A
137	N/A	Yes	No	No	Neg	N/A	Neg	Neg	N/A	Pos	Pos	Neg



138	N/A	Yes	No	Yes	Neg	N/A	Neg	N/A	Neg	N/A	Neg	N/A
139	N/A	Yes	No	Yes	Neg	N/A	Neg	N/A	Neg	N/A	Neg	N/A
140	N/A	Yes	No	Yes	Neg	N/A	Neg	N/A	Neg	N/A	Neg	N/A
141 <sup>a,c</sup>												
KP313/THA,2019												
142	N/A	Yes	Yes	Yes	Neg	N/A	Neg	N/A	Pos	N/A	Pos	N/A
143	N/A	Yes	Yes	Yes	Neg	N/A	Neg	N/A	Pos	N/A	Pos	N/A
144	N/A	No	No	No	Neg	N/A	Neg	N/A	Neg	N/A	Neg	N/A
145	N/A	Yes	No	Yes	Neg	Neg	Neg	N/A	Pos	Neg	Pos	N/A
146	N/A	No	No	Yes	Neg	Neg	Neg	Neg	Pos	Neg	Pos	Neg
147	N/A	Yes	No	Yes	Neg	Neg	Neg	Neg	Neg	Neg	Neg	Neg
148	N/A	Yes	No	Yes	Neg	Neg	Neg	Neg	Neg	Neg	Neg	Neg
149 <sup>a,b</sup>												
KP331/THA,2020												
150	N/A	Yes	No	Yes	Neg	Neg	Neg	N/A	Neg	Neg	Neg	N/A
151	N/A	Yes	No	Yes	Neg	Neg	Neg	Neg	Neg	Neg	Neg	Neg
152 <sup>a,b</sup>												
KP339/THA,2020												
153	N/A	Yes	No	Yes	Pos	Pos	Neg	Neg	Neg	Neg	Neg	Neg





154	N/A	N/A	No	Yes	Neg	Neg	Neg	Pos	Pos	Pos	Pos	Pos
155 <sup>b</sup>	N/A	Yes	No	Yes	Pos	Neg	Pos	Neg	Neg	Neg	Neg	Neg
KP351/THA/2021												
156 <sup>b</sup>	N/A	No	Yes	No	Pos	Neg	Pos	Neg	Neg	Neg	Neg	Neg
KP354/THA/2021												
157	N/A	No	No	Yes	Neg	Neg	Neg	Pos	Pos	Pos	Pos	Neg
158 <sup>#,d</sup>	N/A	No	No	Yes	Pos	N/A	N/A	N/A	N/A	Pos	Pos	N/A
KP361/THA/2021												
159 <sup>#</sup>	N/A	N/A	No	No	Neg	N/A	N/A	N/A	N/A	Pos	Pos	N/A
160 <sup>#</sup>	N/A	N/A	No	No	Neg	N/A	N/A	N/A	N/A	Pos	Pos	N/A
161 <sup>a,b</sup>	N/A	Yes	Yes	Yes	Pos	N/A	Pos	N/A	N/A	Neg	Neg	N/A
KP365/THA/2021												
162 <sup>#</sup>	N/A	N/A	No	No	Neg	N/A	N/A	N/A	N/A	Neg	Neg	N/A
163 <sup>#</sup>	N/A	No	Yes	Yes	Pos	N/A	N/A	N/A	N/A	Neg	Neg	N/A
164 <sup>#</sup>	N/A	N/A	No	No	Neg	N/A	N/A	N/A	N/A	Neg	Neg	N/A
165 <sup>#</sup>	N/A	N/A	No	No	Neg	N/A	N/A	N/A	N/A	Neg	Pos	N/A
166 <sup>#</sup>	N/A	N/A	No	No	Neg	N/A	N/A	N/A	N/A	Neg	Pos	N/A
167 <sup>#</sup>	N/A	No	No	No	Pos	N/A	N/A	N/A	N/A	Neg	Neg	N/A
168 <sup>#</sup>	N/A	N/A	No	No	Neg	N/A	N/A	N/A	N/A	Neg	Neg	N/A
169 <sup>#</sup>	N/A	N/A	No	No	Neg	N/A	N/A	N/A	N/A	Neg	Neg	N/A



170<sup>#,b</sup>  
 KP374/THA/2021

171 <sup>#</sup>	N/A	No	Yes	Yes	Pos	N/A	N/A	N/A	Neg	N/A	N/A	N/A
172 <sup>#</sup>	N/A	Yes	No	No	Neg	N/A	N/A	N/A	Pos	N/A	N/A	N/A
173 <sup>#</sup>	N/A	N/A	No	No	Neg	N/A	N/A	N/A	Pos	N/A	N/A	N/A
174 <sup>#</sup>	N/A	N/A	No	No	Neg	N/A	N/A	N/A	Pos	N/A	N/A	N/A
175 <sup>#</sup>	N/A	N/A	No	No	Neg	N/A	N/A	N/A	Pos	N/A	N/A	N/A
176 <sup>#</sup>	N/A	N/A	No	No	Neg	N/A	N/A	N/A	Pos	N/A	N/A	N/A
177 <sup>#</sup>	N/A	N/A	No	No	Neg	N/A	N/A	N/A	Pos	N/A	N/A	N/A
178	N/A	Yes	No	Yes	Pos	Pos	Pos	N/A	Pos	Pos	Pos	N/A
179	N/A	Yes	No	Yes	Neg	Neg	Neg	N/A	Neg	Neg	Neg	N/A
180	N/A	Yes	No	Yes	Neg	Neg	Neg	N/A	Pos	Pos	Pos	N/A
181	N/A	Yes	No	Yes	Neg	Neg	Neg	N/A	Pos	Pos	Pos	N/A
182 <sup>#</sup>	N/A	N/A	No	Yes	Neg	N/A	N/A	N/A	Pos	N/A	N/A	N/A
183	N/A	Yes	No	Yes	Neg	Neg	Neg	N/A	Neg	Neg	Neg	N/A
184	N/A	Yes	Yes	No	Neg	Neg	Neg	N/A	Neg	Neg	Neg	N/A



REFERENCES



จุฬาลงกรณ์มหาวิทยาลัย  
**CHULALONGKORN UNIVERSITY**

- Abd-Eldaim M, Potgieter L and Kennedy M. 2005. Genetic analysis of feline caliciviruses associated with a hemorrhagic-like disease. *J Vet Diagn Invest.* 17(5): 420-429.
- Abd-Eldaim MM, Wilkes RP, Thomas KV and Kennedy MA. 2009. Development and validation of a TaqMan real-time reverse transcription-PCR for rapid detection of feline calicivirus. *Arch Virol.* 154(4): 555-560.
- Abente EJ, Sosnovtsev SV, Sandoval-Jaime C, Parra GI, Bok K and Green KY. 2013. The feline calicivirus leader of the capsid protein is associated with cytopathic effect. *J Virol.* 87(6): 3003-3017.
- Addie D, Belak S, Boucraut-Baralon C, Egberink H, Frymus T, Gruffydd-Jones T, Hartmann K, Hosie MJ, Lloret A, Lutz H, Marsilio F, Pennisi MG, Radford AD, Thiry E, Truyen U and Horzinek MC. 2009. Feline infectious peritonitis. ABCD guidelines on prevention and management. *J Feline Med Surg.* 11(7): 594-604.
- Addie D, Poulet H, Golder MC, McDonald M, Brunet S, Thibault JC and Hosie MJ. 2008. Ability of antibodies to two new caliciviral vaccine strains to neutralise feline calicivirus isolates from the UK. *Vet Rec.* 163(12): 355-357.
- Afonso MM, Pinchbeck GL, Smith SL, Daly JM, Gaskell RM, Dawson S and Radford AD. 2017. A multi-national European cross-sectional study of feline calicivirus epidemiology, diversity and vaccine cross-reactivity. *Vaccine.* 35(20): 2753-2760.
- Bannasch MJ and Foley JE. 2005. Epidemiologic evaluation of multiple respiratory pathogens in cats in animal shelters. *J Feline Med Surg.* 7(2): 109-119.
- Battilani M, Vaccari F, Carelle MS, Morandi F, Benazzi C, Kipar A, Dondi F and Scagliarini A. 2013. Virulent feline calicivirus disease in a shelter in Italy: a case description. *Res Vet Sci.* 95(1): 283-290.
- Bordicchia M, Fumian TM, Van Brussel K, Russo AG, Carrai M, Le SJ, Pesavento PA, Holmes EC, Martella V, White P, Beatty JA, Shi M and Barrs VR. 2021. Feline Calicivirus Virulent Systemic Disease: Clinical Epidemiology, Analysis of Viral Isolates and In Vitro Efficacy of Novel Antivirals in Australian Outbreaks. *Viruses.* 13(10).

- Brunet S, Sigoillot-Claude C, Pialot D and Poulet H. 2019. Multiple Correspondence Analysis on Amino Acid Properties within the Variable Region of the Capsid Protein Shows Differences between Classical and Virulent Systemic Feline Calicivirus Strains. *Viruses*. 11(12).
- Bull RA, Eden JS, Rawlinson WD and White PA. 2010. Rapid evolution of pandemic noroviruses of the GII.4 lineage. *PLoS Pathog*. 6(3): e1000831.
- Bull RA, Hyde J, Mackenzie JM, Hansman GS, Oka T, Takeda N and White PA. 2011. Comparison of the replication properties of murine and human calicivirus RNA-dependent RNA polymerases. *Virus Genes*. 42(1): 16-27.
- Caringella F, Elia G, Decaro N, Martella V, Lanave G, Varello K, Catella C, Diakoudi G, Carelli G, Colaianni ML, Bo S and Buonavoglia C. 2019. Feline calicivirus infection in cats with virulent systemic disease, Italy. *Res Vet Sci*. 124: 46-51.
- Castro TX, Cubel Garcia Rde C, Fumian TM, Costa EM, Mello R, White PA and Leite JP. 2015. Detection and molecular characterization of caliciviruses (vesivirus and norovirus) in an outbreak of acute diarrhea in kittens from Brazil. *Vet J*. 206(1): 115-117.
- Chaiyasak S, Piewbang C, Rungsipipat A and Techangamsuwan S. 2020. Molecular epidemiology and genome analysis of feline morbillivirus in household and shelter cats in Thailand. *BMC Vet Res*. 16(1): 240.
- Chaiyasak S, Piewbang C, Yostawonkul J, Boonrungsiman S, Kasantikul T, Rungsipipat A and Techangamsuwan S. 2021. Renal epitheliotropism of feline morbillivirus in two cats. *Vet Pathol*. 3009858211045441.
- Chua KH, Lim SC, Ng CC, Lee PC, Lim YA, Lau TP and Chai HC. 2015. Development of High Resolution Melting Analysis for the Diagnosis of Human Malaria. *Sci Rep*. 5: 15671.
- Conley MJ, McElwee M, Azmi L, Gabrielsen M, Byron O, Goodfellow IG and Bhella D. 2019. Calicivirus VP2 forms a portal-like assembly following receptor engagement. *Nature*. 565(7739): 377-381.
- Coyne KP, Christley RM, Pybus OG, Dawson S, Gaskell RM and Radford AD. 2012. Large-scale spatial and temporal genetic diversity of feline calicivirus. *J Virol*. 86(20): 11356-11367.

- Coyne KP, Dawson S, Radford AD, Cripps PJ, Porter CJ, McCracken CM and Gaskell RM. 2006a. Long-term analysis of feline calicivirus prevalence and viral shedding patterns in naturally infected colonies of domestic cats. *Vet Microbiol.* 118(1-2): 12-25.
- Coyne KP, Edwards D, Radford AD, Cripps P, Jones D, Wood JL, Gaskell RM and Dawson S. 2007a. Longitudinal molecular epidemiological analysis of feline calicivirus infection in an animal shelter: a model for investigating calicivirus transmission within high-density, high-turnover populations. *J Clin Microbiol.* 45(10): 3239-3244.
- Coyne KP, Gaskell RM, Dawson S, Porter CJ and Radford AD. 2007b. Evolutionary mechanisms of persistence and diversification of a calicivirus within endemically infected natural host populations. *J Virol.* 81(4): 1961-1971.
- Coyne KP, Jones BR, Kipar A, Chantrey J, Porter CJ, Barber PJ, Dawson S, Gaskell RM and Radford AD. 2006b. Lethal outbreak of disease associated with feline calicivirus infection in cats. *Vet Rec.* 158(16): 544-550.
- Coyne KP, Reed FC, Porter CJ, Dawson S, Gaskell RM and Radford AD. 2006c. Recombination of Feline calicivirus within an endemically infected cat colony. *J Gen Virol.* 87(Pt 4): 921-926.
- Cubillos-Zapata C, Angulo I, Almanza H, Borrego B, Zamora-Ceballos M, Caston JR, Mena I, Blanco E and Barcena J. 2020. Precise location of linear epitopes on the capsid surface of feline calicivirus recognized by neutralizing and non-neutralizing monoclonal antibodies. *Vet Res.* 51(1): 59.
- Dawson S, Bennett D, Carter SD, Bennett M, Meanger J, Turner PC, Carter MJ, Milton I and Gaskell RM. 1994. Acute arthritis of cats associated with feline calicivirus infection. *Res Vet Sci.* 56(2): 133-143.
- Di Martino B, Lanave G, Di Profio F, Melegari I, Marsilio F, Camero M, Catella C, Capozza P, Banyai K, Barrs VR, Buonavoglia C and Martella V. 2020. Identification of feline calicivirus in cats with enteritis. *Transbound Emerg Dis.*
- Domingo E, Escarmis C, Sevilla N, Moya A, Elena SF, Quer J, Novella IS and Holland JJ. 1996. Basic concepts in RNA virus evolution. *FASEB J.* 10(8): 859-864.

- Ebnet K, Suzuki A, Ohno S and Vestweber D. 2004. Junctional adhesion molecules (JAMs): more molecules with dual functions? *J Cell Sci.* 117(Pt 1): 19-29.
- Fastier LB. 1957. A new feline virus isolated in tissue culture. *Am J Vet Res.* 18(67): 382-389.
- Fernandez M, Manzanilla EG, Lloret A, Leon M and Thibault JC. 2017. Prevalence of feline herpesvirus-1, feline calicivirus, *Chlamydomydia felis* and *Mycoplasma felis* DNA and associated risk factors in cats in Spain with upper respiratory tract disease, conjunctivitis and/or gingivostomatitis. *J Feline Med Surg.* 19(4): 461-469.
- Foley J, Hurley K, Pesavento PA, Poland A and Pedersen NC. 2006. Virulent systemic feline calicivirus infection: local cytokine modulation and contribution of viral mutants. *J Feline Med Surg.* 8(1): 55-61.
- Gaskell RM, Dawson S and Radford A. 2012. Feline respiratory disease. In: *Infectious Diseases of the Dog and Cat.* 4th ed. Greene C. E. (ed.). St. Louis, MO, USA: Elsevier Saunders. 151-162.
- Geissler K, Schneider K and Truyen U. 2002. Mapping neutralizing and non-neutralizing epitopes on the capsid protein of feline calicivirus. *J Vet Med B Infect Dis Vet Public Health.* 49(1): 55-60.
- Giglio S, Monis PT and Saint CP. 2003. Demonstration of preferential binding of SYBR Green I to specific DNA fragments in real-time multiplex PCR. *Nucleic Acids Res.* 31(22): e136.
- Gourkow N, Lawson JH, Hamon SC and Phillips CJ. 2013. Descriptive epidemiology of upper respiratory disease and associated risk factors in cats in an animal shelter in coastal western Canada. *Can Vet J.* 54(2): 132-138.
- Guo H, Miao Q, Zhu J, Yang Z and Liu G. 2018. Isolation and molecular characterization of a virulent systemic feline calicivirus isolated in China. *Infect Genet Evol.* 65: 425-429.
- Helps C, Lait P, Tasker S and Harbour D. 2002. Melting curve analysis of feline calicivirus isolates detected by real-time reverse transcription PCR. *J Virol Methods.* 106(2): 241-244.

- Henzel A, Sa e Silva M, Luo S, Lovato LT and Weiblen R. 2012. Genetic and phylogenetic analyses of capsid protein gene in feline calicivirus isolates from Rio Grande do Sul in southern Brazil. *Virus Res.* 163(2): 667-671.
- Hou J, Sánchez-Vizcaíno F, McGahie D, Lesbros C, Almeras T, Howarth D, O'Hara V, Dawson S and Radford AD. 2016. European molecular epidemiology and strain diversity of feline calicivirus. *Vet Rec.* 178(5): 114-115.
- Hurley KE, Pesavento PA, Pedersen NC, Poland AM, Wilson E and Foley JE. 2004. An outbreak of virulent systemic feline calicivirus disease. *J Am Vet Med Assoc.* 224(2): 241-249.
- Hurley KF and Sykes JE. 2003. Update on feline calicivirus: new trends. *Vet Clin North Am Small Anim Pract.* 33(4): 759-772.
- Kalunda M, Lee KM, Holmes DF and Gillespie JH. 1975. Serologic classification of feline caliciviruses by plaque-reduction neutralization and immunodiffusion. *Am J Vet Res.* 36(4 Pt.1): 353-356.
- Katayama K, Horikoshi-Shirato H and Takeda N. 2002a. [Phylogenetic analysis of 14 strains of Norwalk-like viruses: identification of the region in the genome for genotyping]. *Nihon Rinsho.* 60(6): 1165-1174.
- Katayama K, Shirato-Horikoshi H, Kojima S, Kageyama T, Oka T, Hoshino F, Fukushi S, Shinohara M, Uchida K, Suzuki Y, Gojobori T and Takeda N. 2002b. Phylogenetic analysis of the complete genome of 18 Norwalk-like viruses. *Virology.* 299(2): 225-239.
- Kojima S, Kageyama T, Fukushi S, Hoshino FB, Shinohara M, Uchida K, Natori K, Takeda N and Katayama K. 2002. Genogroup-specific PCR primers for detection of Norwalk-like viruses. *J Virol Methods.* 100(1-2): 107-114.
- Koyuncu OO, Hogue IB and Enquist LW. 2013. Virus infections in the nervous system. *Cell Host Microbe.* 13(4): 379-393.
- Ksiazek TG, Erdman D, Goldsmith CS, Zaki SR, Peret T, Emery S, Tong S, Urbani C, Comer JA, Lim W, Rollin PE, Dowell SF, Ling AE, Humphrey CD, Shieh WJ, Guarner J, Paddock CD, Rota P, Fields B, DeRisi J, Yang JY, Cox N, Hughes JM, LeDuc JW, Bellini WJ, Anderson LJ and Group SW. 2003. A novel coronavirus



- associated with severe acute respiratory syndrome. *N Engl J Med.* 348(20): 1953-1966.
- Kumar S, Stecher G, Li M, Knyaz C and Tamura K. 2018. MEGA X: Molecular Evolutionary Genetics Analysis across Computing Platforms. *Mol Biol Evol.* 35(6): 1547-1549.
- Lauritzen A, Jarrett O and Sabara M. 1997. Serological analysis of feline calicivirus isolates from the United States and United Kingdom. *Vet Microbiol.* 56(1-2): 55-63.
- Liew M, Pryor R, Palais R, Meadows C, Erali M, Lyon E and Wittwer C. 2004. Genotyping of single-nucleotide polymorphisms by high-resolution melting of small amplicons. *Clin Chem.* 50(7): 1156-1164.
- Liu Y, Nusrat A, Schnell FJ, Reaves TA, Walsh S, Pochet M and Parkos CA. 2000. Human junction adhesion molecule regulates tight junction resealing in epithelia. *J Cell Sci.* 113 ( Pt 13): 2363-2374.
- Lu Z, Ledgerwood ED, Hinchman MM, Dick R and Parker JSL. 2018. Conserved Surface Residues on the Feline Calicivirus Capsid Are Essential for Interaction with Its Receptor Feline Junctional Adhesion Molecule A (fJAM-A). *J Virol.* 92(8).
- Maclachlan NJ, Dubovi EJ, Barthold SW, Swayne DE and Winton JR. 2016. Fenner's veterinary virology. Fifth ed. In: Elsevier.
- Maggs DJ and Clarke HE. 2005. Relative sensitivity of polymerase chain reaction assays used for detection of feline herpesvirus type 1 DNA in clinical samples and commercial vaccines. *Am J Vet Res.* 66(9): 1550-1555.
- Mahar JE, Bok K, Green KY and Kirkwood CD. 2013. The importance of intergenic recombination in norovirus GII.3 evolution. *J Virol.* 87(7): 3687-3698.
- Makino A, Shimojima M, Miyazawa T, Kato K, Tohya Y and Akashi H. 2006. Junctional adhesion molecule 1 is a functional receptor for feline calicivirus. *J Virol.* 80(9): 4482-4490.
- Mao F, Leung WY and Xin X. 2007. Characterization of EvaGreen and the implication of its physicochemical properties for qPCR applications. *BMC Biotechnol.* 7: 76.

- Marin MS, Quintana S, Leunda MR, Recavarren M, Pagnuco I, Späth E, Pérez S and Odeón A. 2016. A new method for simultaneous detection and discrimination of Bovine herpesvirus types 1 (BoHV-1) and 5 (BoHV-5) using real time PCR with high resolution melting (HRM) analysis. *Journal of Virological Methods*. 227: 14-22.
- Marsilio F, Di Martino B, Decaro N and Buonavoglia C. 2005. A novel nested PCR for the diagnosis of calicivirus infections in the cat. *Vet Microbiol*. 105(1): 1-7.
- Meyer A, Kershaw O and Klopfleisch R. 2011. Feline calicivirus-associated virulent systemic disease: not necessarily a local epizootic problem. *Vet Rec*. 168(22): 589.
- Mochizuki M. 1992. Different stabilities to bile among feline calicivirus strains of respiratory and enteric origin. *Veterinary Microbiology*. 31(2): 297-302.
- Mochizuki M, Horiuchi M, Hiragi H, San Gabriel MC, Yasuda N and Uno T. 1996. Isolation of canine parvovirus from a cat manifesting clinical signs of feline panleukopenia. *J Clin Microbiol*. 34(9): 2101-2105.
- Monne Rodriguez J, Kohler K and Kipar A. 2018. Calicivirus co-infections in herpesvirus pneumonia in kittens. *Vet J*. 236: 1-3.
- Monne Rodriguez JM, Soare T, Malbon A, Blundell R, Papoula-Pereira R, Leeming G, Kohler K and Kipar A. 2014. Alveolar macrophages are the main target cells in feline calicivirus-associated pneumonia. *Vet J*. 201(2): 156-165.
- Neill JD, Sosnovtsev SV and Green KY. 2000. Recovery and altered neutralization specificities of chimeric viruses containing capsid protein domain exchanges from antigenically distinct strains of feline calicivirus. *J Virol*. 74(3): 1079-1084.
- Ohe K, Sakai S, Takahasi T, Sunaga F, Murakami M, Kiuchi A, Fukuyama M, Furuhashi K, Hara M, Ishikawa Y and Taneno A. 2007. Genogrouping of vaccine breakdown strains (VBS) of feline calicivirus in Japan. *Vet Res Commun*. 31(4): 497-507.
- Ossiboff RJ, Zhou Y, Lightfoot PJ, Prasad BV and Parker JS. 2010. Conformational changes in the capsid of a calicivirus upon interaction with its functional receptor. *J Virol*. 84(11): 5550-5564.

- Pedersen NC, Elliott JB, Glasgow A, Poland A and Keel K. 2000a. An isolated epizootic of hemorrhagic-like fever in cats caused by a novel and highly virulent strain of feline calicivirus. *Veterinary Microbiology*. 73(4): 281-300.
- Pedersen NC, Elliott JB, Glasgow A, Poland A and Keel K. 2000b. An isolated epizootic of hemorrhagic-like fever in cats caused by a novel and highly virulent strain of feline calicivirus. *Vet Microbiol*. 73(4): 281-300.
- Penafior-Tellez Y, Trujillo-Uscanga A, Escobar-Almazan JA and Gutierrez-Escolano AL. 2019. Immune Response Modulation by Caliciviruses. *Front Immunol*. 10: 2334.
- Pereira JJ, Baumworcel N, Fioretti JM, Domingues CF, Moraes LF, Marinho R, Vieira MCR, Pinto AMV and de Castro TX. 2018. Molecular characterization of feline calicivirus variants from multicat household and public animal shelter in Rio de Janeiro, Brazil. *Braz J Microbiol*.
- Pesavento PA, Chang KO and Parker JS. 2008. Molecular virology of feline calicivirus. *Vet Clin North Am Small Anim Pract*. 38(4): 775-786, vii.
- Pesavento PA, MacLachlan NJ, Dillard-Telm L, Grant CK and Hurley KF. 2004. Pathologic, immunohistochemical, and electron microscopic findings in naturally occurring virulent systemic feline calicivirus infection in cats. *Vet Pathol*. 41(3): 257-263.
- Phongroop K, Rattanasrisomporn J, Rungsipipat A and Techangamsuwan S. 2018a. Molecular Detection of Feline Calicivirus Infection in Thailand. The 17<sup>th</sup> Chulalongkorn University Veterinary Conference, CUVC2018: Research in Practice. P 35.
- Phongroop K, Rattanasrisomporn J, Rungsipipat A and Techangamsuwan S. 2018b. Occurrence of Feline Herpesvirus-1 and Feline Calicivirus Infection in Thailand. The 11th VPAT Regional Veterinary Congress 2018. P 33-35.
- Piewbang C, Kasantikul T, Pringproa K and Techangamsuwan S. 2019. Feline bocavirus-1 associated with outbreaks of hemorrhagic enteritis in household cats: potential first evidence of a pathological role, viral tropism and natural genetic recombination. *Sci Rep*. 9(1): 16367.

- Piewbang C, Wardhani SW, Chaiyasak S, Yostawonkul J, Chai-In P, Boonrungsiman S, Kasantikul T and Techangamsuwan S. 2020. Insights into the genetic diversity, recombination, and systemic infections with evidence of intracellular maturation of hepadnavirus in cats. *PLoS One*. 15(10): e0241212.
- Piewbang C, Wardhani SW, Chanseanroj J, Yostawonkul J, Boonrungsiman S, Saengkrit N, Kongmakee P, Banlunara W, Poovorawan Y, Kasantikul T and Techangamsuwan S. 2021a. Natural infection of parvovirus in wild fishing cats (*Prionailurus viverrinus*) reveals extant viral localization in kidneys. *PLoS One*. 16(3): e0247266.
- Piewbang C, Wardhani SW, Dankaona W, Lacharoje S, Chai-In P, Yostawonkul J, Chanseanroj J, Boonrungsiman S, Kasantikul T, Poovorawan Y and Techangamsuwan S. 2021b. Canine bocavirus-2 infection and its possible association with encephalopathy in domestic dogs. *PLoS One*. 16(8): e0255425.
- Pond SL and Frost SD. 2005. Datamonkey: rapid detection of selective pressure on individual sites of codon alignments. *Bioinformatics*. 21(10): 2531-2533.
- Posada D, Crandall KA and Holmes EC. 2002. Recombination in evolutionary genomics. *Annu Rev Genet*. 36: 75-97.
- Poulet H, Brunet S, Soulier M, Leroy V, Goutebroze S and Chappuis G. 2000. Comparison between acute oral/respiratory and chronic stomatitis/gingivitis isolates of feline calicivirus: pathogenicity, antigenic profile and cross-neutralisation studies. *Arch Virol*. 145(2): 243-261.
- Povey C and Ingersoll J. 1975. Cross-protection among feline caliciviruses. *Infect Immun*. 11(5): 877-885.
- Prikhodko VG, Sandoval-Jaime C, Abente EJ, Bok K, Parra GI, Rogozin IB, Ostlund EN, Green KY and Sosnovtsev SV. 2014. Genetic characterization of feline calicivirus strains associated with varying disease manifestations during an outbreak season in Missouri (1995-1996). *Virus Genes*. 48(1): 96-110.
- Radford AD, Addie D, Belak S, Boucraut-Baralon C, Egberink H, Frymus T, Gruffydd-Jones T, Hartmann K, Hosie MJ, Lloret A, Lutz H, Marsilio F, Pennisi MG, Thiry

- E, Truyen U and Horzinek MC. 2009. Feline calicivirus infection. ABCD guidelines on prevention and management. *J Feline Med Surg.* 11(7): 556-564.
- Radford AD, Bennett M, McArdle F, Dawson S, Turner PC, Glenn MA and Gaskell RM. 1997. The use of sequence analysis of a feline calicivirus (FCV) hypervariable region in the epidemiological investigation of FCV related disease and vaccine failures. *Vaccine.* 15(12-13): 1451-1458.
- Radford AD, Coyne KP, Dawson S, Porter CJ and Gaskell RM. 2007. Feline calicivirus. *Vet Res.* 38(2): 319-335.
- Radford AD, Dawson S, Coyne KP, Porter CJ and Gaskell RM. 2006. The challenge for the next generation of feline calicivirus vaccines. *Vet Microbiol.* 117(1): 14-18.
- Radford AD, Sommerville L, Ryvar R, Cox MB, Johnson DR, Dawson S and Gaskell RM. 2001a. Endemic infection of a cat colony with a feline calicivirus closely related to an isolate used in live attenuated vaccines. *Vaccine.* 19(31): 4358-4362.
- Radford AD, Sommerville LM, Dawson S, Kerins AM, Ryvar R and Gaskell RM. 2001b. Molecular analysis of isolates of feline calicivirus from a population of cats in a rescue shelter. *Vet Rec.* 149(16): 477-481.
- Radford AD, Turner PC, Bennett M, McArdle F, Dawson S, Glenn MA, Williams RA and Gaskell RM. 1998. Quasispecies evolution of a hypervariable region of the feline calicivirus capsid gene in cell culture and in persistently infected cats. *J Gen Virol.* 79 ( Pt 1): 1-10.
- Radford AD, Willoughby K, Dawson S, McCracken C and Gaskell RM. 1999. The capsid gene of feline calicivirus contains linear B-cell epitopes in both variable and conserved regions. *J Virol.* 73(10): 8496-8502.
- Reed GH, Kent JO and Wittwer CT. 2007. High-resolution DNA melting analysis for simple and efficient molecular diagnostics. *Pharmacogenomics.* 8(6): 597-608.
- Reed GH and Wittwer CT. 2004. Sensitivity and specificity of single-nucleotide polymorphism scanning by high-resolution melting analysis. *Clin Chem.* 50(10): 1748-1754.
- Reynolds BS, Poulet H, Pingret JL, Jas D, Brunet S, Lemeter C, Etievant M and Boucraut-Baralon C. 2009. A nosocomial outbreak of feline calicivirus

- associated virulent systemic disease in France. *J Feline Med Surg.* 11(8): 633-644.
- Rong S, Slade D, Floyd-Hawkins K and Wheeler D. 2006. Characterization of a highly virulent feline calicivirus and attenuation of this virus. *Virus Res.* 122(1-2): 95-108.
- Royall E and Locker N. 2016. Translational Control during Calicivirus Infection. *Viruses.* 8(4): 104.
- Ruch-Gallie RA, Veir JK, Hawley JR and Lappin MR. 2011. Results of molecular diagnostic assays targeting feline herpesvirus-1 and feline calicivirus in adult cats administered modified live vaccines. *J Feline Med Surg.* 13(8): 541-545.
- Sato Y, Ohe K, Fukuyama M, Furuhashi K, Kishikawa S, Sakai S, Kiuchi A, Hara M, Watanabe T, Ishikawa Y and Taneno A. 2004. Properties of a calicivirus isolated from cats dying in an agitated state. *Vet Rec.* 155(25): 800-805.
- Sato Y, Ohe K, Murakami M, Fukuyama M, Furuhashi K, Kishikawa S, Suzuki Y, Kiuchi A, Hara M, Ishikawa Y and Taneno A. 2002. Phylogenetic analysis of field isolates of feline calicivirus (FCV) in Japan by sequencing part of its capsid gene. *Vet Res Commun.* 26(3): 205-219.
- Schorr-Evans EM, Poland A, Johnson WE and Pedersen NC. 2003. An epizootic of highly virulent feline calicivirus disease in a hospital setting in New England. *J Feline Med Surg.* 5(4): 217-226.
- Schulz BS, Hartmann K, Unterer S, Eichhorn W, Majzoub M, Homeier-Bachmann T, Truyen U, Ellenberger C and Huebner J. 2011. Two outbreaks of virulent systemic feline calicivirus infection in cats in Germany. *Berl Munch Tierarztl Wochenschr.* 124(5-6): 186-193.
- Schulz C, Hartmann K, Mueller RS, Helps C and Schulz BS. 2015. Sampling sites for detection of feline herpesvirus-1, feline calicivirus and *Chlamydia felis* in cats with feline upper respiratory tract disease. *J Feline Med Surg.* 1098612X15569615.
- Smertina E, Urakova N, Strive T and Frese M. 2019. Calicivirus RNA-Dependent RNA Polymerases: Evolution, Structure, Protein Dynamics, and Function. *Front Microbiol.* 10: 1280.

- Smith SL, Afonso MM, Pinchbeck GL, Gaskell RM, Dawson S and Radford AD. 2020. Temporally separated feline calicivirus isolates do not cluster phylogenetically and are similarly neutralised by high-titre vaccine strain FCV-F9 antisera in vitro. *J Feline Med Surg.* 22(6): 602-607.
- Sosnovtsev SV, Sosnovtseva SA and Green KY. 1998. Cleavage of the feline calicivirus capsid precursor is mediated by a virus-encoded proteinase. *J Virol.* 72(4): 3051-3059.
- Spiri AM, Riond B, Stirn M, Novacco M, Meli ML, Boretti FS, Herbert I, Hosie MJ and Hofmann-Lehmann R. 2021. Modified-Live Feline Calicivirus Vaccination Reduces Viral RNA Loads, Duration of RNAemia, and the Severity of Clinical Signs after Heterologous Feline Calicivirus Challenge. *Viruses.* 13(8): 1505.
- Stone AE, Brummet GO, Carozza EM, Kass PH, Petersen EP, Sykes J and Westman ME. 2020. 2020 AAHA/AAFP Feline Vaccination Guidelines. *J Feline Med Surg.* 22(9): 813-830.
- Stuart AD and Brown TD. 2006. Entry of feline calicivirus is dependent on clathrin-mediated endocytosis and acidification in endosomes. *J Virol.* 80(15): 7500-7509.
- Sun Y, Cheng Y, Lin P, Zhang H, Yi L, Tong M, Cao Z, Li S, Cheng S and Wang J. 2019. Simultaneous detection and differentiation of canine parvovirus and feline parvovirus by high resolution melting analysis. *BMC Vet Res.* 15(1): 141.
- Symes SJ, Job N, Ficorilli N, Hartley CA, Browning GF and Gilkerson JR. 2015. Novel assay to quantify recombination in a calicivirus. *Veterinary Microbiology.* 177(1): 25-31.
- Tajiri-Utagawa E, Hara M, Takahashi K, Watanabe M and Wakita T. 2009. Development of a Rapid High-Throughput Method for High-Resolution Melting Analysis for Routine Detection and Genotyping of Noroviruses. *Journal of Clinical Microbiology.* 47(2): 435.
- Tamburro M and Ripabelli G. 2017. High Resolution Melting as a rapid, reliable, accurate and cost-effective emerging tool for genotyping pathogenic bacteria and enhancing molecular epidemiological surveillance: a comprehensive review of the literature. *Ann Ig.* 29(4): 293-316.

- Thomas S, Lappin DF, Spears J, Bennett D, Nile C and Riggio MP. 2017. Prevalence of feline calicivirus in cats with odontoclastic resorptive lesions and chronic gingivostomatitis. *Res Vet Sci.* 111: 124-126.
- Tohya Y, Yokoyama N, Maeda K, Kawaguchi Y and Mikami T. 1997. Mapping of antigenic sites involved in neutralization on the capsid protein of feline calicivirus. *J Gen Virol.* 78 ( Pt 2): 303-305.
- Toi CS and Dwyer DE. 2008a. Differentiation between vaccine and wild-type varicella-zoster virus genotypes by high-resolution melt analysis of single nucleotide polymorphisms. *Journal of Clinical Virology.* 43(1): 18-24.
- Toi CS and Dwyer DE. 2008b. Differentiation between vaccine and wild-type varicella-zoster virus genotypes by high-resolution melt analysis of single nucleotide polymorphisms. *J Clin Virol.* 43(1): 18-24.
- Truyen U, Geissler K and Hirschberger J. 1999. Tissue distribution of virus replication in cats experimentally infected with distinct feline calicivirus isolates. *Berl Munch Tierarztl Wochenschr.* 112(9): 355-358.
- Urban C and Luttermann C. 2020. Major Capsid Protein Synthesis from the Genomic RNA of Feline Calicivirus. *J Virol.* 94(15).
- Uri D. 2014. Feline Upper Respiratory Disease Complex: The detection and epidemiology of respiratory pathogens in Midwestern feline shelter populations. Iowa State University, Graduate Theses and Dissertations.
- Vaz PK, Legione AR, Hartley CA and Devlin JM. 2019. Detection and Differentiation of Two Koala Gammaherpesviruses by Use of High-Resolution Melt (HRM) Analysis Reveals Differences in Viral Prevalence and Clinical Associations in a Large Study of Free-Ranging Koalas. *Journal of Clinical Microbiology.* 57(3): e01478-01418.
- Vinje J, Estes MK, Esteves P, Green KY, Katayama K, Knowles NJ, L'Homme Y, Martella V, Vennema H, White PA and Ictv Report C. 2019. ICTV Virus Taxonomy Profile: Caliciviridae. *J Gen Virol.* 100(11): 1469-1470.
- Vossen RH, Aten E, Roos A and den Dunnen JT. 2009. High-resolution melting analysis (HRMA): more than just sequence variant screening. *Hum Mutat.* 30(6): 860-866.



- Wardhani SW, Wongsakul B, Kasantikul T, Piewbang C and Techangamsuwan S. 2021. Molecular and Pathological Investigations of Selected Viral Neuropathogens in Rabies-Negative Brains of Cats and Dogs Revealed Neurotropism of Carnivore Protoparvovirus-1. *Front Vet Sci.* 8: 710701.
- Wardley RC. 1976. Feline calicivirus carrier state. A study of the host/virus relationship. *Arch Virol.* 52(3): 243-249.
- Weiblen R, Lovato LT and Henzel A. 2016. Feline Calicivirus. In: *Molecular Detection of Animal Viral Pathogens.* ed. Liu D. (ed.). New York: CRC Press, Taylor&Francis Group. 121-127.
- Wilhelm S and Truyen U. 2006. Real-time reverse transcription polymerase chain reaction assay to detect a broad range of feline calicivirus isolates. *J Virol Methods.* 133(1): 105-108.
- Willi B, Spiri AM, Meli ML, Samman A, Hoffmann K, Sydler T, Cattori V, Graf F, Diserens KA, Padrucci I, Nesina S, Berger A, Ruetten M, Riond B, Hosie MJ and Hofmann-Lehmann R. 2016. Molecular characterization and virus neutralization patterns of severe, non-epizootic forms of feline calicivirus infections resembling virulent systemic disease in cats in Switzerland and in Liechtenstein. *Vet Microbiol.* 182: 202-212.
- Wobus CE, Karst SM, Thackray LB, Chang KO, Sosnovtsev SV, Belliot G, Krug A, Mackenzie JM, Green KY and Virgin HW. 2004. Replication of Norovirus in cell culture reveals a tropism for dendritic cells and macrophages. *PLoS Biol.* 2(12): e432.
- Wong WT, Kelman M and Ward MP. 2013. Surveillance of upper respiratory tract disease in owned cats in Australia, 2009–2012. *Preventive Veterinary Medicine.* 112(1): 150-155.
- Zhang W, Li L, Deng X, Kapusinszky B, Pesavento PA and Delwart E. 2014. Faecal virome of cats in an animal shelter. *J Gen Virol.* 95(Pt 11): 2553-2564.
- Zhao Y, Chen X, Ying Y, Wang K, Dong H, Gao C, Yang S and Hu G. 2017. Isolation and phylogenetic analysis of three feline calicivirus strains from domestic cats in Jilin Province, China. *Arch Virol.* 162(9): 2579-2589.

Zhou L, Fu N, Ding L, Li Y, Huang J, Sha X, Zhou Q, Song X and Zhang B. 2021. Molecular Characterization and Cross-Reactivity of Feline Calicivirus Circulating in Southwestern China. *Viruses*. 13(9).



## VITA

<b>NAME</b>	Kannika Phongroop
<b>DATE OF BIRTH</b>	27 August 1978
<b>PLACE OF BIRTH</b>	Bangkok
<b>INSTITUTIONS ATTENDED</b>	<ol style="list-style-type: none"> <li>1. Diplomate, Thai Board of Veterinary Medicine (DTBVM)</li> <li>2. M.S. (Health Science), Chiang Mai University</li> <li>3. D.V.M., Kasetsart University</li> </ol>
<b>HOME ADDRESS</b>	208/15 Moo Baan Sriwalee-Lake view, Suthep subdistrick, Muang District, Chiang Mai, Thailand
<b>PUBLICATION</b>	<ol style="list-style-type: none"> <li>1. (Accepted abstract) Genetic variation of feline calicivirus from shelter and stray cats in Thailand, WSAVA 2020</li> <li>2. (Poster presentation) Detection of Feline Calicivirus in fecal sample of cats, ISWAVLD 2019</li> <li>3. (Poster presentation) Occurrence of Feline Herpesvirus-1 and Feline Calicivirus Infection in Thailand, VRVC 2018</li> <li>4. (Poster presentation) Molecular Detection of Feline Calicivirus Infection in Thailand, CUVC 2018</li> </ol>